

Search for Higgs boson decays into a pair of pseudoscalar particles in the $bb\mu\mu$ final state with the ATLAS detector in pp collisions at $\sqrt{s} = 13$ TeV

G. Aad *et al.**
(ATLAS Collaboration)

 (Received 4 October 2021; accepted 22 November 2021; published 11 January 2022)

This paper presents a search for decays of the Higgs boson with a mass of 125 GeV into a pair of new pseudoscalar particles, $H \rightarrow aa$, where one a -boson decays into a b -quark pair and the other into a muon pair. The search uses 139 fb^{-1} of proton-proton collision data at a center-of-mass energy of $\sqrt{s} = 13$ TeV recorded between 2015 and 2018 by the ATLAS experiment at the LHC. A narrow dimuon resonance is searched for in the invariant mass spectrum between 16 GeV and 62 GeV. The largest excess of events above the Standard Model backgrounds is observed at a dimuon invariant mass of 52 GeV and corresponds to a local (global) significance of 3.3σ (1.7σ). Upper limits at 95% confidence level are placed on the branching ratio of the Higgs boson to the $bb\mu\mu$ final state, $\mathcal{B}(H \rightarrow aa \rightarrow bb\mu\mu)$, and are in the range $0.2\text{--}4.0 \times 10^{-4}$, depending on the signal mass hypothesis.

DOI: [10.1103/PhysRevD.105.012006](https://doi.org/10.1103/PhysRevD.105.012006)

I. INTRODUCTION

Light (pseudo) scalars that couple to the 125 GeV Higgs boson [1,2] appear in many well-motivated extensions of the Standard Model (SM) [3–8]. These include models addressing the baryon asymmetry of the universe [9,10], offering a solution to the naturalness problem [11,12], or providing insights into the nature of dark matter [13–19]. Light bosons produced in Higgs boson decays could also be mediators to dark sectors that do not couple to the SM otherwise [20–24]. Furthermore, pseudoscalar mediators appear in models, such as those described in Ref. [25], that were proposed to explain the anomalous muon magnetic moment [26]. A combination of ATLAS measurements of the Higgs boson production cross sections and branching ratios constrains the branching ratios into invisible and undetected states to be $\mathcal{B}(H \rightarrow \text{inv}) < 30\%$ and $\mathcal{B}(H \rightarrow \text{undetected}) < 21\%$, respectively, whereas the overall branching fraction of the Higgs boson into beyond-the-SM (BSM) states is determined to be less than 47% at 95% confidence level (CL) [27]. Combined measurements of Higgs boson couplings performed by the CMS Collaboration set upper limits of $\mathcal{B}(H \rightarrow \text{inv}) < 22\%$ and $\mathcal{B}(H \rightarrow \text{undetected}) < 38\%$ at 95% CL [28]. This motivates searches for light states in the Higgs boson decays that probe this potentially large $\mathcal{B}(H \rightarrow \text{BSM})$.

This paper presents a search for decays of the 125 GeV Higgs boson into two pseudoscalars, denoted by a , in proton-proton (pp) collisions at the LHC [29]. The search is performed in events where one a -boson decays into two b -quarks and the other into two muons, $H \rightarrow aa \rightarrow b\bar{b}\mu^+\mu^-$.¹ The a -bosons are assumed to have a decay width that is narrow compared to the detector resolution. As pseudoscalar couplings are generally proportional to mass, which is for example the case in two-Higgs-doublet models [20,30], the $bb\mu\mu$ final state provides a good balance between a high branching ratio from the $a \rightarrow bb$ decay and a clean, high mass-resolution, dimuon resonance signature that is easy to trigger on from the $a \rightarrow \mu\mu$ decay. In scenarios with enhanced lepton couplings, the $a \rightarrow \mu\mu$ branching ratio can also be relatively large, resulting in $\mathcal{B}(H \rightarrow aa \rightarrow bb\mu\mu)/\mathcal{B}(H \rightarrow aa)$ of up to 0.16% [31].

Light resonances in Higgs boson decays have been searched for by ATLAS and CMS in many different channels, i.e., in the final states involving 4μ [32,33], $2\mu 2\tau$ or 4τ [34–38], $2b2\tau$ [39], $4b$ [40,41], 4γ [42], and $2\gamma + 2$ -jets [43]. A search for a dimuon resonance produced in association with b -jets has been performed by CMS [44] and a light resonance decaying to two muons has been searched for by LHCb [45]. CMS has performed a search for $H \rightarrow aa \rightarrow bb\mu\mu$ in 35.9 fb^{-1} of pp collision data at a center-of-mass energy of $\sqrt{s} = 13$ TeV that sets upper limits on $\mathcal{B}(H \rightarrow aa \rightarrow bb\mu\mu)$ of $(1\text{--}7) \times 10^{-4}$ for a -boson masses (m_a) in the range $20 \leq m_a \leq 62.5$ GeV [46]. The ATLAS search based on 36 fb^{-1} of Run 2 data [47] sets

*Full author list given at the end of the article.

Published by the American Physical Society under the terms of the [Creative Commons Attribution 4.0 International license](https://creativecommons.org/licenses/by/4.0/). Further distribution of this work must maintain attribution to the author(s) and the published article's title, journal citation, and DOI. Funded by SCOAP³.

¹Denoted by $H \rightarrow aa \rightarrow b\bar{b}\mu\mu$ from now on for the rest of the paper.

upper limits on $\mathcal{B}(H \rightarrow aa \rightarrow bb\mu\mu)$ between 1.2×10^{-4} and 8.4×10^{-4} for a -boson masses in the range $20 \leq m_a \leq 60$ GeV. In this paper, the full Run 2 dataset corresponding to an integrated luminosity of 139 fb^{-1} is used and the search is extended down to $m_a = 16$ GeV and up to $m_a = 62$ GeV. Additionally, boosted decision tree (BDT) techniques are used to improve the separation of the signal from the SM backgrounds, increasing the analysis sensitivity, especially for higher m_a .

II. ATLAS DETECTOR

The ATLAS experiment [48,49] is a multipurpose particle detector with a forward-backward symmetric cylindrical geometry and a nearly 4π coverage in solid angle.² It consists of an inner detector (ID) surrounded by a thin superconducting solenoid providing a 2 T axial magnetic field, electromagnetic (EM), and hadron calorimeters, and a muon spectrometer (MS). The inner tracking detector covers the pseudorapidity range $|\eta| < 2.5$. It consists of silicon pixel, silicon microstrip, and transition radiation tracking detectors. Lead/liquid-argon (LAr) sampling calorimeters provide electromagnetic energy measurements with high granularity. A steel/scintillator-tile hadron calorimeter covers the central pseudorapidity range $|\eta| < 1.7$. The endcap and forward regions are instrumented with LAr calorimeters for both the EM and hadronic energy measurements up to $|\eta| = 4.9$. The MS surrounds the calorimeters and is based on three large superconducting air-core toroidal magnets with eight coils each. The field integral of the toroids ranges between 2.0 Tm and 6.0 Tm across most of the detector. The MS includes a system of precision tracking chambers and fast detectors for triggering. A two-level trigger system is used to select events. The first-level trigger is implemented in hardware and uses a subset of the detector information to accept events at a rate below 100 kHz [50]. This is followed by a software-based trigger that reduces the accepted event rate to 1 kHz on average. An extensive software suite [51] is used in the reconstruction and analysis of real and simulated data, in detector operations, and in the trigger and data acquisition systems of the experiment.

III. DATASET AND SIMULATED EVENTS

The data used in this analysis were collected in Run 2 of the LHC during the 2015–2018 data-taking period with pp

collisions at a center-of-mass energy of $\sqrt{s} = 13$ TeV. The dataset corresponds to an integrated luminosity of 139 fb^{-1} . The lowest-threshold unscaled single-muon and dimuon triggers are used to select the events [52]. Single-muon triggers require the transverse momentum (p_T) of the muon to be above 20 or 26 GeV, depending on the data-taking period, while the dimuon trigger requires both muons to have a p_T above 14 GeV.

Simulated events are used in the estimation of the SM backgrounds. SHERPA 2.2.1 [53,54] was used as the baseline generator for the Drell–Yan (DY) + jets, $W(\rightarrow \ell\nu)$ + jets, diboson and triboson backgrounds. It is a multiparton matrix element and parton shower (PS) generator including hadronization [55–59], with the NNPDF3.0 parton distribution function (PDF) set at next-to-next-to-leading-order (NNLO) accuracy [60]. The DY + jets and multiboson samples were generated with a minimum dilepton mass of 10 and 4 GeV, respectively. The $t\bar{t}$ and single-top-quark samples were generated with Powheg-Box v2 [61–65] using the NNPDF3.0NLO PDF in matrix element interfaced to PYTHIA 8.230 [66] for the PS. For the underlying-event description a set of tuned parameters called the A14 tune [67] was used, along with the NNPDF2.3LO PDF [68]. The $t\bar{t}$ + vector-boson processes ($t\bar{t} + V$) were generated with MadGraph5_aMC@NLO 2.3.3 [69] interfaced to PYTHIA 8.210 for the PS. The underlying-event tune was the same as for the $t\bar{t}$ sample. EvtGen [70] was used for the properties of the bottom and charm hadron decays in all simulated samples, except those simulated with SHERPA.

Higgs boson production through gluon–gluon fusion (ggF) was generated using the NNLOPS program [71,72] with Powheg-Box v2 [61,63,73,74]. The vector-boson fusion (VBF) processes were generated with Powheg-Box v2 at NLO accuracy [75]. The Higgs boson mass was set to 125 GeV. For both the ggF and VBF production processes, Powheg-Box was interfaced with PYTHIA 8.212 using the AZNLO tune [76] for the simulation of the $H \rightarrow aa \rightarrow bb\mu\mu$ decays, where the a -boson is a pseudoscalar, as well as for parton showering, hadronization and the underlying event. The ggF Higgs boson production rate is normalized to the total cross section predicted at next-to-next-to-next-to-leading-order accuracy in QCD with NLO electroweak corrections applied [77–81] and amounts to 48.58 pb. The VBF production rate is normalized to an approximate NNLO cross section with the NLO electroweak corrections applied [82–85], which amounts to 3.8 pb. The contribution from the associated production of a Higgs boson and a vector boson (VH) is calculated to be 3.5% of the total ggF + VBF cross section and is accounted for by scaling the simulated ggF and VBF samples. The contribution from Higgs boson production in association with a pair of top quarks is found to be negligible (below the percent level) and is neglected in the analysis. Thirteen mass points were simulated for the ggF and VBF production modes, with the

²ATLAS uses a right-handed coordinate system with its origin at the nominal interaction point (IP) in the center of the detector and the z -axis along the beam pipe. The x -axis points from the IP to the center of the LHC ring, and the y -axis points upwards. Cylindrical coordinates (r, ϕ) are used in the transverse plane, ϕ being the azimuthal angle around the z -axis. The pseudorapidity is defined in terms of the polar angle θ as $\eta = -\ln \tan(\theta/2)$. Angular distance is measured in units of $\Delta R \equiv \sqrt{(\Delta\eta)^2 + (\Delta\phi)^2}$.

a -boson mass in the range $m_a = 16\text{--}62$ GeV.³ Below $m_a = 16$ GeV the b -quarks coming from the decays of the a -boson tend to be so collimated due to its boost that they cannot be reconstructed as two separate b -jets (with a radius parameter of $R = 0.4$). Another effect is that in the highly asymmetric decays of low-mass a -bosons, the subleading b -jet falls below the jet reconstruction threshold of 20 GeV [86]. As a result, the signal acceptance falls below 0.2% and the analysis loses sensitivity.

The effects of additional interactions in the same and neighboring beam-bunch crossings (pileup) were modeled for all simulated events by overlaying additional pp collisions generated with PYTHIA 8.186 using the NNPDF2.3LO PDF set and the A3 tune [87]. Simulated event samples are weighted to reproduce the distribution of the number of pileup interactions observed in the data. All the generated background and signal samples are processed through the ATLAS detector simulation [88] based on GEANT4 [89] and reconstructed using the same software as for the data.

IV. EVENT RECONSTRUCTION AND SELECTION

Muons are reconstructed by combining track information from the MS with tracks found in the ID [90]. They also have to satisfy $p_T > 5$ GeV and $|\eta| < 2.7$ (for $|\eta| > 2.5$, only tracking information from the MS is used), and pass the *LowPt* working point identification requirement defined in Ref. [90]. Muon tracks must have a longitudinal impact parameter z_0 satisfying $|z_0 \sin \theta| < 0.5$ mm and a transverse impact parameter significance $|d_0|/\sigma_{d_0} < 3$ relative to the primary interaction vertex, chosen as the reconstructed vertex with the highest sum of the p_T^2 of its associated tracks. Furthermore, muons are required to be isolated from the surrounding detector activity by requiring that the scalar sum of the p_T of additional inner detector tracks and the sum of the transverse momentum E_T of calorimeter energy deposits within a cone of size $\Delta R = 0.2$ around a muon be less than 15% and 30% of the muon p_T , respectively.

Jets are reconstructed using the anti- k_t algorithm [91] implemented in the *FastJet* package [92] with a radius parameter of $R = 0.4$. The inputs to the jet clustering are built by combining the information from both the calorimeters and the ID using a particle-flow algorithm [86,93]. Jets with $p_T < 60$ GeV originating from pileup are suppressed with the jet-vertex-tagger (JVT) [94], a multivariate algorithm combining track-based variables. Selected jets are required to have $p_T > 20$ GeV and $|\eta| < 2.5$. An algorithm (MV2c10) relying on multivariate techniques, taking as input the properties of displaced tracks and vertices reconstructed within a jet, is employed

to identify (tag) jets containing b -hadrons [95]. The MV2c10 tagger is used at 77% b -jet identification efficiency, with an approximate misidentification probability of 25% for jets arising from charm quarks, 6.3% for hadronically decaying τ -leptons, and 0.8% for light-flavor jets as measured in simulated $t\bar{t}$ events.

The missing transverse momentum (E_T^{miss}) is calculated as the magnitude of the negative vector sum of the transverse momenta of all the reconstructed and calibrated objects in the event, including a soft term that accounts for charged particles that are associated with the primary vertex, but not with any reconstructed object [96,97].

The events selected for the analysis are required to have two muons of opposite charge, either with the leading and subleading muons satisfying $p_T^{\text{leading}} > 27$ GeV and $p_T^{\text{subleading}} > 5$ GeV, and the event being triggered by a single-muon trigger, or with both muons having $p_T > 15$ GeV, and the event being triggered by a dimuon trigger. The dimuon invariant mass, $m_{\mu\mu}$, is required to be between 15 and 65 GeV. Furthermore, the events must contain exactly two b -tagged jets with p_T above 20 GeV.

A kinematic likelihood (KL) [98] fit exploiting the equal invariant masses of the bb and $\mu\mu$ systems in $H \rightarrow aa$ decays is performed to improve the four-body invariant mass ($m_{bb\mu\mu}$) resolution and reduce the SM backgrounds. The same fit approach as considered in the previous ATLAS publication [47] is used. The dimuon invariant mass, $m_{\mu\mu}$, is used to constrain the di- b -jet mass, as the former has a resolution approximately ten times better than the latter. The $m_{\mu\mu}$ resolution ranges between 0.4 GeV at $m_a = 16$ GeV and 1.3 GeV at $m_a = 62$ GeV. The fit maximizes the likelihood by shifting the b -jet energies within the resolution in order to satisfy the constraint $m_{\mu\mu} \simeq m_{bb}$. The output of the fit is the logarithm of the maximum likelihood value, $\ln(L^{\text{max}})$, which quantifies how well the event matches the $m_{\mu\mu} = m_{bb}$ hypothesis, characteristic of signal events. The four-body invariant mass, recomputed after the KL fit, is denoted by $m_{bb\mu\mu}^{\text{KL}}$ and is used for further event categorization.

Signal-like events are chosen by requiring that $110 < m_{bb\mu\mu}^{\text{KL}} < 140$ GeV, and that $\ln(L^{\text{max}}) > -8$, which ensures that m_{bb} is compatible with $m_{\mu\mu}$. Finally, E_T^{miss} is required to be less than 60 GeV to reduce the background from $t\bar{t}$ events, which is one of the two major backgrounds and can contain large E_T^{miss} from neutrinos in top-quark decays. This selection defines the “inclusive” signal region (SRincl) and is summarized in Table I, along with the selection requirements for other analysis regions described later in the text.

A BDT classifier implemented using the TMVA framework [99] is employed to further reduce the SM backgrounds. Its training is done in partially overlapping 8-GeV-wide $m_{\mu\mu}$ windows centered at the m_a values of

³More specifically, the simulated mass points are at $m_a = 16, 18, 20, 25, 30, 35, 40, 45, 50, 52, 55, 60, \text{ and } 62$ GeV.

TABLE I. Summary of the selection requirements for the control (TCR and DYCR), validation (VR1 and VR2), and inclusive signal (SRincl) regions in the analysis, as well as the final SR bins. The control and validation regions are defined in Sec. V.

	TCR	DYCR	SRincl	VR1	VR2
$m_{\mu\mu}$ (GeV)	[15, 65]				
$m_{bb\mu\mu}^{\text{KL}}$ (GeV)	[110, 140]	[80, 110] or [140, 170]	[110, 140]	[170, 300]	[110, 140]
E_T^{miss} (GeV)	>60	<60			
$\ln(L^{\text{max}})$	> -8			[-11, -8]	
SR bins	SRincl & $\text{BDT}m_a > 0.2$				
	2-GeV-wide (3-GeV-wide) $m_{\mu\mu}$ bins for $m_a \leq 45$ GeV ($m_a > 45$ GeV)				

each of the 12 generated signals,⁴ in order to fully exploit their kinematic differences. The background sample consists of $t\bar{t}$ and DY + jets events, the two dominant backgrounds, combined in the proportions extracted from the background validation fit described in Sec. VII. The signal samples

used for the training include ggF and VBF Higgs boson production samples combined according to their cross sections. The seven kinematic variables included in the training are:

- (i) m_{bb} ,
- (ii) $\ln(L^{\text{max}})$,
- (iii) $\Delta R_{b_1 b_2}$ (the angular distance between the two b -jets),
- (iv) $\text{diff}\Delta R_b R_\mu = \Delta R_{b_1 b_2} - \Delta R_{\mu_1 \mu_2}$ (the difference between the angular separations between the two b -jets and the two muons),
- (v) $\Delta R_{bb\mu\mu}$ (the angular distance between the bb and $\mu\mu$ systems),
- (vi) $\overline{\Delta R}_{b,\mu} = [\Delta R_{b_1 \mu_1} + \Delta R_{b_1 \mu_2} + \Delta R_{b_2 \mu_1} + \Delta R_{b_2 \mu_2}]/4$ (the average angular distance of all four combinations of a b -jet and a muon),
- (vii) $\overline{m}_{b\mu} = [m_{b_1 \mu_1} + m_{b_1 \mu_2} + m_{b_2 \mu_1} + m_{b_2 \mu_2}]/4$ (the average mass of all four combinations of a b -jet and a muon).

The distributions of these variables for the background and three representative signal masses are shown in Fig. 1.

The m_{bb} variable helps separate the low-mass signal from the backgrounds, as m_{bb} peaks around 60 GeV for the $t\bar{t}$ and DY processes. The $\ln(L^{\text{max}})$ peaks at higher values as the signal mass becomes smaller.

Due to a higher boost of a lighter a -boson, its decay products are collimated, resulting in $\Delta R_{b_1 b_2}$ and $\Delta R_{\mu_1 \mu_2}$ being much smaller than for a signal from a heavier a -boson or for background processes. As a consequence, $\text{diff}\Delta R_b R_\mu$ shows a narrow distribution centered around zero, while the background and a higher-mass signal exhibit a much broader $\text{diff}\Delta R_b R_\mu$ distribution.

⁴One BDT was trained for each generated signal MC sample, except for $m_a = 52$ GeV, as this sample was produced only at a later analysis stage.

The $\Delta R_{bb\mu\mu}$ variable helps enhance the sensitivity to higher signal masses. Heavier a -bosons are produced approximately at rest, resulting in the $\Delta R_{bb\mu\mu}$ distribution being relatively flat with a small peak at low values. As the signal mass decreases, the $\Delta R_{bb\mu\mu}$ distribution transitions into a “back-to-back” topology, characteristic of both a low-mass signal and the background events.

Finally, the $\overline{\Delta R}_{b,\mu}$ and $\overline{m}_{b,\mu}$ variables provide another measure of how close the two a -bosons are in ΔR . In the back-to-back topology for lower signal masses, the muons are, on average, further away from the b -jets, while for heavier a -bosons produced approximately at rest, the average distance between the muons and the b -jets is smaller. Consequently, $\overline{\Delta R}_{b,\mu}$ and $\overline{m}_{b,\mu}$ peak at high (low) values for low (high) signal masses, while the backgrounds peak somewhere between the two extreme signal topologies.

The output score of the BDT trained for a signal with mass m_a is denoted by $\text{BDT}m_a$. The $\text{BDT}m_a$ distributions for $m_a = 20, 40, \text{ and } 60$ GeV are shown in Fig. 2.

The final signal region (SR) bin for each signal mass is defined by imposing two requirements in addition to the SRincl selection: $m_a - X < m_{\mu\mu} < m_a + X$ and $\text{BDT}m_a > 0.2$, where $X = 1$ GeV ($X = 1.5$ GeV) for $m_a \leq 45$ GeV ($m_a > 45$ GeV). The widths of the SR bins and the $\text{BDT}m_a$ cut value are optimized to maximize the significance of signal over background events. For masses at which no signal sample was generated, and, consequently, no BDT was trained, the BDT trained for the m_a closest to the one being tested is used. For example, when testing the $m_a = 32$ GeV hypothesis, the requirement $\text{BDT}30 > 0.2$ is applied to select the events for the SR bin. Signal yields for mass points where no signal sample was generated ($m_a = 32$ GeV in this example) are obtained by selecting events with BDT scores above 0.2 for the same $\text{BDT}m_a$ (BDT30 in this case) in all simulated mass points and interpolating using third-order splines. To assess the uncertainty, the yields of the neighboring simulated mass points ($m_a = 30$ GeV and $m_a = 35$ GeV in this case) are interpolated using a linear function. The difference between the yields obtained using the splines and a linear function for the interpolation is assigned as a systematic uncertainty on the interpolated signal yield.

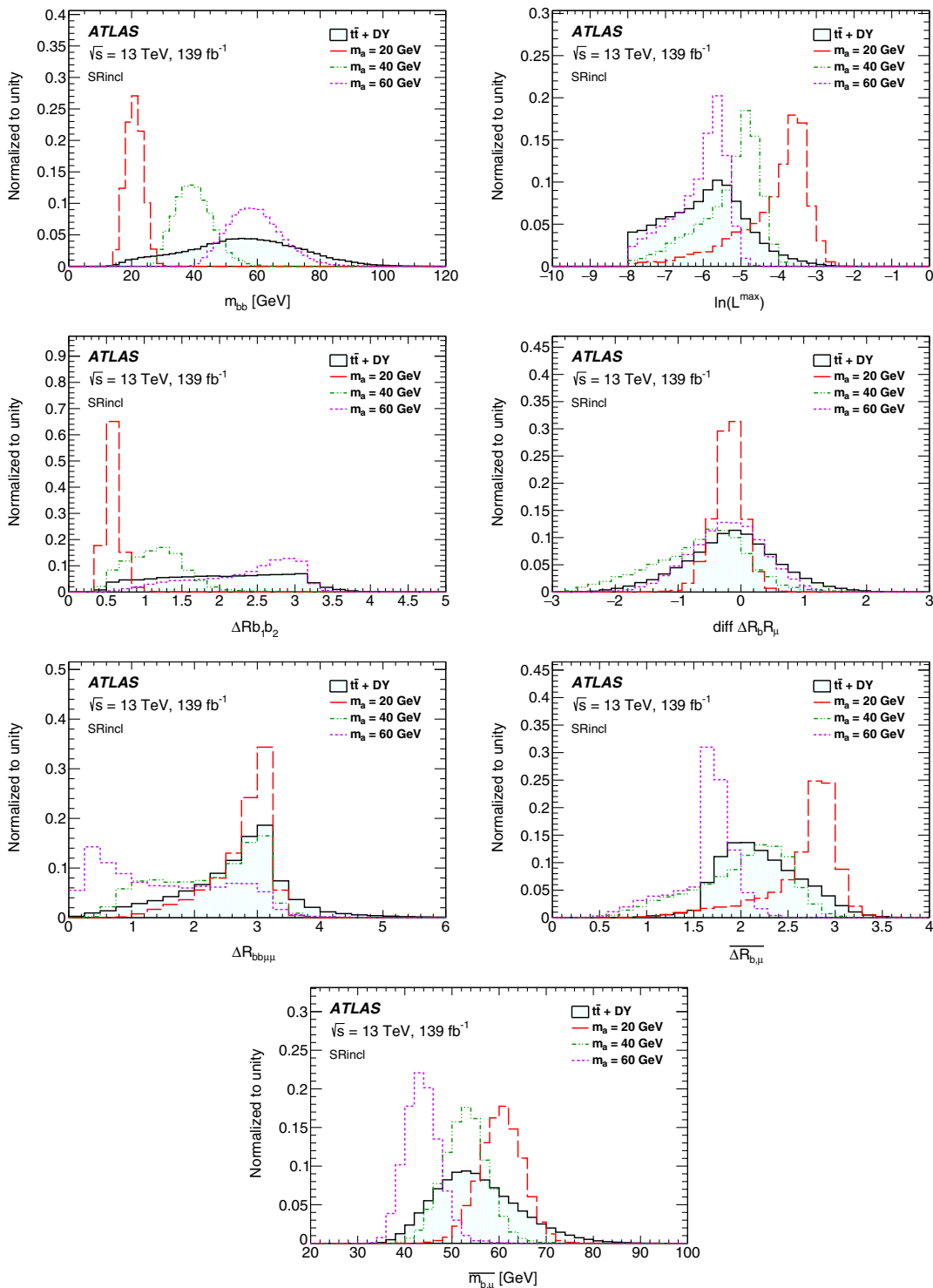


FIG. 1. Kinematic variables used as inputs to the BDT training. From top left to bottom right: m_{bb} , $\ln(L^{\max})$, $\Delta R_{b_1 b_2}$, $\text{diff} \Delta R_b R_\mu$, $\Delta R_{bb\mu\mu}$, $\overline{\Delta R_{b,\mu}}$, $\overline{m_{b,\mu}}$. The variables are plotted in SRincl. All the distributions are normalized to unit area. The background histogram is the sum of the $t\bar{t}$ and DY event templates, combined in the proportions extracted from the background validation fit described in Sec. VII.

Using a BDT at a mass for which the training was not performed results in a negligible loss of significance relative to a BDT that was optimized for that mass point.

The signal acceptance \times efficiency varies between 0.3% and 2.5% for ggF Higgs boson production and between 0.2% and 3.0% for VBF production, where the lowest

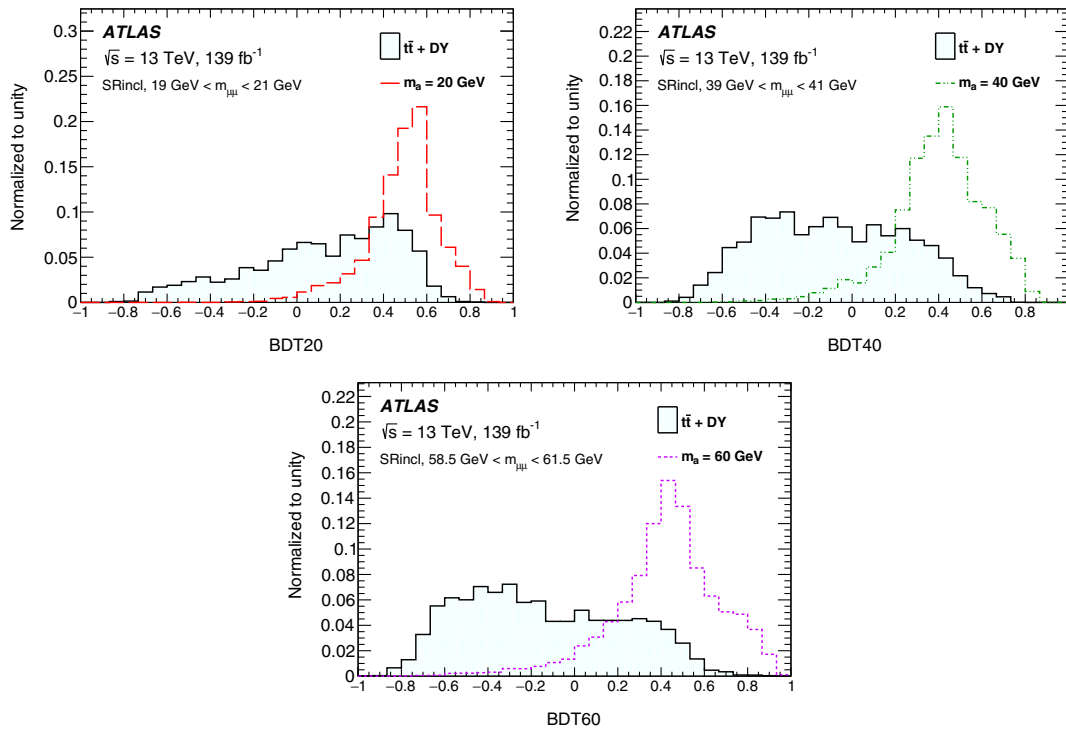


FIG. 2. Three BDT_{m_a} distributions, BDT20, BDT40, and BDT60, plotted in the $m_{\mu\mu}$ windows of SRincl, as indicated in the figures. The distributions are normalized to unit area. The background histogram is the sum of the $t\bar{t}$ and DY event templates, combined in the proportions extracted from the background validation fit described in Sec. VII.

acceptance \times efficiency is obtained for the lowest m_a , and grows as m_a increases. The largest loss of acceptance occurs when requiring that there are two b -jets in the event, as one of the signal jets tends to fall below the reconstruction threshold of 20 GeV. The fraction of signal events passing the two- b -jet requirement is less than 20% for all mass points.

V. BACKGROUND ESTIMATION

The dominant backgrounds in the analysis arise from the DY dimuon process in association with b -quarks and pair production of top quarks ($t\bar{t}$) where each W boson decays into a muon and a neutrino. These two backgrounds account for more than 96% of background events in all analysis regions.

Two control regions are designed to constrain the $t\bar{t}$ and DY backgrounds. They are chosen so that they have negligible signal contamination, are kinematically as close as possible to SRincl, and maximize the contribution of one of the respective background processes. A top-quark control region (TCR) is defined by inverting the E_T^{miss} selection criterion in SRincl to $E_T^{\text{miss}} > 60$ GeV. This results in an event sample approximately 93% pure in $t\bar{t}$ events. The DY control region (DYCR) is defined in the 30 GeV-wide $m_{bb\mu\mu}^{\text{KL}}$ sidebands of SRincl, i.e., by requiring $80 < m_{bb\mu\mu}^{\text{KL}} < 110$ GeV or $140 < m_{bb\mu\mu}^{\text{KL}} < 170$ GeV. Approximately 50% of the events in DYCR originate from the DY process, whereas the rest mostly come from $t\bar{t}$

production. Two validation regions (VR1 and VR2) are used to validate the normalizations of the backgrounds. VR1 is defined in the $170 < m_{bb\mu\mu}^{\text{KL}} < 300$ GeV range, while VR2 is obtained by inverting the $\ln(L^{\text{max}})$ selection criterion of SRincl to $-11 < \ln(L^{\text{max}}) < -8$. All the analysis regions are summarized in Table I and illustrated in Fig. 3.

The shapes of the $t\bar{t}$ kinematic variable distributions are obtained from simulation, while the overall normalization

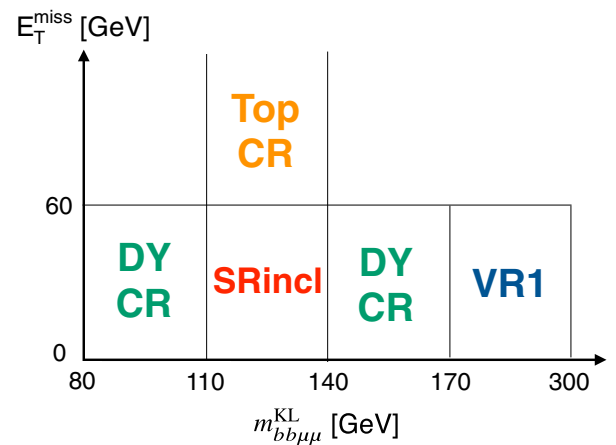


FIG. 3. Illustration of the signal, control, and validation regions used in the analysis. VR2 (not shown) is defined by the same selection as SRincl, except that the requirement on $\ln(L^{\text{max}})$ is inverted to $-11 < \ln(L^{\text{max}}) < -8$.

is extracted from the fits described in Sec. VII. The distributions for the DY background are taken from data templates because the limited sizes of the simulated event samples do not allow a reliable estimate. The template regions are defined in the same way as the analysis regions in Table I, except that the two- b -tag requirement is replaced by a zero- b -tag requirement. The template regions are $>95\%$ pure in DY events. Contributions from other processes, namely $t\bar{t}$, W + jets, diboson and single-top, are subtracted using simulation. Following the subtraction, the DY templates are corrected to account for kinematic differences between event samples dominated by jets originating from light quarks or gluons (template regions) and event samples dominated by b -jets (analysis regions). The correction is applied as a per-event weight, where the reweighting is derived from a comparison between two- b -tag and zero- b -tag kinematic distributions in simulated DY events. Two sets of event weights are derived and applied sequentially. First, the jet multiplicity of the zero- b -tag MC sample is reweighted to the one in the two- b -tag sample. It is the distribution with the largest difference between the zero- and two- b -tag samples and was hence corrected first. Second, a BDT-based reweighting is employed to further correct the zero- b -tag template kinematics. A BDT is trained on the zero- b -tag versus the two- b -tag simulated DY samples. The BDT input consists of kinematic properties and angular distributions of the b -jets, muons and the two corresponding a -boson candidates, as well as E_T^{miss} and $m_{bb\mu\mu}^{\text{KL}}$. The ratio of the BDT score distributions obtained for the two- b -tag and zero- b -tag simulated events is then applied as a weight to every event from the zero- b -tag DY template, as a function of its BDT score. Following the BDT-based reweighting, the $m_{bb\mu\mu}^{\text{KL}}$ and E_T^{miss} distributions are corrected by up to 20%. The DY templates are normalized to data in the fits described in Sec. VII.

Minor backgrounds include diboson and single-top-quark production, production of a $t\bar{t}$ pair in association with a vector boson, and W boson production in association with b -jets. The estimation of these minor backgrounds relies purely on simulation normalized to the best available theoretical prediction. The events where a jet is misidentified as a muon are taken into account as follows: non-prompt/misidentified muons in W + jets and $t\bar{t}$ events are included in the analysis on the basis of simulation, any contribution of nonprompt/misidentified muons in the DY + jets component is accounted for by the data template, and the potential contribution from multijet events is found to be negligible.

VI. SYSTEMATIC UNCERTAINTIES

Systematic uncertainties in the analysis are divided into three categories: experimental uncertainties affecting the simulated background and signal processes, uncertainties in the modeling of the DY template, and theoretical

uncertainties of the simulated background and signal samples. Table II shows a summary of the dominant systematic uncertainties in the total background and signal yields in the signal region bins, as resulting from the fits described in Sec. VII and hereafter denoted by “postfit”.

Among the experimental uncertainties, the leading effects come from those associated with the calibration and resolution of jet energies [100], and with the measurement of the b -tagging efficiency [95]. The impact of these uncertainties on the total background (signal) yields in the SR bins is as large as 3% (10%). The uncertainty in the combined 2015–2018 integrated luminosity is 1.7% [101], obtained using the LUCID-2 detector [102] for the primary luminosity measurement. Other uncertainties, such as those arising from the muon identification efficiency, momentum scale and resolution [90,103], and pileup are found to have a negligible impact on the final yields.

The uncertainty arising from limited MC sample sizes ranges from 8% to as large as 40% in the low m_a mass bins due to there being few $t\bar{t}$ events in this region.

Five sources of uncertainty in the data-driven DY template are considered. The uncertainty in subtracting non-DY events from the non-reweighted template in the

TABLE II. Summary of the dominant postfit systematic uncertainties in the background and signal yields. The uncertainties are expressed as a percentage of the total background and signal yields per $m_{\mu\mu}$ bin of the signal region. Only uncertainties exceeding 2% in at least one SR bin are shown.

Category	Source	Total background (%)	Signal (%)
DY	BDT m_a selection	7–14	...
	Normalization	5–10	...
	$m_{\mu\mu}$ shape	1–8	...
	Kinematics	0.3–6	...
	Background subtraction	0.6–3	...
$t\bar{t}$	Hadronization/PS	0.3–4	...
	Hard-scatter generation	0.2–3	...
	Normalization	0.2–3	...
Overall MC	Sample statistics	8–40	1–2
Jets	b -tagging	0.03–0.7	9–10
	Jet-energy resolution	1–3	6–7
	Jet-energy scale	1–3	4–5
Signal	FSR	...	5
	PS	...	4
	VH contribution	...	3.5
	MPI	...	3
	QCD scale	...	3
	ISR	...	3
	ggF cross section		
	-missing higher-order QCD	...	5
	-PDF & α_s	...	3

analysis regions is assessed by comparing the nominal template, for which the simulated non-DY backgrounds had been subtracted before reweighting, with an alternative template for which no subtraction had been performed. The uncertainties in the template kinematics modeling are derived by comparing the DY template with simulation in two key variables: E_T^{miss} and $m_{bb\mu\mu}^{\text{KL}}$. The ratios of the template to the simulated DY events are fit with linear functions and used in assigning uncertainties to the shapes of the E_T^{miss} and $m_{bb\mu\mu}^{\text{KL}}$ distributions. Similarly, the uncertainty in the $m_{\mu\mu}$ template shape is assessed by comparing the template with the smoothed simulated sample and applying the observed difference as a systematic uncertainty. The uncertainty in the normalization of the DY template is obtained from the fits to data. Finally, the uncertainty in the efficiency of the $\text{BDT}m_a$ selection criteria is evaluated by taking the difference in the $\text{BDT}m_a$ cut efficiency, $N_{\text{DY events SR}}^{\text{BDT}m_a > 0.2} / N_{\text{DY events SR}}^{\text{no BDT}m_a \text{ cut}}$, between the template and the simulation. All one-sided DY template uncertainties are symmetrized around the nominal value.

To assess the uncertainties in the generation of the hard-scatter $t\bar{t}$ process, the Powheg sample is compared with a sample generated using MadGraph5_aMC@NLO 2.3.3. The hadronization and fragmentation uncertainties in the PS are evaluated by comparing the nominal sample showered by PYTHIA 8.230 with an alternative sample generated by Powheg using the same PDF in matrix element as for the nominal sample, but showered with HERWIG 7.0.4 [104,105]. The initial- and final-state radiation (ISR and FSR) uncertainties of the $t\bar{t}$ sample are assessed by varying the internal PYTHIA 8.230 showering parameters. Finally, the uncertainties due to the PDF choice are evaluated using the internal variations of the nominal PDF4LHC15_NLO_30 set [106].

Uncertainties in the calculation of the ggF and VBF Higgs boson production cross sections are assessed by following the recommendations of the LHC Higgs Working Group given in Refs. [77,82]. As no VH signal sample was generated, a conservative 100% uncertainty is assigned to the estimated VH yield. To evaluate the uncertainties due to the PDF choice, the yields obtained with the baseline NNPDF30_NLO_AS_0118 set are compared with the yields obtained using the internal variations of NNPDF30_NLO_AS_0118 and with the yields obtained with the nominal MMHT2014NLO68CLAS118 [107] and CT14NLO [108] sets. The largest difference is taken as the overall PDF uncertainty for all signal mass points. Furthermore, the effects of uncertainties in the ISR, FSR, multiparton interactions (MPI) in PYTHIA, parton showering, and renormalization and factorization scales are also assessed. Uncertainties from these sources have an impact of 1–6% on the signal yields, with the largest contributions arising from the ggF production cross section and FSR uncertainties.

VII. ANALYSIS AND RESULTS

The final background and signal estimates are obtained in a set of binned likelihood fits [109] using the HistFitter [110] package. The likelihood is a product of Poisson probability functions, describing the observed and predicted numbers of events in each region, and Gaussian distributions that constrain the nuisance parameters associated with the systematic uncertainties. In the background validation fit, the data in TCR and DYCR are used to extract the normalization of the $t\bar{t}$ and DY backgrounds, respectively. As the $t\bar{t}$ sample in TCR is modeled very well, it is implemented as only one bin in the fit, whereas DYCR is divided into five equal-width bins in $m_{\mu\mu}$ to provide greater sensitivity to the DY template shape. The purpose of this fit is to validate the modeling of the background in the control and validation regions and in SRincl. The fitted $t\bar{t}$ normalization factor is $\mu_{t\bar{t}} = 1.07_{-0.07}^{+0.06}$, while the value of μ_{DY} has no physical meaning because it is scaled from a template region and is thus not quoted. Figures 4 and 5 show postfit distributions of $m_{bb\mu\mu}^{\text{KL}}$, E_T^{miss} , $\ln(L^{\text{max}})$, and $m_{\mu\mu}$ spanning various analysis regions, while Fig. 6 shows BDT20 and BDT50 in SRincl. Good agreement between the estimated backgrounds and the data is observed in the kinematic distributions. In SRincl, 1185 events are observed, which is compatible with the total estimated background of 1155.3 ± 13.6 . The yields in several representative SR bins, i.e., $m_{\mu\mu}$ windows after applying the BDT selection, as obtained from the background validation fit above, are shown in Table III. When comparing the systematic uncertainty with the statistical uncertainty, it can be seen that the analysis is clearly statistically limited. Figure 7 shows the data and the estimated backgrounds in all final SR bins. Due to the limited statistics of the background samples, the estimates are not perfectly smooth; however, the bin-to-bin fluctuations are much smaller than the statistical uncertainty of the data. Larger jumps, which occur at $m_a = 23, 28, 33, 38$ GeV etc., appear when the BDT discriminant used for the selection changes from the one trained in the lower mass range to the one trained in the higher mass range.

To test for the presence of new phenomena, fits are performed for each of the 47 hypothesized signal masses in the range $16 \leq m_{\mu\mu} \leq 62$ GeV in 1 GeV steps. It was verified that the analysis is also sufficiently sensitive to a signal with $m_{\mu\mu}$ centered in between these 1 GeV steps. TCR, DYCR, and the respective SR bin are included in each fit in order to constrain the backgrounds and the signal to the data.

A model-independent fit, i.e., not including any signal sample, is performed to test whether the data are compatible with the background-only hypothesis. The result is a scan of p_0 -values as shown in Fig. 8. The largest discrepancy is found at $m_{\mu\mu} = 52$ GeV, corresponding to a local (global) p_0 -value of 0.00054 (0.048) and a local (global)

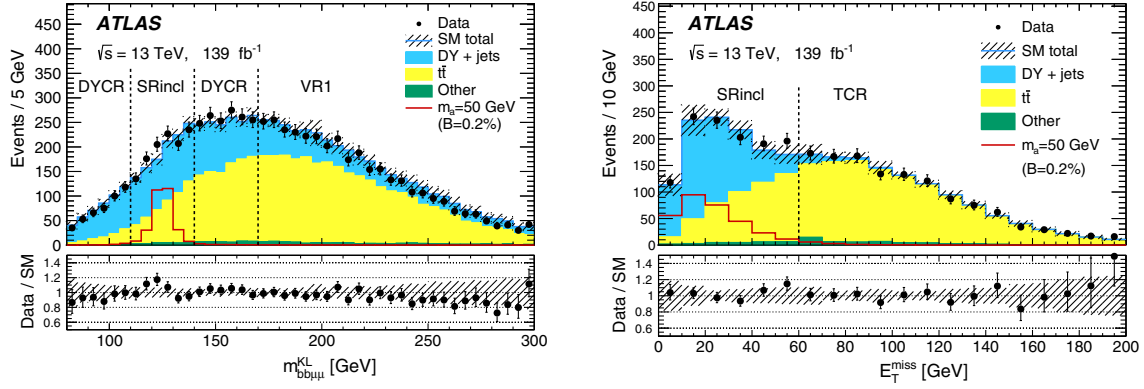


FIG. 4. Postfit $m_{bb\mu\mu}^{KL}$ in DYCR, SRincl, and VR1 (left); E_T^{miss} in SRincl and TCR (right). No selection based on the BDT discriminants is applied in the analysis regions shown in the figures. The signal distributions are normalized to the SM Higgs boson cross section (including ggF, VBF, and VH production) and assume $\mathcal{B}(H \rightarrow aa \rightarrow bb\mu\mu)$ as indicated in the legends of the figures (chosen to ensure good visibility in the plot). The hatched bands show the total postfit statistical and systematic uncertainties of the backgrounds. The histogram labeled as “Other” in the legend includes the contributions from the diboson, single-top-quark, $t\bar{t} + V$ and $W + \text{jets}$ backgrounds.

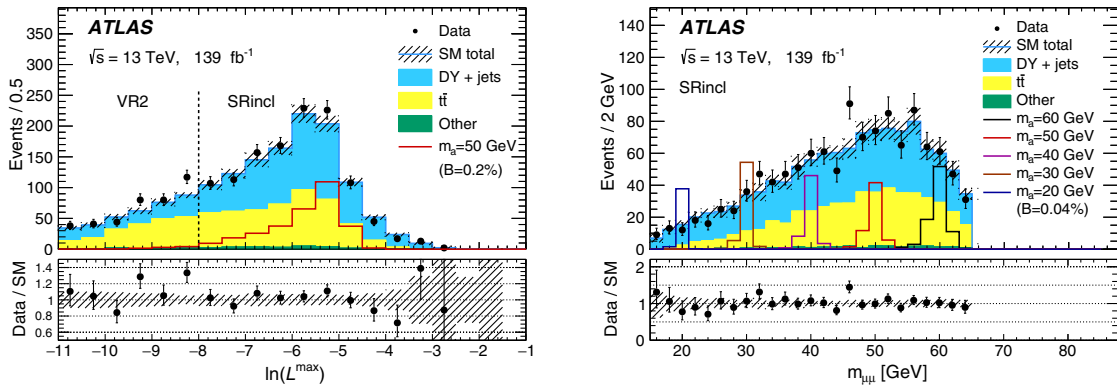


FIG. 5. Postfit $\ln(L^{\max})$ in VR2 and SRincl (left); $m_{\mu\mu}$ in SRincl (right). No selection based on the BDT discriminants is applied in the analysis regions shown in the figures. The signal distributions are normalized to the SM Higgs boson cross section (including ggF, VBF, and VH production) and assume $\mathcal{B}(H \rightarrow aa \rightarrow bb\mu\mu)$ as indicated in the legends of the figures (chosen to ensure good visibility in the plot). The hatched bands show the total postfit statistical and systematic uncertainties of the backgrounds. The histogram labeled as “Other” in the legend includes the contributions from the diboson, single-top-quark, $t\bar{t} + V$, and $W + \text{jets}$ backgrounds.

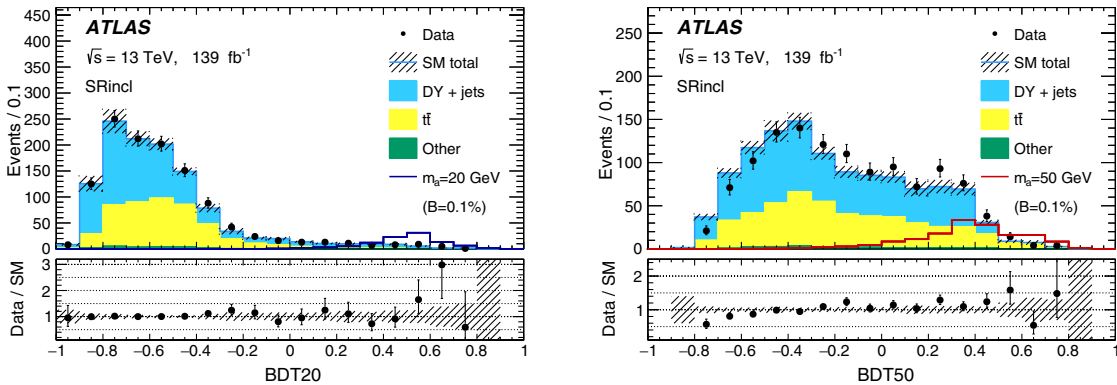


FIG. 6. Postfit BDT20 (left) and BDT50 (right) distributions in SRincl. The signal distributions are normalized to the SM Higgs boson cross section (including ggF, VBF, and VH production) and assume $\mathcal{B}(H \rightarrow aa \rightarrow bb\mu\mu)$ as indicated in the legends of the figures (chosen to ensure good visibility in the plot). The hatched bands show the total postfit statistical and systematic uncertainties of the backgrounds. The histogram labeled as “Other” in the legend includes the contributions from the diboson, single-top-quark, $t\bar{t} + V$, and $W + \text{jets}$ backgrounds.

TABLE III. Total and individual background yields in six representative $m_{\mu\mu}$ bins of the signal region after the BDT selection is applied. The yields are the postfit values as determined by the background validation fit. The uncertainties shown include all systematic and statistical uncertainties. As the diboson, single top quark, $t\bar{t}V$, and W + jets contributions are very small, they are summed in the table under “Other”.

$m_{\mu\mu}$ bin (GeV)	[15–17]	[24–26]	[34–36]	[44–46]	[50.5–53.5]	[60.5–63.5]
Observed events	6	9	19	17	39	8
Total background	4.8 ± 2.2	9.0 ± 1.8	11.9 ± 1.6	15.5 ± 2.0	19.3 ± 2.7	9.3 ± 1.7
DY	4.6 ± 2.1	6.4 ± 1.5	5.7 ± 1.1	6.4 ± 1.5	8.3 ± 2.1	5.3 ± 1.4
$t\bar{t}$	0.2 ± 0.1	2.6 ± 0.8	6.0 ± 1.1	8.5 ± 1.4	10.4 ± 2.4	3.5 ± 0.9
Other	0.03 ± 0.01	0.03 ± 0.00	0.24 ± 0.12	0.50 ± 0.40	0.50 ± 0.12	0.45 ± 0.19

significance of 3.3σ (1.7σ). The global significance was calculated from the asymptotic formulas in Refs. [109,111].

Upper limits, derived using the CL_s technique [112,113], are set on $\mathcal{B}(H \rightarrow aa \rightarrow bb\mu\mu)$ in a series of conditional fits, this time also including the signal samples. The limits as a function of m_a are shown in Fig. 9. Uniform sensitivity is achieved for all masses above 18 GeV, while for lower signal masses, $m_a \leq 18$ GeV, the sensitivity of the analysis decreases due to b -jets falling below the reconstruction threshold or merging into one reconstructed jet. Figure 10 shows $m_{\mu\mu}$ and $BDTm_a$ distributions after the signal + background fit for two SR bins, $m_a = 35$ GeV and $m_a = 52$ GeV, where the two largest deviations from the background-only hypothesis are observed. The signal in the plots is scaled to the best-fit value, corresponding to $\mathcal{B}(H \rightarrow aa \rightarrow bb\mu\mu) = 6.4 \times 10^{-5}$ (1.9×10^{-4}) for $m_a = 35$ GeV ($m_a = 52$ GeV).

The upper limits at 95% CL on $\mathcal{B}(H \rightarrow aa \rightarrow bb\mu\mu)$ range between 0.2×10^{-4} and 4.0×10^{-4} , depending on m_a . These limits improve upon the previous ATLAS result based on 36 fb^{-1} of data [47] by a factor of 2–5 over the

full $m_{\mu\mu}$ range. A factor of ~ 2 improvement in sensitivity comes from the larger dataset, and a further factor of ~ 2 is achieved thanks to the use of multivariate techniques to discriminate between the signal and the SM backgrounds. Due to small number of background events at lower signal masses m_a , the BDT training is less efficient in this region, and the gain from applying the $BDTm_a$ selection criteria is higher at higher m_a . Taking as an example the favorable scenario with $\mathcal{B}(H \rightarrow aa \rightarrow bb\mu\mu)/\mathcal{B}(H \rightarrow aa) = 0.16\%$, the analysis probes the Higgs boson branching fraction into pseudoscalars down to $\mathcal{B}(H \rightarrow aa) = 1.3\%$, much lower than the limits derived from combinations of the Higgs boson measurements.

So as not to restrict the analysis sensitivity solely to models where the a -particle is a pseudoscalar, upper limits obtained without employing the BDT discriminants are also derived as shown in Fig. 11. In addition to being less sensitive to the particle’s CP properties, the limits in SRincl without the BDT selection also facilitate reinterpretations of the analysis. These limits are derived in the same way as described above, i.e., by scanning the $m_{\mu\mu}$ windows of

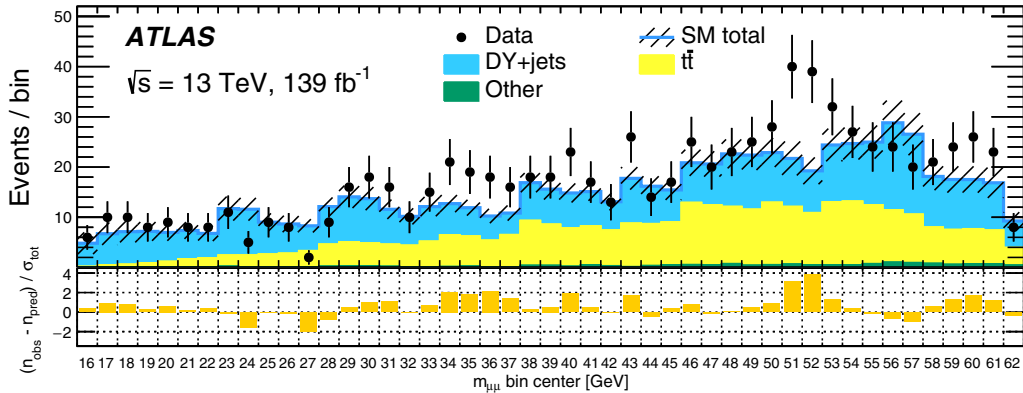


FIG. 7. Postbackground-validation-fit number of events in all SR bins (after applying the BDT selection) that are tested for the presence of signal. The bin widths are 2 GeV (3 GeV) in $m_{\mu\mu}$ for $m_a \leq 45$ GeV ($m_a > 45$ GeV). Neighboring bins partially overlap, hence they are not statistically independent. The bottom panel shows the pull in each bin, defined as $(n_{\text{obs}} - n_{\text{pred}})/\sigma_{\text{tot}}$, where n_{obs} is the number of events in the data, n_{pred} is the number of fitted background events and σ_{tot} is the total (systematic and statistical, added in quadrature) uncertainty in the fitted background yield. Discontinuities in the background predictions appear when the BDT discriminant used for the selection changes from the one trained in the lower mass range to the one trained in the higher mass range. The histogram labeled as “Other” in the legend includes the contributions from the diboson, single-top-quark, $t\bar{t} + V$, and W + jets backgrounds.

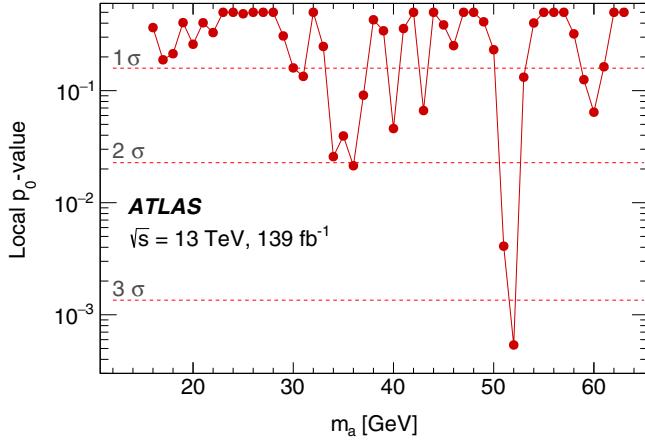


FIG. 8. The local p_0 -values are quantified in standard deviations σ and plotted as a function of the signal mass hypothesis. Between the points, the p_0 -values are interpolated and may not be fully representative of the actual sensitivity.

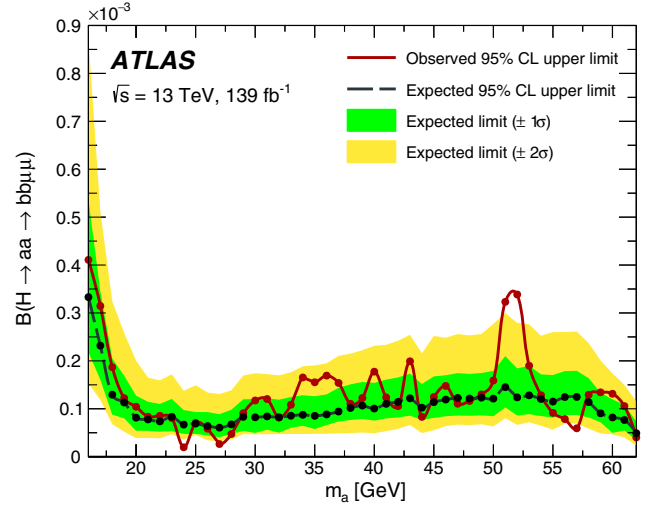


FIG. 9. Upper limits on $\mathcal{B}(H \rightarrow aa \rightarrow bb\mu\mu)$ at 95% CL, including the BDT selection, as a function of the signal mass hypothesis. Black and red dots show masses for which the hypothesis testing was done. Between these points, the limits are interpolated and may not be fully representative of the actual sensitivity.

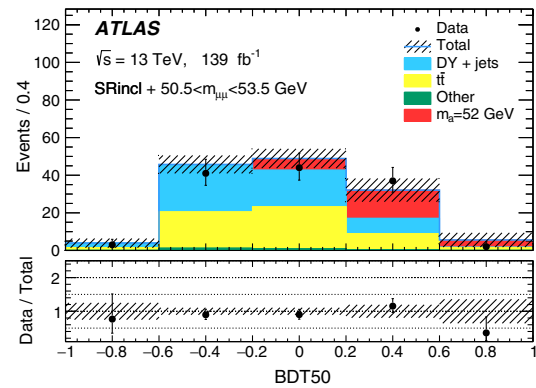
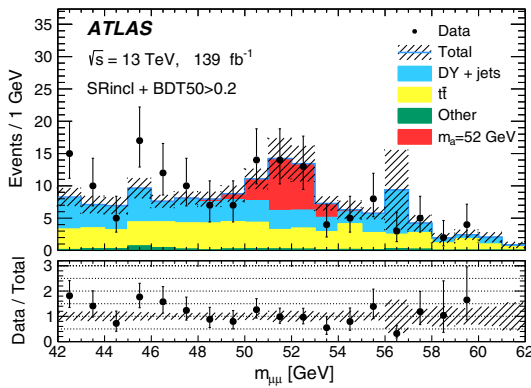
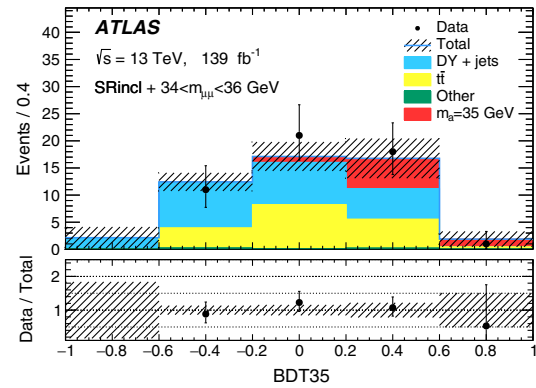
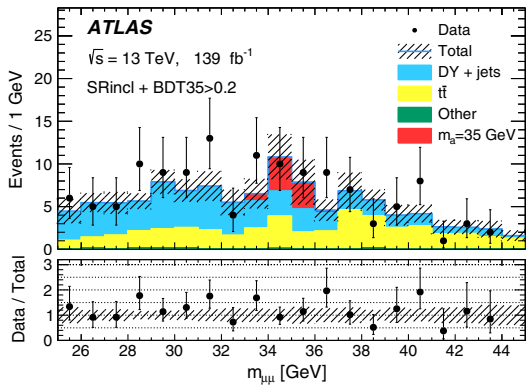


FIG. 10. $m_{\mu\mu}$ distributions in the SRincl after the BDT35 > 0.2 selection (top left) and BDT50 > 0.2 selection (bottom left), and BDT35 (top right) and BDT50 (bottom right) distributions in the SRincl in the $m_{\mu\mu}$ window 34–36 GeV and 50.5–53.5 GeV, respectively. The signal is scaled to the best-fit value, $\mathcal{B}(H \rightarrow aa \rightarrow bb\mu\mu) = 6.4 \times 10^{-5}$ for the top plots, and 1.9×10^{-4} for the bottom plots, assuming the SM Higgs boson cross section (including ggF, VBF, and VH production). The hatched bands show the total postfit statistical and systematic uncertainties of the backgrounds and the signal. The histogram labeled as “Other” in the legend includes the contributions from the diboson, single-top-quark, $t\bar{t} + V$, and $W + \text{jets}$ backgrounds.

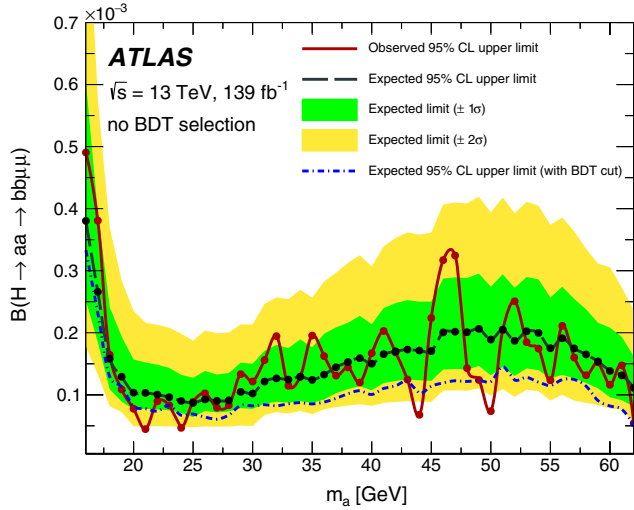


FIG. 11. Upper limits on $\mathcal{B}(H \rightarrow aa \rightarrow bb\mu\mu)$ at 95% CL, with no BDT selection applied, as a function of the signal mass hypothesis. The dash-dotted blue line indicates the expected limit set in the analysis with the BDT selection. Black and red dots show masses for which the hypothesis testing was done. Between these points, the limits are interpolated and may not be fully representative of the actual sensitivity.

SRincl, but omitting the final selection on the BDT discriminants. The expected limits obtained when employing the baseline analysis strategy are also shown in Fig. 11 for comparison, illustrating the significant improvement in sensitivity to pseudoscalars when using the BDTs. The excess observed at $m_{\mu\mu} = 52$ GeV in the BDT analysis is not supported by the limits derived without the BDTs.

Figure 12 shows the data and the estimated backgrounds in all final SR bins, without applying the BDT selection.

VIII. CONCLUSION

A search for light pseudoscalar particles (denoted by a) in the decays of the 125 GeV Higgs boson in the final state with two muons and two b -tagged jets, $H \rightarrow aa \rightarrow bb\mu\mu$, is presented. The analysis is performed using 139 fb^{-1} of $\sqrt{s} = 13$ TeV pp collision data recorded by the ATLAS detector at the LHC between 2015 and 2018. A narrow resonance is searched for in the dimuon invariant mass spectrum in the range $16 \leq m_{\mu\mu} \leq 62$ GeV. BDT classifiers are trained to distinguish the $H \rightarrow aa$ signal, where a is a pseudoscalar, from the SM backgrounds. Additionally, the result without selection on the BDT discriminants is also provided to ensure sensitivity to models where the a -particle is not necessarily a pseudoscalar, as well as to facilitate reinterpretations of the analysis. No significant excess of the data above the SM backgrounds is observed. In the BDT analysis, the lowest local p_0 -value of 0.00054 is observed at $m_{\mu\mu} = 52$ GeV and corresponds to a local significance of 3.3σ . The global significance of that excess is determined to be 1.7σ . Upper limits at 95% CL including (excluding) the BDT selection criteria are set on $\mathcal{B}(H \rightarrow aa \rightarrow bb\mu\mu)$ and range between 0.2×10^{-4} and 4.0×10^{-4} (0.5×10^{-4} and 5.0×10^{-4}), depending on m_a . The result including the BDT selection criteria improves upon previous ATLAS and CMS limits by about a factor of 2–5 for $m_a > 20$ GeV, while both results (with and without the BDT) extend the search down to m_a values of 16 GeV.

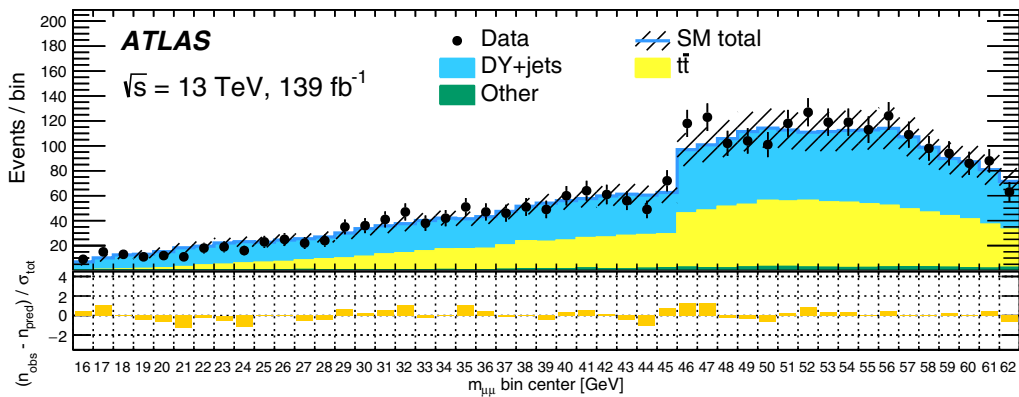


FIG. 12. Postbackground-validation-fit number of events in all SR bins (without applying the BDT selection) that are tested for the presence of signal. The bin widths are 2 GeV (3 GeV) in $m_{\mu\mu}$ for $m_a \leq 45$ GeV ($m_a > 45$ GeV). Neighboring bins partially overlap, hence they are not statistically independent. The bottom panel shows the pull in each bin, defined as $(n_{\text{obs}} - n_{\text{pred}}) / \sigma_{\text{tot}}$, where n_{obs} is the number of events in the data, n_{pred} is the number of fitted background events, and σ_{tot} is the total (systematic and statistical, added in quadrature) uncertainty in the fitted background yield. The discontinuity at $m_a = 45$ GeV appears where the $m_{\mu\mu}$ window size is changed. The histogram labeled as “Other” in the legend includes the contributions from the diboson, single-top-quark, $t\bar{t} + V$, and $W + \text{jets}$ backgrounds.

ACKNOWLEDGMENTS

We thank CERN for the very successful operation of the LHC, as well as the support staff from our institutions without whom ATLAS could not be operated efficiently. We acknowledge the support of ANPCyT, Argentina; YerPhI, Armenia; ARC, Australia; BMWFW and FWF, Austria; ANAS, Azerbaijan; SSTC, Belarus; CNPq and FAPESP, Brazil; NSERC, NRC and CFI, Canada; CERN; ANID, Chile; CAS, MOST and NSFC, China; Minciencias, Colombia; MSMT CR, MPO CR and VSC CR, Czech Republic; DNRF and DNSRC, Denmark; IN2P3-CNRS and CEA-DRF/IRFU, France; SRNSFG, Georgia; BMBF, HGF and MPG, Germany; GSRI, Greece; RGC and Hong Kong SAR, China; ISF and Benozio Center, Israel; INFN, Italy; MEXT and JSPS, Japan; CNRST, Morocco; NWO, Netherlands; RCN, Norway; MEiN, Poland; FCT, Portugal; MNE/IFA, Romania; JINR; MES of Russia and NRC KI, Russian Federation; MESTD, Serbia; MSSR, Slovakia; ARRS and MIZŠ, Slovenia; DSI/NRF, South Africa; MICINN, Spain; SRC and Wallenberg Foundation, Sweden; SERI, SNSF and Cantons of Bern and Geneva, Switzerland; MOST, Taiwan; TAEK, Turkey; STFC, United Kingdom; DOE and NSF, United States of America. In addition, individual

groups and members have received support from BCKDF, CANARIE, Compute Canada and CRC, Canada; COST, ERC, ERDF, Horizon 2020 and Marie Skłodowska-Curie Actions, European Union; Investissements d’Avenir Labex, Investissements d’Avenir Idex and ANR, France; DFG and AvH Foundation, Germany; Herakleitos, Thales and Aristeia programmes co-financed by EU-ESF and the Greek NSRF, Greece; BSF-NSF and GIF, Israel; Norwegian Financial Mechanism 2014–2021, Norway; NCN and NAWA, Poland; La Caixa Banking Foundation, CERCA Programme Generalitat de Catalunya and PROMETEO and GenT Programmes Generalitat Valenciana, Spain; Göran Gustafssons Stiftelse, Sweden; The Royal Society and Leverhulme Trust, United Kingdom. The crucial computing support from all WLCG partners is acknowledged gratefully, in particular from CERN, the ATLAS Tier-1 facilities at TRIUMF (Canada), NDGF (Denmark, Norway, Sweden), CC-IN2P3 (France), KIT/GridKA (Germany), INFN-CNAF (Italy), NL-T1 (Netherlands), PIC (Spain), ASGC (Taiwan), RAL (UK) and BNL (USA), the Tier-2 facilities worldwide and large non-WLCG resource providers. Major contributors of computing resources are listed in Ref. [114].

-
- [1] ATLAS Collaboration, Observation of a new particle in the search for the Standard Model Higgs boson with the ATLAS detector at the LHC, *Phys. Lett. B* **716**, 1 (2012).
 - [2] CMS Collaboration, Observation of a new boson at a mass of 125 GeV with the CMS experiment at the LHC, *Phys. Lett. B* **716**, 30 (2012).
 - [3] B. A. Dobrescu and K. T. Matchev, Light axion within the next-to-minimal supersymmetric standard model, *J. High Energy Phys.* **09** (2000) 031.
 - [4] U. Ellwanger, J. F. Gunion, C. Hugonie, and S. Moretti, Towards a no-lose theorem for NMSSM Higgs discovery at the LHC, [arXiv:hep-ph/0305109](https://arxiv.org/abs/hep-ph/0305109).
 - [5] R. Dermisek and J. F. Gunion, Escaping the Large Fine Tuning and Little Hierarchy Problems in the Next to Minimal Supersymmetric Model and $h \rightarrow aa$ Decays, *Phys. Rev. Lett.* **95**, 041801 (2005).
 - [6] S. Chang, R. Dermisek, J. F. Gunion, and N. Weiner, Nonstandard Higgs boson decays, *Annu. Rev. Nucl. Part. Sci.* **58**, 75 (2008).
 - [7] D. E. Morrissey and A. Pierce, Modified Higgs boson phenomenology from gauge or gaugino mediation in the next-to-minimal supersymmetric standard model, *Phys. Rev. D* **78**, 075029 (2008).
 - [8] G. Belanger, B. Dumont, U. Ellwanger, J. F. Gunion, and S. Kraml, Status of invisible Higgs decays, *Phys. Lett. B* **723**, 340 (2013).
 - [9] S. Profumo, M. J. Ramsey-Musolf, and G. Shaughnessy, Singlet Higgs phenomenology and the electroweak phase transition, *J. High Energy Phys.* **08** (2007) 010.
 - [10] N. Blinov, J. Kozaczuk, D. E. Morrissey, and C. Tamarit, Electroweak baryogenesis from exotic electroweak symmetry breaking, *Phys. Rev. D* **92**, 035012 (2015).
 - [11] N. Craig, A. Katz, M. Strassler, and R. Sundrum, Naturalness in the dark at the LHC, *J. High Energy Phys.* **07** (2015) 105.
 - [12] D. Curtin and C. B. Verhaaren, Discovering uncolored naturalness in exotic Higgs decays, *J. High Energy Phys.* **12** (2015) 072.
 - [13] V. Silveira and A. Zee, Scalar phantoms, *Phys. Lett.* **161B**, 136 (1985).
 - [14] M. Pospelov, A. Ritz, and M. B. Voloshin, Secluded WIMP dark matter, *Phys. Lett. B* **662**, 53 (2008).
 - [15] P. Draper, T. Liu, C. E. M. Wagner, L.-T. Wang, and H. Zhang, Dark Light-Higgs Bosons, *Phys. Rev. Lett.* **106**, 121805 (2011).
 - [16] S. Ipek, D. McKeen, and A. E. Nelson, Renormalizable model for the galactic center gamma-ray excess from dark matter annihilation, *Phys. Rev. D* **90**, 055021 (2014).
 - [17] A. Martin, J. Shelton, and J. Unwin, Fitting the galactic center gamma-ray excess with cascade annihilations, *Phys. Rev. D* **90**, 103513 (2014).

- [18] C. Boehm, M. J. Dolan, C. McCabe, M. Spannowsky, and C. J. Wallace, Extended gamma-ray emission from coy dark matter, *J. Cosmol. Astropart. Phys.* **05** (2014) 009.
- [19] K. C. Yang, Hidden Higgs portal vector dark matter for the Galactic center gamma-ray excess from the two-step cascade annihilation, and muon $g-2$, *J. High Energy Phys.* **08** (2018) 99.
- [20] D. Curtin *et al.*, Exotic decays of the 125 GeV Higgs boson, *Phys. Rev. D* **90**, 075004 (2014).
- [21] T. Robens and T. Stefaniak, Status of the Higgs singlet extension of the standard model after LHC run 1, *Eur. Phys. J. C* **75**, 104 (2015).
- [22] T. Robens and T. Stefaniak, LHC benchmark scenarios for the real Higgs singlet extension of the standard model, *Eur. Phys. J. C* **76**, 268 (2016).
- [23] T. S. Robens and J. T. Wittbrodt, Two-real-scalar-singlet extension of the SM: LHC phenomenology and benchmark scenarios, *Eur. Phys. J. C* **80**, 151 (2020).
- [24] M. Bauer, M. Neubert, and A. Thamm, Collider probes of axion-like particles, *J. High Energy Phys.* **12** (2017) 044.
- [25] J. Liu, C. E. M. Wagner, and X.-P. Wang, A light complex scalar for the electron and muon anomalous magnetic moments, *J. High Energy Phys.* **03** (2019) 008.
- [26] B. Abi *et al.* (Muon $g-2$ Collaboration), Measurement of the Positive Muon Anomalous Magnetic Moment to 0.46 ppm, *Phys. Rev. Lett.* **126**, 141801 (2021).
- [27] ATLAS Collaboration, Combined measurements of Higgs boson production and decay using up to 80 fb⁻¹ of proton-proton collision data at $\sqrt{s} = 13$ TeV collected with the ATLAS experiment, *Phys. Rev. D* **101**, 012002 (2020).
- [28] CMS Collaboration, Combined measurements of Higgs boson couplings in proton-proton collisions at $\sqrt{s} = 13$ TeV, *Eur. Phys. J. C* **79**, 421 (2019).
- [29] L. Evans and P. Bryant, LHC machine, *J. Instrum.* **3**, S08001 (2008).
- [30] G. Branco, P. M. Ferreira, L. Lavoura, M. N. Rebelo, M. Sher, and J. P. Silva, Theory and phenomenology of two-Higgs-doublet models, *Phys. Rep.* **516**, 1 (2012).
- [31] D. Curtin, R. Essig, and Y. M. Zhong, Uncovering light scalars with exotic Higgs decays to $b\bar{b}\mu^+\mu^-$, *J. High Energy Phys.* **06** (2015) 025.
- [32] CMS Collaboration, A search for pair production of new light bosons decaying into muons in proton-proton collisions at 13 TeV, *Phys. Lett. B* **796**, 131 (2019).
- [33] ATLAS Collaboration, Search for Higgs boson decays to beyond-the-Standard-Model light bosons in four-lepton events with the ATLAS detector at $\sqrt{s} = 13$ TeV, *J. High Energy Phys.* **06** (2018) 166.
- [34] CMS Collaboration, Search for a light pseudoscalar Higgs boson in the boosted $\mu\mu\tau\tau$ final state in proton-proton collisions at $\sqrt{s} = 13$ TeV, *J. High Energy Phys.* **08** (2020) 139.
- [35] CMS Collaboration, Search for light pseudoscalar boson pairs produced from decays of the 125 GeV Higgs boson in final states with two muons and two nearby tracks in p p collisions at $\sqrt{s} = 13$ TeV, *Phys. Lett. B* **800**, 135087 (2020).
- [36] CMS Collaboration, Search for an exotic decay of the Higgs boson to a pair of light pseudoscalars in the final state of two muons and two τ leptons in proton-proton collisions at $\sqrt{s} = 13$ TeV, *J. High Energy Phys.* **11** (2018) 018.
- [37] CMS Collaboration, Search for light bosons in decays of the 125 GeV Higgs boson in proton-proton collisions at $\sqrt{s} = 8$ TeV, *J. High Energy Phys.* **10** (2017) 076.
- [38] ATLAS Collaboration, Search for Higgs bosons decaying to aa in the $\mu\mu\tau\tau$ final state in p p collisions at $\sqrt{s} = 8$ TeV with the ATLAS experiment, *Phys. Rev. D* **92**, 052002 (2015).
- [39] CMS Collaboration, Search for an exotic decay of the Higgs boson to a pair of light pseudoscalars in the final state with two b quarks and two τ leptons in proton-proton collisions at $\sqrt{s} = 13$ TeV, *Phys. Lett. B* **785**, 462 (2018).
- [40] ATLAS Collaboration, Search for the Higgs boson produced in association with a vector boson and decaying into two spin-zero particles in the $H \rightarrow aa \rightarrow 4b$ channel in p p collisions at $\sqrt{s} = 13$ TeV with the ATLAS detector, *J. High Energy Phys.* **10** (2018) 031.
- [41] ATLAS Collaboration, Search for Higgs boson decays into two new low-mass spin-0 particles in the 4b channel with the ATLAS detector using p p collisions at $\sqrt{s} = 13$ TeV, *Phys. Rev. D* **102**, 112006 (2020).
- [42] ATLAS Collaboration, Search for new phenomena in events with at least three photons collected in p p collisions at $\sqrt{s} = 8$ TeV with the ATLAS detector, *Eur. Phys. J. C* **76**, 210 (2016).
- [43] ATLAS Collaboration, Search for Higgs boson decays into pairs of light (pseudo)scalar particles in the $\gamma\gamma jj$ final state in p p collisions at $\sqrt{s} = 13$ TeV with the ATLAS detector, *Phys. Lett. B* **782**, 750 (2018).
- [44] A. M. Sirunyan *et al.*, Search for resonances in the mass spectrum of muon pairs produced in association with b quark jets in proton-proton collisions at $\sqrt{s} = 8$ and 13 TeV, *J. High Energy Phys.* **11** (2018) 161.
- [45] R. Aaij *et al.*, Searches for low-mass dimuon resonances, *J. High Energy Phys.* **10** (2020) 156.
- [46] CMS Collaboration, Search for an exotic decay of the Higgs boson to a pair of light pseudoscalars in the final state with two muons and two b quarks in p p collisions at 13 TeV, *Phys. Lett. B* **795**, 398 (2019).
- [47] ATLAS Collaboration, Search for Higgs boson decays into a pair of light bosons in the $b\bar{b}\mu\mu$ final state in pp collision at $\sqrt{s} = 13$ TeV with the ATLAS detector, *Phys. Lett. B* **790**, 1 (2019).
- [48] ATLAS Collaboration, The ATLAS experiment at the CERN large hadron collider, *J. Instrum.* **3**, S08003 (2008).
- [49] B. Abbott *et al.*, Production and integration of the ATLAS insertable B-layer, *J. Instrum.* **13**, T05008 (2018).
- [50] ATLAS Collaboration, Performance of the ATLAS trigger system in 2015, *Eur. Phys. J. C* **77**, 317 (2017).
- [51] ATLAS Collaboration, ATLAS computing acknowledgements, Report No. ATL-SOFT-PUB-2020-001, <https://cds.cern.ch/record/2717821>.
- [52] ATLAS Collaboration, Performance of the ATLAS muon triggers in Run 2, *J. Instrum.* **15**, P09015 (2020).
- [53] T. Gleisberg, S. Höche, F. Krauss, M. Schönherr, S. Schumann, F. Siegert, and J. Winter, Event generation with SHERPA 1.1, *J. High Energy Phys.* **02** (2009) 007.
- [54] E. Bothmann *et al.*, Event generation with Sherpa 2.2, *SciPost Phys.* **7**, 034 (2019).

- [55] S. Schumann and F. Krauss, A parton shower algorithm based on Catani–Seymour dipole factorisation, *J. High Energy Phys.* **03** (2008) 038.
- [56] S. Höche, F. Krauss, M. Schönherr, and F. Siegert, A critical appraisal of NLO + PS matching methods, *J. High Energy Phys.* **09** (2012) 049.
- [57] S. Höche, F. Krauss, M. Schönherr, and F. Siegert, QCD matrix elements + parton showers. The NLO case, *J. High Energy Phys.* **04** (2013) 027.
- [58] S. Catani, F. Krauss, R. Kuhn, and B.R. Webber, QCD matrix elements + parton showers, *J. High Energy Phys.* **11** (2001) 063.
- [59] S. Höche, F. Krauss, S. Schumann, and F. Siegert, QCD matrix elements and truncated showers, *J. High Energy Phys.* **05** (2009) 053.
- [60] R. D. Ball *et al.*, Parton distributions for the LHC run II, *J. High Energy Phys.* **04** (2015) 040.
- [61] S. Frixione, P. Nason, and C. Oleari, Matching NLO QCD computations with parton shower simulations: The POWHEG method, *J. High Energy Phys.* **11** (2007) 070.
- [62] P. Nason, A new method for combining NLO QCD with shower Monte Carlo algorithms, *J. High Energy Phys.* **11** (2004) 040.
- [63] S. Alioli, P. Nason, C. Oleari, and E. Re, A general framework for implementing NLO calculations in shower Monte Carlo programs: The POWHEG BOX, *J. High Energy Phys.* **06** (2010) 043.
- [64] S. Frixione, P. Nason, and G. Ridolfi, A positive-weight next-to-leading-order Monte Carlo for heavy flavour hadroproduction, *J. High Energy Phys.* **09** (2007) 126.
- [65] E. Re, Single-top Wt-channel production matched with parton showers using the POWHEG method, *Eur. Phys. J. C* **71**, 1547 (2011).
- [66] T. Sjöstrand, S. Ask, J.R. Christiansen, R. Corke, N. Desai, P. Ilten, S. Mrenna, S. Prestel, C. O. Rasmussen, and P.Z. Skands, An introduction to PYTHIA 8.2, *Comput. Phys. Commun.* **191**, 159 (2015).
- [67] ATLAS Collaboration, ATLAS Pythia8 tunes to 7 TeV data, Report No. ATL-PHYS-PUB-2014-021, 2014, <https://cds.cern.ch/record/1966419/>.
- [68] R. D. Ball *et al.*, Parton distributions with LHC data, *Nucl. Phys.* **B867**, 244 (2013).
- [69] J. Alwall, R. Frederix, S. Frixione, V. Hirschi, F. Maltoni, O. Mattelaer, H.-S. Shao, T. Stelzer, P. Torrielli, and M. Zaro, The automated computation of tree-level and next-to-leading order differential cross sections, and their matching to parton shower simulations, *J. High Energy Phys.* **07** (2014) 079.
- [70] D. J. Lange, The EvtGen particle decay simulation package, *Nucl. Instrum. Methods Phys. Res., Sect. A* **462**, 152 (2001).
- [71] K. Hamilton, P. Nason, and G. Zanderighi, MINLO: Multi-scale improved NLO, *J. High Energy Phys.* **10** (2012) 155.
- [72] K. Hamilton, P. Nason, and G. Zanderighi, Finite quark-mass effects in the NNLOPS POWHEG + MinLO Higgs generator, *J. High Energy Phys.* **05** (2015) 140.
- [73] J.M. Campbell, R.K. Ellis, R. Frederix, P. Nason, C. Oleari, and C. Williams, NLO Higgs boson production plus one and two jets using the POWHEG BOX, MadGraph4 and MCFM, *J. High Energy Phys.* **07** (2012) 092.
- [74] K. Hamilton, P. Nason, C. Oleari, and G. Zanderighi, Merging $H/W/Z + 0$ and 1 jet at NLO with no merging scale: A path to parton shower + NNLO matching, *J. High Energy Phys.* **05** (2013) 082.
- [75] P. Nason and C. Oleari, NLO Higgs boson production via vector-boson fusion matched with shower in POWHEG, *J. High Energy Phys.* **02** (2010) 037.
- [76] ATLAS Collaboration, Measurement of the Z/γ^* boson transverse momentum distribution in p p collisions at $\sqrt{s} = 7$ TeV with the ATLAS detector, *J. High Energy Phys.* **09** (2014) 145.
- [77] *Handbook of LHC Higgs Cross Sections: 4. Deciphering the Nature of the Higgs Sector*, edited by D. de Florian *et al.* (CERN, Geneva, 2017).
- [78] C. Anastasiou, C. Duhr, F. Dulat, F. Herzog, and B. Mistlberger, Higgs Boson Gluon-Fusion Production in QCD at Three Loops, *Phys. Rev. Lett.* **114**, 212001 (2015).
- [79] C. Anastasiou, C. Duhr, F. Dulat, E. Furlan, T. Gehrmann, F. Herzog, A. Lazopoulos, and B. Mistlberger, High precision determination of the gluon fusion Higgs boson cross section at the LHC, *J. High Energy Phys.* **05** (2016) 058.
- [80] S. Actis, G. Passarino, C. Sturm, and S. Uccirati, NLO electroweak corrections to Higgs boson production at hadron colliders, *Phys. Lett. B* **670**, 12 (2008).
- [81] C. Anastasiou, R. Boughezal, and F. Petriello, Mixed QCD-electroweak corrections to Higgs boson production in gluon fusion, *J. High Energy Phys.* **04** (2009) 003.
- [82] J.R. Andersen *et al.*, *Handbook of LHC Higgs Cross Sections: 3. Higgs Properties*, edited by S. Heinemeyer, C. Mariotti, G. Passarino, and R. Tanaka (CERN, Geneva, 2013).
- [83] M. Ciccolini, A. Denner, and S. Dittmaier, Strong and Electroweak Corrections to the Production of a Higgs Boson + 2Jets via Weak Interactions at the Large Hadron Collider, *Phys. Rev. Lett.* **99**, 161803 (2007).
- [84] M. Ciccolini, A. Denner, and S. Dittmaier, Electroweak and QCD corrections to Higgs production via vector-boson fusion at the CERN LHC, *Phys. Rev. D* **77**, 013002 (2008).
- [85] P. Bolzoni, F. Maltoni, S.-O. Moch, and M. Zaro, Higgs Boson Production via Vector-Boson Fusion at Next-to-Next-to-Leading Order in QCD, *Phys. Rev. Lett.* **105**, 011801 (2010).
- [86] ATLAS Collaboration, Jet reconstruction and performance using particle flow with the ATLAS detector, *Eur. Phys. J. C* **77**, 466 (2017).
- [87] T. Sjöstrand, S. Mrenna, and P. Skands, A brief introduction to PYTHIA 8.1, *Comput. Phys. Commun.* **178**, 852 (2008).
- [88] ATLAS Collaboration, The ATLAS Simulation Infrastructure, *Eur. Phys. J. C* **70**, 823 (2010).
- [89] S. Agostinelli *et al.*, Geant4—a simulation toolkit, *Nucl. Instrum. Methods Phys. Res., Sect. A* **506**, 250 (2003).
- [90] ATLAS Collaboration, Muon reconstruction and identification efficiency in ATLAS using the full Run 2 p p collision data set at $\sqrt{s} = 13$ TeV, *Eur. Phys. J. C* **81**, 578 (2020).
- [91] M. Cacciari, G.P. Salam, and G. Soyez, The anti- k_t jet clustering algorithm, *J. High Energy Phys.* **04** (2008) 063.
- [92] M. Cacciari, G.P. Salam, and G. Soyez, FastJet user manual, *Eur. Phys. J. C* **72**, 1896 (2012).

- [93] ATLAS Collaboration, Jet energy scale and resolution measured in proton-proton collisions at $\sqrt{s} = 13$ TeV with the ATLAS detector, *Eur. Phys. J. C* **81**, 689 (2021).
- [94] ATLAS Collaboration, Tagging and suppression of pileup jets with the ATLAS detector, Technical Report No. ATLAS-CONF-2014-018, CERN, 2014, <https://cds.cern.ch/record/1700870>.
- [95] ATLAS Collaboration, ATLAS b-jet identification performance and efficiency measurement with $t\bar{t}$ events in p p collisions at $\sqrt{s} = 13$ TeV, *Eur. Phys. J. C* **79**, 970 (2019).
- [96] ATLAS Collaboration, Performance of missing transverse momentum reconstruction with the ATLAS detector using proton-proton collisions at $\sqrt{s} = 13$ TeV, *Eur. Phys. J. C* **78**, 903 (2018).
- [97] ATLAS Collaboration, E_T^{miss} performance in the ATLAS detector using 2015–2016 LHC p p collisions, Report No. ATLAS-CONF-2018-023, 2018, <https://cds.cern.ch/record/2625233>.
- [98] J. Erdmann, S. Guindon, K. Kröninger, B. Lemmer, O. Nackenhorst, A. Quadt, and P. Stolte, A likelihood-based reconstruction algorithm for top-quark pairs and the KLFFitter framework, *Nucl. Instrum. Methods Phys. Res., Sect. A* **748**, 18 (2014).
- [99] P. Speckmayer, A. Hocker, J. Stelzer, and H. Voss, The toolkit for multivariate data analysis, TMVA 4, *J. Phys. Conf. Ser.* **219**, 032057 (2010).
- [100] ATLAS Collaboration, Jet energy scale measurements and their systematic uncertainties in proton-proton collisions at $\sqrt{s} = 13$ TeV with the ATLAS detector, *Phys. Rev. D* **96**, 072002 (2017).
- [101] ATLAS Collaboration, Luminosity determination in p p collisions at $\sqrt{s} = 13$ TeV using the ATLAS detector at the LHC, Report No. ATLAS-CONF-2019-021, 2019, <https://cds.cern.ch/record/2677054>.
- [102] G. Avoni *et al.*, The new LUCID-2 detector for luminosity measurement and monitoring in ATLAS, *J. Instrum.* **13**, P07017 (2018).
- [103] ATLAS Collaboration, Muon reconstruction performance of the ATLAS detector in proton-proton collision data at $\sqrt{s} = 13$ TeV, *Eur. Phys. J. C* **76**, 292 (2016).
- [104] M. Bähr *et al.*, Herwig++ physics and manual, *Eur. Phys. J. C* **58**, 639 (2008).
- [105] J. Bellm *et al.*, Herwig 7.0/Herwig++ 3.0 release note, *Eur. Phys. J. C* **76**, 196 (2016).
- [106] J. Butterworth *et al.*, PDF4LHC recommendations for LHC Run II, *J. Phys. G* **43**, 023001 (2016).
- [107] L. Harland-Lang, A. Martin, P. Motylinski, and R. Thorne, Parton distributions in the LHC era: MMHT 2014 PDFs, *Eur. Phys. J. C* **75**, 204 (2015).
- [108] S. Dulat, T.-J. Hou, J. Gao, M. Guzzi, J. Huston, P. Nadolsky, J. Pumplin, C. Schmidt, D. Stump, and C.-P. Yuan, New parton distribution functions from a global analysis of quantum chromodynamics, *Phys. Rev. D* **93**, 033006 (2016).
- [109] G. Cowan, K. Cranmer, E. Gross, and O. Vitells, Asymptotic formulae for likelihood-based tests of new physics, *Eur. Phys. J. C* **71**, 1554 (2011).
- [110] M. Baak, G. J. Besjes, D. Côté, A. Koutsman, J. Lorenz, and D. Short, HistFitter software framework for statistical data analysis, *Eur. Phys. J. C* **75**, 153 (2015).
- [111] E. Gross and O. Vitells, Trial factors for the look elsewhere effect in high energy physics, *Eur. Phys. J. C* **70**, 525 (2010).
- [112] A. L. Read, Presentation of search results: The CL_S technique, *J. Phys. G* **28**, 2693 (2002).
- [113] T. Junk, Confidence level computation for combining searches with small statistics, *Nucl. Instrum. Methods Phys. Res., Sect. A* **434**, 435 (1999).
- [114] ATLAS Collaboration, ATLAS Computing Acknowledgements, Report No. ATL-SOFT-PUB-2021-003, 2021, <https://cds.cern.ch/record/2776662>.

G. Aad,⁹⁸ B. Abbott,¹²³ D. C. Abbott,⁹⁹ A. Abed Abud,³⁴ K. Abeling,⁵¹ D. K. Abhayasinghe,⁹¹ S. H. Abidi,²⁷ A. Aboulhorma,^{33e} H. Abramowicz,¹⁵⁶ H. Abreu,¹⁵⁵ Y. Abulaiti,⁵ A. C. Abusleme Hoffman,^{141a} B. S. Acharya,^{64a,64b,b} B. Achkar,⁵¹ L. Adam,⁹⁶ C. Adam Bourdarios,⁴ L. Adamczyk,^{81a} L. Adamek,¹⁶¹ S. V. Addepalli,²⁴ J. Adelman,¹¹⁶ A. Adiguzel,^{11c,c} S. Adorni,⁵² T. Adye,¹³⁸ A. A. Affolder,¹⁴⁰ Y. Afik,³⁴ C. Agapopoulou,⁶² M. N. Agaras,¹² J. Agarwala,^{68a,68b} A. Aggarwal,¹¹⁴ C. Agheorghiesei,^{25c} J. A. Aguilar-Saavedra,^{134f,134a,d} A. Ahmad,³⁴ F. Ahmadov,⁷⁷ W. S. Ahmed,¹⁰⁰ X. Ai,⁴⁴ G. Aielli,^{71a,71b} I. Aizenberg,¹⁷⁴ S. Akatsuka,⁸³ M. Akbiyik,⁹⁶ T. P. A. Åkesson,⁹⁴ A. V. Akimov,¹⁰⁷ K. Al Khoury,³⁷ G. L. Alberghi,^{21b} J. Albert,¹⁷⁰ P. Albicocco,⁴⁹ M. J. Alconada Verzini,⁸⁶ S. Alderweireldt,⁴⁸ M. Aleksa,³⁴ I. N. Aleksandrov,⁷⁷ C. Alexa,^{25b} T. Alexopoulos,⁹ A. Alfonsi,¹¹⁵ F. Alfonsi,^{21b} M. Alhroob,¹²³ B. Ali,¹³⁶ S. Ali,¹⁵³ M. Aliev,¹⁶⁰ G. Alimonti,^{66a} C. Allaire,³⁴ B. M. M. Allbrooke,¹⁵¹ P. P. Allport,¹⁹ A. Aloisio,^{67a,67b} F. Alonso,⁸⁶ C. Alpigiani,¹⁴³ E. Alunno Camelia,^{71a,71b} M. Alvarez Estevez,⁹⁵ M. G. Alviggi,^{67a,67b} Y. Amaral Coutinho,^{78b} A. Ambler,¹⁰⁰ L. Ambroz,¹²⁹ C. Amelung,³⁴ D. Amidei,¹⁰² S. P. Amor Dos Santos,^{134a} S. Amoroso,⁴⁴ C. S. Amrouche,⁵² V. Ananiev,¹²⁸ C. Anastopoulos,¹⁴⁴ N. Andari,¹³⁹ T. Andeen,¹⁰ J. K. Anders,¹⁸ S. Y. Andreatan,^{43a,43b} A. Andreatza,^{66a,66b} S. Angelidakis,⁸ A. Angerami,³⁷ A. V. Anisenkov,^{117b,117a} A. Annovi,^{69a} C. Antel,⁵² M. T. Anthony,¹⁴⁴ E. Antipov,¹²⁴ M. Antonelli,⁴⁹ D. J. A. Antrim,¹⁶ F. Anulli,^{70a} M. Aoki,⁷⁹ J. A. Aparisi Pozo,¹⁶⁸ M. A. Aparo,¹⁵¹ L. Aperio Bella,⁴⁴ N. Aranzabal,³⁴ V. Araujo Ferraz,^{78a} C. Arcangeletti,⁴⁹ A. T. H. Arce,⁴⁷ E. Arena,⁸⁸ J.-F. Arguin,¹⁰⁶ S. Argyropoulos,⁵⁰ J.-H. Arling,⁴⁴ A. J. Armbruster,³⁴ A. Armstrong,¹⁶⁵ O. Arnaez,¹⁶¹ H. Arnold,³⁴ Z. P. Arrubarrena Tame,¹¹⁰ G. Artoni,¹²⁹ H. Asada,¹¹²

K. Asai,¹²¹ S. Asai,¹⁵⁸ N. A. Asbah,⁵⁷ E. M. Asimakopoulou,¹⁶⁶ L. Asquith,¹⁵¹ J. Assahsah,^{33d} K. Assamagan,²⁷
 R. Astalos,^{26a} R. J. Atkin,^{31a} M. Atkinson,¹⁶⁷ N. B. Atlay,¹⁷ H. Atmani,^{58b} P. A. Atmasiddha,¹⁰² K. Augsten,¹³⁶
 S. Auricchio,^{67a,67b} V. A. Austrup,¹⁷⁶ G. Avner,¹⁵⁵ G. Avolio,³⁴ M. K. Ayoub,^{13c} G. Azuelos,^{106,e} D. Babal,^{26a}
 H. Bachacou,¹³⁹ K. Bachas,¹⁵⁷ A. Bachiu,³² F. Backman,^{43a,43b} A. Badea,⁵⁷ P. Bagnaia,^{70a,70b} H. Bahrasemani,¹⁴⁷
 A. J. Bailey,¹⁶⁸ V. R. Bailey,¹⁶⁷ J. T. Baines,¹³⁸ C. Bakalis,⁹ O. K. Baker,¹⁷⁷ P. J. Bakker,¹¹⁵ E. Bakos,¹⁴ D. Bakshi Gupta,⁷
 S. Balaji,¹⁵² R. Balasubramanian,¹¹⁵ E. M. Baldin,^{117b,117a} P. Balek,¹³⁷ E. Ballabene,^{66a,66b} F. Balli,¹³⁹ W. K. Balunas,¹²⁹
 J. Balz,⁹⁶ E. Banas,⁸² M. Bandieramonte,¹³³ A. Bandyopadhyay,¹⁷ S. Bansal,²² L. Barak,¹⁵⁶ E. L. Barberio,¹⁰¹
 D. Barberis,^{53b,53a} M. Barbero,⁹⁸ G. Barbour,⁹² K. N. Barends,^{31a} T. Barillari,¹¹¹ M-S. Barisits,³⁴ J. Barkeloo,¹²⁶
 T. Barklow,¹⁴⁸ B. M. Barnett,¹³⁸ R. M. Barnett,¹⁶ A. Baroncelli,^{58a} G. Barone,²⁷ A. J. Barr,¹²⁹ L. Barranco Navarro,^{43a,43b}
 F. Barreiro,⁹⁵ J. Barreiro Guimarães da Costa,^{13a} U. Barron,¹⁵⁶ S. Barsov,¹³² F. Bartels,^{59a} R. Bartoldus,¹⁴⁸ G. Bartolini,⁹⁸
 A. E. Barton,⁸⁷ P. Bartos,^{26a} A. Basalaeu,⁴⁴ A. Basan,⁹⁶ M. Baselga,⁴⁴ I. Bashta,^{72a,72b} A. Bassalat,⁶² M. J. Basso,¹⁶¹
 C. R. Basson,⁹⁷ R. L. Bates,⁵⁵ S. Batlamous,^{33e} J. R. Batley,³⁰ B. Batool,¹⁴⁶ M. Battaglia,¹⁴⁰ M. Bauce,^{70a,70b} F. Bauer,^{139,a}
 P. Bauer,²² H. S. Bawa,²⁹ A. Bayirli,^{11c} J. B. Beacham,⁴⁷ T. Beau,¹³⁰ P. H. Beauchemin,¹⁶⁴ F. Becherer,⁵⁰ P. Bechtel,²²
 H. P. Beck,^{18,f} K. Becker,¹⁷² C. Becot,⁴⁴ A. J. Beddall,^{11a} V. A. Bednyakov,⁷⁷ C. P. Bee,¹⁵⁰ T. A. Beermann,³⁴ M. Begalli,^{78b}
 M. Begel,²⁷ A. Behera,¹⁵⁰ J. K. Behr,⁴⁴ C. Beirao Da Cruz E Silva,³⁴ J. F. Beirer,^{51,34} F. Beisiegel,²² M. Belfkir,⁴ G. Bella,¹⁵⁶
 L. Bellagamba,^{21b} A. Bellerive,³² P. Bellos,¹⁹ K. Beloborodov,^{117b,117a} K. Belotskiy,¹⁰⁸ N. L. Belyaev,¹⁰⁸ D. Benckekroun,^{33a}
 Y. Benhammou,¹⁵⁶ D. P. Benjamin,²⁷ M. Benoit,²⁷ J. R. Bensinger,²⁴ S. Bentvelsen,¹¹⁵ L. Beresford,³⁴ M. Beretta,⁴⁹
 D. Berge,¹⁷ E. Bergeas Kuutmann,¹⁶⁶ N. Berger,⁴ B. Bergmann,¹³⁶ L. J. Bergsten,²⁴ J. Beringer,¹⁶ S. Berlendis,⁶
 G. Bernardi,¹³⁰ C. Bernius,¹⁴⁸ F. U. Bernlochner,²² T. Berry,⁹¹ P. Berta,¹³⁷ A. Berthold,⁴⁶ I. A. Bertram,⁸⁷
 O. Bessidskaia Bylund,¹⁷⁶ S. Bethke,¹¹¹ A. Betti,⁴⁰ A. J. Bevan,⁹⁰ S. Bhatta,¹⁵⁰ D. S. Bhattacharya,¹⁷¹ P. Bhattacharai,²⁴
 V. S. Bhopatkar,⁵ R. Bi,¹³³ R. M. Bianchi,¹³³ O. Biebel,¹¹⁰ R. Bielski,¹²⁶ N. V. Biesuz,^{69a,69b} M. Biglietti,^{72a}
 T. R. V. Billoud,¹³⁶ M. Bindi,⁵¹ A. Bingul,^{11d} C. Bini,^{70a,70b} S. Biondi,^{21b,21a} A. Biondini,⁸⁸ C. J. Birch-sykes,⁹⁷
 G. A. Bird,^{19,138} M. Birman,¹⁷⁴ T. Bisanz,³⁴ J. P. Biswal,² D. Biswas,^{175,g} A. Bitadze,⁹⁷ C. Bittrich,⁴⁶ K. Björke,¹²⁸ I. Bloch,⁴⁴
 C. Blocker,²⁴ A. Blue,⁵⁵ U. Blumenschein,⁹⁰ J. Blumenthal,⁹⁶ G. J. Bobbink,¹¹⁵ V. S. Bobrovnikov,^{117b,117a} M. Boehler,⁵⁰
 D. Bogavac,¹² A. G. Bogdanchikov,^{117b,117a} C. Bohm,^{43a} V. Boisvert,⁹¹ P. Bokan,⁴⁴ T. Bold,^{81a} M. Bomben,¹³⁰ M. Bona,⁹⁰
 M. Boonekamp,¹³⁹ C. D. Booth,⁹¹ A. G. Borbély,⁵⁵ H. M. Borecka-Bielska,¹⁰⁶ L. S. Borgna,⁹² G. Borissov,⁸⁷
 D. Bortoletto,¹²⁹ D. Boscherini,^{21b} M. Bosman,¹² J. D. Bossio Sola,³⁴ K. Bouaouda,^{33a} J. Boudreau,¹³³
 E. V. Bouhova-Thacker,⁸⁷ D. Boumediene,³⁶ R. Bouquet,¹³⁰ A. Boveia,¹²² J. Boyd,³⁴ D. Boye,²⁷ I. R. Boyko,⁷⁷
 A. J. Bozson,⁹¹ J. Bracinik,¹⁹ N. Brahimy,^{58d,58c} G. Brandt,¹⁷⁶ O. Brandt,³⁰ F. Braren,⁴⁴ B. Brau,⁹⁹ J. E. Brau,¹²⁶
 W. D. Breaden Madden,⁵⁵ K. Brendlinger,⁴⁴ R. Brenner,¹⁷⁴ L. Brenner,³⁴ R. Brenner,¹⁶⁶ S. Bressler,¹⁷⁴ B. Brickwedde,⁹⁶
 D. L. Briglin,¹⁹ D. Britton,⁵⁵ D. Britzger,¹¹¹ I. Brock,²² R. Brock,¹⁰³ G. Brooijmans,³⁷ W. K. Brooks,^{141f} E. Brost,²⁷
 P. A. Bruckman de Renstrom,⁸² B. Brüers,⁴⁴ D. Bruncko,^{26b} A. Bruni,^{21b} G. Bruni,^{21b} M. Bruschi,^{21b} N. Brusino,^{70a,70b}
 L. Bryngemark,¹⁴⁸ T. Buanes,¹⁵ Q. Buat,¹⁵⁰ P. Buchholz,¹⁴⁶ A. G. Buckley,⁵⁵ I. A. Budagov,⁷⁷ M. K. Bugge,¹²⁸
 O. Bulekov,¹⁰⁸ B. A. Bullard,⁵⁷ S. Burdin,⁸⁸ C. D. Burgard,⁴⁴ A. M. Burger,¹²⁴ B. Burghgrave,⁷ J. T. P. Burr,⁴⁴
 C. D. Burton,¹⁰ J. C. Burzynski,⁹⁹ E. L. Busch,³⁷ V. Büscher,⁹⁶ P. J. Bussey,⁵⁵ J. M. Butler,²³ C. M. Buttar,⁵⁵
 J. M. Butterworth,⁹² W. Buttinger,¹³⁸ C. J. Buxo Vazquez,¹⁰³ A. R. Buzykaev,^{117b,117a} G. Cabras,^{21b} S. Cabrera Urbán,¹⁶⁸
 D. Caforio,⁵⁴ H. Cai,¹³³ V. M. M. Cairo,¹⁴⁸ O. Cakir,^{3a} N. Calace,³⁴ P. Calafiura,¹⁶ G. Calderini,¹³⁰ P. Calfayan,⁶³ G. Callea,⁵⁵
 L. P. Caloba,^{78b} S. Calvente Lopez,⁹⁵ D. Calvet,³⁶ S. Calvet,³⁶ T. P. Calvet,⁹⁸ M. Calvetti,^{69a,69b} R. Camacho Toro,¹³⁰
 S. Camarda,³⁴ D. Camarero Munoz,⁹⁵ P. Camarri,^{71a,71b} M. T. Camerlingo,^{72a,72b} D. Cameron,¹²⁸ C. Camincher,¹⁷⁰
 M. Campanelli,⁹² A. Camplani,³⁸ V. Canale,^{67a,67b} A. Canesse,¹⁰⁰ M. Cano Bret,⁷⁵ J. Cantero,¹²⁴ Y. Cao,¹⁶⁷ F. Capocasa,²⁴
 M. Capua,^{39b,39a} A. Carbone,^{66a,66b} R. Cardarelli,^{71a} J. C. J. Cardenas,⁷ F. Cardillo,¹⁶⁸ G. Carducci,^{39b,39a} T. Carli,³⁴
 G. Carlino,^{67a} B. T. Carlson,¹³³ E. M. Carlson,^{170,162a} L. Carminati,^{66a,66b} M. Carnesale,^{70a,70b} R. M. D. Carney,¹⁴⁸
 S. Caron,¹¹⁴ E. Carquin,^{141f} S. Carrá,⁴⁴ G. Carratta,^{21b,21a} J. W. S. Carter,¹⁶¹ T. M. Carter,⁴⁸ D. Casadei,^{31c} M. P. Casado,^{12,h}
 A. F. Casha,¹⁶¹ E. G. Castiglia,¹⁷⁷ F. L. Castillo,^{59a} L. Castillo Garcia,¹² V. Castillo Gimenez,¹⁶⁸ N. F. Castro,^{134a,134e}
 A. Catinaccio,³⁴ J. R. Catmore,¹²⁸ A. Cattai,³⁴ V. Cavaliere,²⁷ N. Cavalli,^{21b,21a} V. Cavasinni,^{69a,69b} E. Celebi,^{11b} F. Celli,¹²⁹
 M. S. Centonze,^{65a,65b} K. Cerny,¹²⁵ A. S. Cerqueira,^{78a} A. Cerri,¹⁵¹ L. Cerrito,^{71a,71b} F. Cerutti,¹⁶ A. Cervelli,^{21b} S. A. Cetin,^{11b}
 Z. Chadi,^{33a} D. Chakraborty,¹¹⁶ M. Chala,^{134f} J. Chan,¹⁷⁵ W. S. Chan,¹¹⁵ W. Y. Chan,⁸⁸ J. D. Chapman,³⁰
 B. Chargeishvili,^{154b} D. G. Charlton,¹⁹ T. P. Charman,⁹⁰ M. Chatterjee,¹⁸ S. Chekanov,⁵ S. V. Chekulaev,^{162a}
 G. A. Chelkov,^{77,i} A. Chen,¹⁰² B. Chen,¹⁵⁶ B. Chen,¹⁷⁰ C. Chen,^{58a} C. H. Chen,⁷⁶ H. Chen,^{13c} H. Chen,²⁷ J. Chen,^{58c}

J. Chen,²⁴ S. Chen,¹³¹ S. J. Chen,^{13c} X. Chen,^{58c} X. Chen,^{13b} Y. Chen,^{58a} Y-H. Chen,⁴⁴ C. L. Cheng,¹⁷⁵ H. C. Cheng,^{60a}
 A. Cheplakov,⁷⁷ E. Cheremushkina,⁴⁴ E. Cherepanova,⁷⁷ R. Cherkaoui El Moursli,^{33e} E. Cheu,⁶ K. Cheung,⁶¹
 L. Chevalier,¹³⁹ V. Chiarella,⁴⁹ G. Chiarelli,^{69a} G. Chiodini,^{65a} A. S. Chisholm,¹⁹ A. Chitan,^{25b} Y. H. Chiu,¹⁷⁰
 M. V. Chizhov,^{77j} K. Choi,¹⁰ A. R. Chomont,^{70a,70b} Y. Chou,⁹⁹ Y. S. Chow,¹¹⁵ T. Chowdhury,^{31g} L. D. Christopher,^{31g}
 M. C. Chu,^{60a} X. Chu,^{13a,13d} J. Chudoba,¹³⁵ J. J. Chwastowski,⁸² D. Cieri,¹¹¹ K. M. Ciesla,⁸² V. Cindro,⁸⁹ I. A. Cioară,^{25b}
 A. Ciocio,¹⁶ F. Ciroto,^{67a,67b} Z. H. Citron,^{174,k} M. Citterio,^{66a} D. A. Ciubotaru,^{25b} B. M. Ciungu,¹⁶¹ A. Clark,⁵² P. J. Clark,⁴⁸
 J. M. Clavijo Columbie,⁴⁴ S. E. Clawson,⁹⁷ C. Clement,^{43a,43b} L. Clissa,^{21b,21a} Y. Coadou,⁹⁸ M. Cobal,^{64a,64c} A. Coccaro,^{53b}
 J. Cochran,⁷⁶ R. F. Coelho Barrue,^{134a} R. Coelho Lopes De Sa,⁹⁹ S. Coelli,^{66a} H. Cohen,¹⁵⁶ A. E. C. Coimbra,³⁴ B. Cole,³⁷
 J. Collot,⁵⁶ P. Conde Muñio,^{134a,134h} S. H. Connell,^{31c} I. A. Connelly,⁵⁵ E. I. Conroy,¹²⁹ F. Conventi,^{67a,l} H. G. Cooke,¹⁹
 A. M. Cooper-Sarkar,¹²⁹ F. Cormier,¹⁶⁹ L. D. Corpe,³⁴ M. Corradi,^{70a,70b} E. E. Corrigan,⁹⁴ F. Corriveau,^{100,m} M. J. Costa,¹⁶⁸
 F. Costanza,⁴ D. Costanzo,¹⁴⁴ B. M. Cote,¹²² G. Cowan,⁹¹ J. W. Cowley,³⁰ K. Cranmer,¹²⁰ S. Crépe-Renaudin,⁵⁶
 F. Crescioli,¹³⁰ M. Cristinziani,¹⁴⁶ M. Cristoforetti,^{73a,73b,n} V. Croft,¹⁶⁴ G. Crosetti,^{39b,39a} A. Cueto,³⁴
 T. Cuhadar Donszelmann,¹⁶⁵ H. Cui,^{13a,13d} A. R. Cukierman,¹⁴⁸ W. R. Cunningham,⁵⁵ F. Curcio,^{39b,39a} P. Czodrowski,³⁴
 M. M. Czurylo,^{59b} M. J. Da Cunha Sargedas De Sousa,^{58a} J. V. Da Fonseca Pinto,^{78b} C. Da Via,⁹⁷ W. Dabrowski,^{81a}
 T. Dado,⁴⁵ S. Dahbi,^{31g} T. Dai,¹⁰² C. Dallapiccola,⁹⁹ M. Dam,³⁸ G. D'amen,²⁷ V. D'Amico,^{72a,72b} J. Damp,⁹⁶ J. R. Dandoy,¹³¹
 M. F. Daneri,²⁸ M. Danninger,¹⁴⁷ V. Dao,³⁴ G. Darbo,^{53b} S. Darmora,⁵ A. Dattagupta,¹²⁶ S. D'Auria,^{66a,66b} C. David,^{162b}
 T. Davidek,¹³⁷ D. R. Davis,⁴⁷ B. Davis-Purcell,³² I. Dawson,⁹⁰ K. De,⁷ R. De Asmundis,^{67a} M. De Beurs,¹¹⁵
 S. De Castro,^{21b,21a} N. De Groot,¹¹⁴ P. de Jong,¹¹⁵ H. De la Torre,¹⁰³ A. De Maria,^{13c} D. De Pedis,^{70a} A. De Salvo,^{70a}
 U. De Sanctis,^{71a,71b} M. De Santis,^{71a,71b} A. De Santo,¹⁵¹ J. B. De Vivie De Regie,⁵⁶ D. V. Dedovich,⁷⁷ J. Degens,¹¹⁵
 A. M. Deiana,⁴⁰ J. Del Peso,⁹⁵ Y. Delabat Diaz,⁴⁴ F. Deliot,¹³⁹ C. M. Delitzsch,⁶ M. Della Pietra,^{67a,67b} D. Della Volpe,⁵²
 A. Dell'Acqua,³⁴ L. Dell'Asta,^{66a,66b} M. Delmastro,⁴ P. A. Delsart,⁵⁶ S. Demers,¹⁷⁷ M. Demichev,⁷⁷ S. P. Denisov,¹¹⁸
 L. D'Eramo,¹¹⁶ D. Derendarz,⁸² J. E. Derkaoui,^{33d} F. Derue,¹³⁰ P. Dervan,⁸⁸ K. Desch,²² K. Dette,¹⁶¹ C. Deutsch,²²
 P. O. Deviveiros,³⁴ F. A. Di Bello,^{70a,70b} A. Di Ciaccio,^{71a,71b} L. Di Ciaccio,⁴ A. Di Domenico,^{70a,70b} C. Di Donato,^{67a,67b}
 A. Di Girolamo,³⁴ G. Di Gregorio,^{69a,69b} A. Di Luca,^{73a,73b} B. Di Micco,^{72a,72b} R. Di Nardo,^{72a,72b} C. Diaconu,⁹⁸ F. A. Dias,¹¹⁵
 T. Dias Do Vale,^{134a} M. A. Diaz,^{141a} F. G. Diaz Capriles,²² J. Dickinson,¹⁶ M. Didenko,¹⁶⁸ E. B. Diehl,¹⁰² J. Dietrich,¹⁷
 S. Díez Cornell,⁴⁴ C. Díez Pardos,¹⁴⁶ A. Dimitrievska,¹⁶ W. Ding,^{13b} J. Dingfelder,²² I-M. Dinu,^{25b} S. J. Dittmeier,^{59b}
 F. Dittus,³⁴ F. Djama,⁹⁸ T. Djobava,^{154b} J. I. Djuvsland,¹⁵ M. A. B. Do Vale,¹⁴² D. Dodsworth,²⁴ C. Doglioni,⁹⁴ J. Dolejsi,¹³⁷
 Z. Dolezal,¹³⁷ M. Donadelli,^{78c} B. Dong,^{58c} J. Donini,³⁶ A. D'onofrio,^{13c} M. D'Onofrio,⁸⁸ J. Dopke,¹³⁸ A. Doria,^{67a}
 M. T. Dova,⁸⁶ A. T. Doyle,⁵⁵ E. Drechsler,¹⁴⁷ E. Dreyer,¹⁴⁷ T. Dreyer,⁵¹ A. S. Drobac,¹⁶⁴ D. Du,^{58a} T. A. du Pree,¹¹⁵
 F. Dubinin,¹⁰⁷ M. Dubovsky,^{26a} A. Dubreuil,⁵² E. Duchovni,¹⁷⁴ G. Duckeck,¹¹⁰ O. A. Ducu,^{34,25b} D. Duda,¹¹¹ A. Dudarev,³⁴
 M. D'uffizi,⁹⁷ L. Dufлот,⁶² M. Dührssen,³⁴ C. Dülsen,¹⁷⁶ A. E. Dumitriu,^{25b} M. Dunford,^{59a} S. Dungs,⁴⁵ K. Dunne,^{43a,43b}
 A. Duperrin,⁹⁸ H. Duran Yildiz,^{3a} M. Düren,⁵⁴ A. Durglishvili,^{154b} B. Dutta,⁴⁴ G. I. Dyckes,¹⁶ M. Dyndal,^{81a} S. Dysch,⁹⁷
 B. S. Dziedzic,⁸² B. Eckerova,^{26a} M. G. Eggleston,⁴⁷ E. Egidio Purcino De Souza,^{78b} L. F. Ehrke,⁵² T. Eifert,⁷ G. Eigen,¹⁵
 K. Einsweiler,¹⁶ T. Ekelof,¹⁶⁶ Y. El Ghazali,^{33b} H. El Jarrari,^{33e} A. El Moussaouy,^{33a} V. Ellajosyula,¹⁶⁶ M. Ellert,¹⁶⁶
 F. Ellinghaus,¹⁷⁶ A. A. Elliot,⁹⁰ N. Ellis,³⁴ J. Elmsheuser,²⁷ M. Elsing,³⁴ D. Emeliyanov,¹³⁸ A. Emerman,³⁷ Y. Enari,¹⁵⁸
 J. Erdmann,⁴⁵ A. Ereditato,¹⁸ P. A. Erland,⁸² M. Errenst,¹⁷⁶ M. Escalier,⁶² C. Escobar,¹⁶⁸ O. Estrada Pastor,¹⁶⁸ E. Etzion,¹⁵⁶
 G. Evans,^{134a} H. Evans,⁶³ M. O. Evans,¹⁵¹ A. Ezhilov,¹³² F. Fabbri,⁵⁵ L. Fabbri,^{21b,21a} G. Facini,¹⁷² V. Fadeyev,¹⁴⁰
 R. M. Fakhruddinov,¹¹⁸ S. Falciano,^{70a} P. J. Falke,²² S. Falke,³⁴ J. Faltova,¹³⁷ Y. Fan,^{13a} Y. Fang,^{13a} Y. Fang,^{13a}
 G. Fanourakis,⁴² M. Fanti,^{66a,66b} M. Faraj,^{58c} A. Farbin,⁷ A. Farilla,^{72a} E. M. Farina,^{68a,68b} T. Farooque,¹⁰³ S. M. Farrington,⁴⁸
 P. Farthouat,³⁴ F. Fassi,^{33e} D. Fassouliotis,⁸ M. Fauci Giannelli,^{71a,71b} W. J. Fawcett,³⁰ L. Fayard,⁶² O. L. Fedin,^{132,o}
 M. Feickert,¹⁶⁷ L. Feligioni,⁹⁸ A. Fell,¹⁴⁴ C. Feng,^{58b} M. Feng,^{13b} M. J. Fenton,¹⁶⁵ A. B. Fenyuk,¹¹⁸ S. W. Ferguson,⁴¹
 J. Ferrando,⁴⁴ A. Ferrari,¹⁶⁶ P. Ferrari,¹¹⁵ R. Ferrari,^{68a} D. Ferrere,⁵² C. Ferretti,¹⁰² F. Fiedler,⁹⁶ A. Filipčič,⁸⁹ F. Filthaut,¹¹⁴
 M. C. N. Fiolhais,^{134a,134c,p} L. Fiorini,¹⁶⁸ F. Fischer,¹⁴⁶ W. C. Fisher,¹⁰³ T. Fitschen,¹⁹ I. Fleck,¹⁴⁶ P. Fleischmann,¹⁰²
 T. Flick,¹⁷⁶ B. M. Flierl,¹¹⁰ L. Flores,¹³¹ M. Flores,^{31g} L. R. Flores Castillo,^{60a} F. M. Follega,^{73a,73b} N. Fomin,¹⁵ J. H. Foo,¹⁶¹
 B. C. Forland,⁶³ A. Formica,¹³⁹ F. A. Förster,¹² A. C. Forti,⁹⁷ E. Fortin,⁹⁸ M. G. Foti,¹²⁹ L. Fountas,⁸ D. Fournier,⁶² H. Fox,⁸⁷
 P. Francavilla,^{69a,69b} S. Francescato,⁵⁷ M. Franchini,^{21b,21a} S. Franchino,^{59a} D. Francis,³⁴ L. Franco,⁴ L. Franconi,¹⁸
 M. Franklin,⁵⁷ G. Frattari,^{70a,70b} A. C. Freegard,⁹⁰ P. M. Freeman,¹⁹ W. S. Freund,^{78b} E. M. Freundlich,⁴⁵ D. Froidevaux,³⁴
 J. A. Frost,¹²⁹ Y. Fu,^{58a} M. Fujimoto,¹²¹ E. Fullana Torregrosa,¹⁶⁸ J. Fuster,¹⁶⁸ A. Gabrielli,^{21b,21a} A. Gabrielli,³⁴ P. Gadow,⁴⁴
 G. Gagliardi,^{53b,53a} L. G. Gagnon,¹⁶ G. E. Gallardo,¹²⁹ E. J. Gallas,¹²⁹ B. J. Gallop,¹³⁸ R. Gamboa Goni,⁹⁰ K. K. Gan,¹²²

S. Ganguly,¹⁷⁴ J. Gao,^{58a} Y. Gao,⁴⁸ Y. S. Gao,^{29,q} F. M. Garay Walls,^{141a} C. García,¹⁶⁸ J. E. García Navarro,¹⁶⁸ J. A. García Pascual,^{13a} M. Garcia-Sciveres,¹⁶ R. W. Gardner,³⁵ D. Garg,⁷⁵ R. B. Garg,¹⁴⁸ S. Gargiulo,⁵⁰ C. A. Garner,¹⁶¹ V. Garonne,¹²⁸ S. J. Gasirowski,¹⁴³ P. Gaspar,^{78b} G. Gaudio,^{68a} P. Gauzzi,^{70a,70b} I. L. Gavrilenko,¹⁰⁷ A. Gavrilyuk,¹¹⁹ C. Gay,¹⁶⁹ G. Gaycken,⁴⁴ E. N. Gazis,⁹ A. A. Geanta,^{25b} C. M. Gee,¹⁴⁰ C. N. P. Gee,¹³⁸ J. Geisen,⁹⁴ M. Geisen,⁹⁶ C. Gemme,^{53b} M. H. Genest,⁵⁶ S. Gentile,^{70a,70b} S. George,⁹¹ W. F. George,¹⁹ T. Gerasis,⁴² L. O. Gerlach,⁵¹ P. Gessinger-Befurt,³⁴ M. Ghasemi Bostanabad,¹⁷⁰ M. Ghneimat,¹⁴⁶ A. Ghosh,¹⁶⁵ A. Ghosh,⁷⁵ B. Giacobbe,^{21b} S. Giagu,^{70a,70b} N. Giangiacomi,¹⁶¹ P. Giannetti,^{69a} A. Giannini,^{67a,67b} S. M. Gibson,⁹¹ M. Gignac,¹⁴⁰ D. T. Gil,^{81b} B. J. Gilbert,³⁷ D. Gillberg,³² G. Gilles,¹¹⁵ N. E. K. Gillwald,⁴⁴ D. M. Gingrich,^{2,e} M. P. Giordani,^{64a,64c} P. F. Giraud,¹³⁹ G. Giugliarelli,^{64a,64c} D. Giugni,^{66a} F. Giuli,^{71a,71b} I. Gkialas,^{8,r} P. Gkoutoumis,⁹ L. K. Gladilin,¹⁰⁹ C. Glasman,⁹⁵ G. R. Gledhill,¹²⁶ M. Glisic,¹²⁶ I. Gnesi,^{39b,s} M. Goblirsch-Kolb,²⁴ D. Godin,¹⁰⁶ S. Goldfarb,¹⁰¹ T. Golling,⁵² D. Golubkov,¹¹⁸ J. P. Gombas,¹⁰³ A. Gomes,^{134a,134b} R. Goncalves Gama,⁵¹ R. Gonçalo,^{134a,134c} G. Gonella,¹²⁶ L. Gonella,¹⁹ A. Gongadze,⁷⁷ F. Gonnella,¹⁹ J. L. Gonski,³⁷ S. González de la Hoz,¹⁶⁸ S. Gonzalez Fernandez,¹² R. Gonzalez Lopez,⁸⁸ C. Gonzalez Renteria,¹⁶ R. Gonzalez Suarez,¹⁶⁶ S. Gonzalez-Sevilla,⁵² G. R. Gonzalvo Rodriguez,¹⁶⁸ R. Y. González Andana,^{141a} L. Goossens,³⁴ N. A. Gorasia,¹⁹ P. A. Gorbounov,¹¹⁹ H. A. Gordon,²⁷ B. Gorini,³⁴ E. Gorini,^{65a,65b} A. Gorišek,⁸⁹ A. T. Goshaw,⁴⁷ M. I. Gostkin,⁷⁷ C. A. Gottardo,¹¹⁴ M. Goughri,^{33b} V. Goumarre,⁴⁴ A. G. Goussiou,¹⁴³ N. Govender,^{31c} C. Goy,⁴ I. Grabowska-Bold,^{81a} K. Graham,³² E. Gramstad,¹²⁸ S. Grancagnolo,¹⁷ M. Grandi,¹⁵¹ V. Gratchev,¹³² P. M. Gravila,^{25f} F. G. Gravili,^{65a,65b} H. M. Gray,¹⁶ C. Grefe,²² I. M. Gregor,⁴⁴ P. Grenier,¹⁴⁸ K. Grevtsov,⁴⁴ C. Grieco,¹² N. A. Grieser,¹²³ A. A. Grillo,¹⁴⁰ K. Grimm,^{29,t} S. Grinstein,^{12,u} J.-F. Grivaz,⁶² S. Groh,⁹⁶ E. Gross,¹⁷⁴ J. Grosse-Knetter,⁵¹ C. Grud,¹⁰² A. Grummer,¹¹³ J. C. Grundy,¹²⁹ L. Guan,¹⁰² W. Guan,¹⁷⁵ C. Gubbels,¹⁶⁹ J. Guenther,³⁴ J. G. R. Guerrero Rojas,¹⁶⁸ F. Guescini,¹¹¹ D. Guest,¹⁷ R. Gugel,⁹⁶ A. Guida,⁴⁴ T. Guillemin,⁴ S. Guindon,³⁴ J. Guo,^{58c} L. Guo,⁶² Y. Guo,¹⁰² R. Gupta,⁴⁴ S. Gurbuz,²² G. Gustavino,¹²³ M. Guth,⁵² P. Gutierrez,¹²³ L. F. Gutierrez Zagazeta,¹³¹ C. Gutscheow,⁹² C. Guyot,¹³⁹ C. Gwenlan,¹²⁹ C. B. Gwilliam,⁸⁸ E. S. Haaland,¹²⁸ A. Haas,¹²⁰ M. Habedank,¹⁷ C. Haber,¹⁶ H. K. Hadavand,⁷ A. Hadeef,⁹⁶ S. Hadzic,¹¹¹ M. Haleem,¹⁷¹ J. Haley,¹²⁴ J. J. Hall,¹⁴⁴ G. Halladjian,¹⁰³ G. D. Hallewell,⁹⁸ L. Halser,¹⁸ K. Hamano,¹⁷⁰ H. Hamdaoui,^{33e} M. Hamer,²² G. N. Hamity,⁴⁸ K. Han,^{58a} L. Han,^{13c} L. Han,^{58a} S. Han,¹⁶ Y. F. Han,¹⁶¹ K. Hanagaki,^{79,v} M. Hance,¹⁴⁰ M. D. Hank,³⁵ R. Hankache,⁹⁷ E. Hansen,⁹⁴ J. B. Hansen,³⁸ J. D. Hansen,³⁸ M. C. Hansen,²² P. H. Hansen,³⁸ K. Hara,¹⁶³ T. Harenberg,¹⁷⁶ S. Harkusha,¹⁰⁴ Y. T. Harris,¹²⁹ P. F. Harrison,¹⁷² N. M. Hartman,¹⁴⁸ N. M. Hartmann,¹¹⁰ Y. Hasegawa,¹⁴⁵ A. Hasib,⁴⁸ S. Hassani,¹³⁹ S. Haug,¹⁸ R. Hauser,¹⁰³ M. Havranek,¹³⁶ C. M. Hawkes,¹⁹ R. J. Hawkins,³⁴ S. Hayashida,¹¹² D. Hayden,¹⁰³ C. Hayes,¹⁰² R. L. Hayes,¹⁶⁹ C. P. Hays,¹²⁹ J. M. Hays,⁹⁰ H. S. Hayward,⁸⁸ S. J. Haywood,¹³⁸ F. He,^{58a} Y. He,¹⁵⁹ Y. He,¹³⁰ M. P. Heath,⁴⁸ V. Hedberg,⁹⁴ A. L. Heggelund,¹²⁸ N. D. Hehir,⁹⁰ C. Heidegger,⁵⁰ K. K. Heidegger,⁵⁰ W. D. Heidorn,⁷⁶ J. Heilman,³² S. Heim,⁴⁴ T. Heim,¹⁶ B. Heinemann,^{44,w} J. G. Heinlein,¹³¹ J. J. Heinrich,¹²⁶ L. Heinrich,³⁴ J. Hejbal,¹³⁵ L. Helary,⁴⁴ A. Held,¹²⁰ C. M. Helling,¹⁴⁰ S. Hellman,^{43a,43b} C. Hensels,³⁴ R. C. W. Henderson,⁸⁷ L. Henkelmann,³⁰ A. M. Henriques Correia,³⁴ H. Herde,¹⁴⁸ Y. Hernández Jiménez,¹⁵⁰ H. Herr,⁹⁶ M. G. Herrmann,¹¹⁰ T. Herrmann,⁴⁶ G. Herten,⁵⁰ R. Hertenberger,¹¹⁰ L. Hervas,³⁴ N. P. Hessey,^{162a} H. Hibi,⁸⁰ S. Higashino,⁷⁹ E. Higón-Rodríguez,¹⁶⁸ K. H. Hiller,⁴⁴ S. J. Hillier,¹⁹ M. Hils,⁴⁶ I. Hinchliffe,¹⁶ F. Hinterkeuser,²² M. Hirose,¹²⁷ S. Hirose,¹⁶³ D. Hirschbuehl,¹⁷⁶ B. Hiti,⁸⁹ O. Hladik,¹³⁵ J. Hobbs,¹⁵⁰ R. Hobincu,^{25e} N. Hod,¹⁷⁴ M. C. Hodgkinson,¹⁴⁴ B. H. Hodgkinson,³⁰ A. Hoecker,³⁴ J. Hofer,⁴⁴ D. Hohn,⁵⁰ T. Holm,²² T. R. Holmes,³⁵ M. Holzbock,¹¹¹ L. B. A. H. Hommels,³⁰ B. P. Honan,⁹⁷ J. Hong,^{58c} T. M. Hong,¹³³ Y. Hong,⁵¹ J. C. Honig,⁵⁰ A. Hönle,¹¹¹ B. H. Hooberman,¹⁶⁷ W. H. Hopkins,⁵ Y. Horii,¹¹² L. A. Horyn,³⁵ S. Hou,¹⁵³ J. Howarth,⁵⁵ J. Hoya,⁸⁶ M. Hrabovsky,¹²⁵ A. Hrynevich,¹⁰⁵ T. Hryn'ova,⁴ P. J. Hsu,⁶¹ S.-C. Hsu,¹⁴³ Q. Hu,³⁷ S. Hu,^{58c} Y. F. Hu,^{13a,13d,x} D. P. Huang,⁹² X. Huang,^{13c} Y. Huang,^{58a} Y. Huang,^{13a} Z. Hubacek,¹³⁶ F. Hubaut,⁹⁸ M. Huebner,²² F. Huegging,²² T. B. Huffman,¹²⁹ M. Huhtinen,³⁴ S. K. Huiberts,¹⁵ R. Hulsken,⁵⁶ N. Huseynov,^{77,y} J. Huston,¹⁰³ J. Huth,⁵⁷ R. Hyneman,¹⁴⁸ S. Hyrych,^{26a} G. Iacobucci,⁵² G. Iakovidis,²⁷ I. Ibragimov,¹⁴⁶ L. Iconomidou-Fayard,⁶² P. Iengo,³⁴ R. Iguchi,¹⁵⁸ T. Iizawa,⁵² Y. Ikegami,⁷⁹ A. Ilg,¹⁸ N. Ilic,¹⁶¹ H. Imam,^{33a} T. Ingebretsen Carlson,^{43a,43b} G. Introzzi,^{68a,68b} M. Iodice,^{72a} V. Ippolito,^{70a,70b} M. Ishino,¹⁵⁸ W. Islam,¹⁷⁵ C. Issever,^{17,44} S. Istin,^{11c,z} J. M. Iturbe Ponce,^{60a} R. Iuppa,^{73a,73b} A. Ivina,¹⁷⁴ J. M. Izen,⁴¹ V. Izzo,^{67a} P. Jacka,¹³⁵ P. Jackson,¹ R. M. Jacobs,⁴⁴ B. P. Jaeger,¹⁴⁷ C. S. Jagfeld,¹¹⁰ G. Jäkel,¹⁷⁶ K. Jakobs,⁵⁰ T. Jakoubek,¹⁷⁴ J. Jamieson,⁵⁵ K. W. Janas,^{81a} G. Jarlskog,⁹⁴ A. E. Jaspán,⁸⁸ N. Javadov,^{77,y} T. Javůrek,³⁴ M. Javurkova,⁹⁹ F. Jeanneau,¹³⁹ L. Jeanty,¹²⁶ J. Jejelava,^{154a,aa} P. Jenni,^{50,bb} S. Jézéquel,⁴ J. Jia,¹⁵⁰ Z. Jia,^{13c} Y. Jiang,^{58a} S. Jiggins,⁴⁸ J. Jimenez Pena,¹¹¹ S. Jin,^{13c} A. Jinaru,^{25b} O. Jinnouchi,¹⁵⁹ H. Jivan,^{31g} P. Johansson,¹⁴⁴ K. A. Johns,⁶ C. A. Johnson,⁶³ D. M. Jones,³⁰ E. Jones,¹⁷² R. W. L. Jones,⁸⁷ T. J. Jones,⁸⁸ J. Jovicevic,⁵¹ X. Ju,¹⁶ J. J. Jungeburth,³⁴ A. Juste Rozas,^{12,u} S. Kabana,^{141e}

A. Kaczmarek,⁸² M. Kado,^{70a,70b} H. Kagan,¹²² M. Kagan,¹⁴⁸ A. Kahn,³⁷ A. Kahn,¹³¹ C. Kahra,⁹⁶ T. Kaji,¹⁷³
 E. Kajomovitz,¹⁵⁵ C. W. Kalderon,²⁷ A. Kamenshchikov,¹¹⁸ M. Kaneda,¹⁵⁸ N. J. Kang,¹⁴⁰ S. Kang,⁷⁶ Y. Kano,¹¹²
 J. Kanzaki,⁷⁹ D. Kar,^{31g} K. Karava,¹²⁹ M. J. Kareem,^{162b} I. Karkanas,¹⁵⁷ S. N. Karpov,⁷⁷ Z. M. Karpova,⁷⁷
 V. Kartvelishvili,⁸⁷ A. N. Karyukhin,¹¹⁸ E. Kasimi,¹⁵⁷ C. Kato,^{58d} J. Katzy,⁴⁴ K. Kawade,¹⁴⁵ K. Kawagoe,⁸⁵ T. Kawaguchi,¹¹²
 T. Kawamoto,¹³⁹ G. Kawamura,⁵¹ E. F. Kay,¹⁷⁰ F. I. Kaya,¹⁶⁴ S. Kazakos,¹² V. F. Kazanin,^{117b,117a} Y. Ke,¹⁵⁰
 J. M. Keaveney,^{31a} R. Keeler,¹⁷⁰ J. S. Keller,³² D. Kelsey,¹⁵¹ J. J. Kempster,¹⁹ J. Kendrick,¹⁹ K. E. Kennedy,³⁷ O. Kepka,¹³⁵
 S. Kersten,¹⁷⁶ B. P. Kerševan,⁸⁹ S. Ketabchi Haghighat,¹⁶¹ M. Khandoga,¹³⁰ A. Khanov,¹²⁴ A. G. Kharlamov,^{117b,117a}
 T. Kharlamova,^{117b,117a} E. E. Khoda,¹⁴³ T. J. Khoo,¹⁷ G. Khoriauli,¹⁷¹ E. Khramov,⁷⁷ J. Khubua,^{154b} S. Kido,⁸⁰ M. Kiehn,³⁴
 A. Kilgallon,¹²⁶ E. Kim,¹⁵⁹ Y. K. Kim,³⁵ N. Kimura,⁹² A. Kirchhoff,⁵¹ D. Kirchmeier,⁴⁶ C. Kirfel,²² J. Kirk,¹³⁸
 A. E. Kiryunin,¹¹¹ T. Kishimoto,¹⁵⁸ D. P. Kisluk,¹⁶¹ C. Kitsaki,⁹ O. Kivernyk,²² T. Klapdor-Kleingrothaus,⁵⁰ M. Klassen,^{59a}
 C. Klein,³² L. Klein,¹⁷¹ M. H. Klein,¹⁰² M. Klein,⁸⁸ U. Klein,⁸⁸ P. Klimek,³⁴ A. Klimentov,²⁷ F. Klimpel,³⁴ T. Klingl,²²
 T. Klioutchnikova,³⁴ F. F. Klitzner,¹¹⁰ P. Kluit,¹¹⁵ S. Kluth,¹¹¹ E. Kneringer,⁷⁴ T. M. Knight,¹⁶¹ A. Knue,⁵⁰ D. Kobayashi,⁸⁵
 M. Kobel,⁴⁶ M. Kocian,¹⁴⁸ T. Kodama,¹⁵⁸ P. Kodys,¹³⁷ D. M. Koeck,¹⁵¹ P. T. Koenig,²² T. Koffas,³² N. M. Köhler,³⁴
 M. Kolb,¹³⁹ I. Koletsou,⁴ T. Komarek,¹²⁵ K. Köneke,⁵⁰ A. X. Y. Kong,¹ T. Kono,¹²¹ V. Konstantinides,⁹² N. Konstantinidis,⁹²
 B. Konya,⁹⁴ R. Kopeliansky,⁶³ S. Koperny,^{81a} K. Korcyl,⁸² K. Kordas,¹⁵⁷ G. Koren,¹⁵⁶ A. Korn,⁹² S. Korn,⁵¹ I. Korolkov,¹²
 E. V. Korolkova,¹⁴⁴ N. Korotkova,¹⁰⁹ B. Kortman,¹¹⁵ O. Kortner,¹¹¹ S. Kortner,¹¹¹ W. H. Kostecka,¹¹⁶
 V. V. Kostyukhin,^{144,160} A. Kotskechagia,⁶² A. Kotwal,⁴⁷ A. Koulouris,³⁴ A. Kourkoumeli-Charalampidi,^{68a,68b}
 C. Kourkoumelis,⁸ E. Kourlitis,⁵ O. Kovanda,¹⁵¹ R. Kowalewski,¹⁷⁰ W. Kozanecki,¹³⁹ A. S. Kozhin,¹¹⁸ V. A. Kramarenko,¹⁰⁹
 G. Kramberger,⁸⁹ P. Kramer,⁹⁶ D. Krasnopevtsev,^{58a} M. W. Krasny,¹³⁰ A. Krasznahorkay,³⁴ J. A. Kremer,⁹⁶ J. Kretschmar,⁸⁸
 K. Kreul,¹⁷ P. Krieger,¹⁶¹ F. Krieter,¹¹⁰ S. Krishnamurthy,⁹⁹ A. Krishnan,^{59b} M. Krivos,¹³⁷ K. Krizka,¹⁶ K. Kroeninger,⁴⁵
 H. Kroha,¹¹¹ J. Kroll,¹³⁵ J. Kroll,¹³¹ K. S. Krowpman,¹⁰³ U. Kruchonak,⁷⁷ H. Krüger,²² N. Krumnack,⁷⁶ M. C. Kruse,⁴⁷
 J. A. Krzysiak,⁸² A. Kubota,¹⁵⁹ O. Kuchinskaia,¹⁶⁰ S. Kuday,^{3a} D. Kuechler,⁴⁴ J. T. Kuechler,⁴⁴ S. Kuehn,³⁴ T. Kuhl,⁴⁴
 V. Kukhtin,⁷⁷ Y. Kulchitsky,^{104,cc} S. Kuleshov,^{141d} M. Kumar,^{31g} N. Kumari,⁹⁸ M. Kuna,⁵⁶ A. Kupco,¹³⁵ T. Kupfer,⁴⁵
 O. Kuprash,⁵⁰ H. Kurashige,⁸⁰ L. L. Kurchaninov,^{162a} Y. A. Kurochkin,¹⁰⁴ A. Kurova,¹⁰⁸ M. G. Kurth,^{13a,13d} E. S. Kuwertz,³⁴
 M. Kuze,¹⁵⁹ A. K. Kvam,¹⁴³ J. Kvita,¹²⁵ T. Kwan,¹⁰⁰ K. W. Kwok,^{60a} C. Lacasta,¹⁶⁸ F. Lacava,^{70a,70b} H. Lacker,¹⁷
 D. Lacour,¹³⁰ N. N. Lad,⁹² E. Ladygin,⁷⁷ R. Lafaye,⁴ B. Laforge,¹³⁰ T. Lagouri,^{141e} S. Lai,⁵¹ I. K. Lakomic,^{81a} N. Lalloue,⁵⁶
 J. E. Lambert,¹²³ S. Lammers,⁶³ W. Lampl,⁶ C. Lampoudis,¹⁵⁷ E. Lançon,²⁷ U. Landgraf,⁵⁰ M. P. J. Landon,⁹⁰ V. S. Lang,⁵⁰
 J. C. Lange,⁵¹ R. J. Langenberg,⁹⁹ A. J. Lankford,¹⁶⁵ F. Lanni,²⁷ K. Lantsch,²² A. Lanza,^{68a} A. Lapertosa,^{53b,53a}
 J. F. Laporte,¹³⁹ T. Lari,^{66a} F. Lasagni Manghi,^{21b} M. Lassnig,³⁴ V. Latonova,¹³⁵ T. S. Lau,^{60a} A. Laudrain,⁹⁶ A. Laurier,³²
 M. Lavorgna,^{67a,67b} S. D. Lawlor,⁹¹ Z. Lawrence,⁹⁷ M. Lazzaroni,^{66a,66b} B. Le,⁹⁷ B. Leban,⁸⁹ A. Lebedev,⁷⁶ M. LeBlanc,³⁴
 T. LeCompte,⁵ F. Ledroit-Guillon,⁵⁶ A. C. A. Lee,⁹² G. R. Lee,¹⁵ L. Lee,⁵⁷ S. C. Lee,¹⁵³ S. Lee,⁷⁶ L. L. Leeuw,^{31c}
 B. Lefebvre,^{162a} H. P. Lefebvre,⁹¹ M. Lefebvre,¹⁷⁰ C. Leggett,¹⁶ K. Lehmann,¹⁴⁷ N. Lehmann,¹⁸ G. Lehmann Miotto,³⁴
 W. A. Leight,⁴⁴ A. Leisos,^{157,dd} M. A. L. Leite,^{78c} C. E. Leitgeb,⁴⁴ R. Leitner,¹³⁷ K. J. C. Leney,⁴⁰ T. Lenz,²² S. Leone,^{69a}
 C. Leonidopoulos,⁴⁸ A. Leopold,¹³⁰ C. Leroy,¹⁰⁶ R. Les,¹⁰³ C. G. Lester,³⁰ M. Levchenko,¹³² J. Levêque,⁴ D. Levin,¹⁰²
 L. J. Levinson,¹⁷⁴ D. J. Lewis,¹⁹ B. Li,^{13b} B. Li,^{58b} C. Li,^{58a} C-Q. Li,^{58c,58d} H. Li,^{58a} H. Li,^{58b} H. Li,^{58b} J. Li,^{58c} K. Li,¹⁴³
 L. Li,^{58c} M. Li,^{13a,13d} Q. Y. Li,^{58a} S. Li,^{58d,58c,ee} T. Li,^{58b} X. Li,⁴⁴ Y. Li,⁴⁴ Z. Li,^{58b} Z. Li,¹²⁹ Z. Li,¹⁰⁰ Z. Li,⁸⁸ Z. Liang,^{13a}
 M. Liberatore,⁴⁴ B. Liberti,^{71a} K. Lie,^{60c} J. Lieber Marin,^{78b} K. Lin,¹⁰³ R. A. Linck,⁶³ R. E. Lindley,⁶ J. H. Lindon,²
 A. Linss,⁴⁴ E. Lipeles,¹³¹ A. Lipniacka,¹⁵ T. M. Liss,^{167,ff} A. Lister,¹⁶⁹ J. D. Little,⁷ B. Liu,^{13a} B. X. Liu,¹⁴⁷ J. B. Liu,^{58a}
 J. K. K. Liu,³⁵ K. Liu,^{58d,58c} M. Liu,^{58a} M. Y. Liu,^{58a} P. Liu,^{13a} X. Liu,^{58a} Y. Liu,⁴⁴ Y. Liu,^{13c,13d} Y. L. Liu,¹⁰² Y. W. Liu,^{58a}
 M. Livan,^{68a,68b} A. Lleres,⁵⁶ J. Llorente Merino,¹⁴⁷ S. L. Lloyd,⁹⁰ E. M. Lobodzinska,⁴⁴ P. Loch,⁶ S. Loffredo,^{71a,71b}
 T. Lohse,¹⁷ K. Lohwasser,¹⁴⁴ M. Lokajicek,¹³⁵ J. D. Long,¹⁶⁷ I. Longarini,^{70a,70b} L. Longo,³⁴ R. Longo,¹⁶⁷ I. Lopez Paz,¹²
 A. Lopez Solis,⁴⁴ J. Lorenz,¹¹⁰ N. Lorenzo Martinez,⁴ A. M. Lory,¹¹⁰ A. Lösle,⁵⁰ X. Lou,^{43a,43b} X. Lou,^{13a} A. Lounis,⁶²
 J. Love,⁵ P. A. Love,⁸⁷ J. J. Lozano Bahilo,¹⁶⁸ G. Lu,^{13a} M. Lu,^{58a} S. Lu,¹³¹ Y. J. Lu,⁶¹ H. J. Lubatti,¹⁴³ C. Luci,^{70a,70b}
 F. L. Lucio Alves,^{13c} A. Lucotte,⁵⁶ F. Luehring,⁶³ I. Luise,¹⁵⁰ L. Luminari,^{70a} O. Lundberg,¹⁴⁹ B. Lund-Jensen,¹⁴⁹
 N. A. Luongo,¹²⁶ M. S. Lutz,¹⁵⁶ D. Lynn,²⁷ H. Lyons,⁸⁸ R. Lysak,¹³⁵ E. Lytken,⁹⁴ F. Lyu,^{13a} V. Lyubushkin,⁷⁷
 T. Lyubushkina,⁷⁷ H. Ma,²⁷ L. L. Ma,^{58b} Y. Ma,⁹² D. M. Mac Donell,¹⁷⁰ G. Maccarrone,⁴⁹ C. M. Macdonald,¹⁴⁴
 J. C. MacDonald,¹⁴⁴ R. Madar,³⁶ W. F. Mader,⁴⁶ M. Madugoda Ralalage Don,¹²⁴ N. Madysa,⁴⁶ J. Maeda,⁸⁰ T. Maeno,²⁷
 M. Maerker,⁴⁶ V. Magerl,⁵⁰ J. Magro,^{64a,64c} D. J. Mahon,³⁷ C. Maidantchik,^{78b} A. Maio,^{134a,134b,134d} K. Maj,^{81a}
 O. Majersky,^{26a} S. Majewski,¹²⁶ N. Makovec,⁶² V. Maksimovic,¹⁴ B. Malaescu,¹³⁰ Pa. Malecki,⁸² V. P. Maleev,¹³²

F. Malek,⁵⁶ D. Malito,^{39b,39a} U. Mallik,⁷⁵ C. Malone,³⁰ S. Maltezos,⁹ S. Malyukov,⁷⁷ J. Mamuzic,¹⁶⁸ G. Mancini,⁴⁹ J. P. Mandalia,⁹⁰ I. Mandić,⁸⁹ L. Manhaes de Andrade Filho,^{78a} I. M. Maniatis,¹⁵⁷ M. Manisha,¹³⁹ J. Manjarres Ramos,⁴⁶ K. H. Mankinen,⁹⁴ A. Mann,¹¹⁰ A. Manousos,⁷⁴ B. Mansoulie,¹³⁹ I. Mantos,¹⁵⁷ S. Manzoni,¹¹⁵ A. Marantis,^{157,dd} G. Marchiori,¹³⁰ M. Marcisovsky,¹³⁵ L. Marcoccia,^{71a,71b} C. Marcon,⁹⁴ M. Marjanovic,¹²³ Z. Marshall,¹⁶ S. Marti-Garcia,¹⁶⁸ T. A. Martin,¹⁷² V. J. Martin,⁴⁸ B. Martin dit Latour,¹⁵ L. Martinelli,^{70a,70b} M. Martinez,^{12,u} P. Martinez Agullo,¹⁶⁸ V. I. Martinez Outschoorn,⁹⁹ S. Martin-Haugh,¹³⁸ V. S. Martoiu,^{25b} A. C. Martyniuk,⁹² A. Marzin,³⁴ S. R. Maschek,¹¹¹ L. Masetti,⁹⁶ T. Mashimo,¹⁵⁸ J. Masik,⁹⁷ A. L. Maslennikov,^{117b,117a} L. Massa,^{21b} P. Massarotti,^{67a,67b} P. Mastrandrea,^{69a,69b} A. Mastroberardino,^{39b,39a} T. Masubuchi,¹⁵⁸ D. Matakias,²⁷ T. Mathisen,¹⁶⁶ A. Matic,¹¹⁰ N. Matsuzawa,¹⁵⁸ J. Maurer,^{25b} B. Maček,⁸⁹ D. A. Maximov,^{117b,117a} R. Mazini,¹⁵³ I. Maznas,¹⁵⁷ S. M. Mazza,¹⁴⁰ C. Mc Ginn,²⁷ J. P. Mc Gowan,¹⁰⁰ S. P. Mc Kee,¹⁰² T. G. McCarthy,¹¹¹ W. P. McCormack,¹⁶ E. F. McDonald,¹⁰¹ A. E. McDougall,¹¹⁵ J. A. McFayden,¹⁵¹ G. Mchedlize,^{154b} M. A. McKay,⁴⁰ K. D. McLean,¹⁷⁰ S. J. McMahon,¹³⁸ P. C. McNamara,¹⁰¹ R. A. McPherson,^{170,m} J. E. Mdhuli,^{31g} Z. A. Meadows,⁹⁹ S. Meehan,³⁴ T. Megy,³⁶ S. Mehlhase,¹¹⁰ A. Mehta,⁸⁸ B. Meirose,⁴¹ D. Melini,¹⁵⁵ B. R. Mellado Garcia,^{31g} A. H. Melo,⁵¹ F. Meloni,⁴⁴ A. Melzer,²² E. D. Mendes Gouveia,^{134a} A. M. Mendes Jacques Da Costa,¹⁹ H. Y. Meng,¹⁶¹ L. Meng,³⁴ S. Menke,¹¹¹ M. Mentink,³⁴ E. Meoni,^{39b,39a} C. Merlassino,¹²⁹ P. Mermod,^{52,a} L. Merola,^{67a,67b} C. Meroni,^{66a} G. Merz,¹⁰² O. Meshkov,^{109,107} J. K. R. Meshreki,¹⁴⁶ J. Metcalfe,⁵ A. S. Mete,⁵ C. Meyer,⁶³ J-P. Meyer,¹³⁹ M. Michetti,¹⁷ R. P. Middleton,¹³⁸ L. Mijović,⁴⁸ G. Mikenberg,¹⁷⁴ M. Mikesstikova,¹³⁵ M. Mikuž,⁸⁹ H. Mildner,¹⁴⁴ A. Milic,¹⁶¹ C. D. Milke,⁴⁰ D. W. Miller,³⁵ L. S. Miller,³² A. Milov,¹⁷⁴ D. A. Milstead,^{43a,43b} T. Min,^{13c} A. A. Minaenko,¹¹⁸ I. A. Minashvili,^{154b} L. Mince,⁵⁵ A. I. Mincer,¹²⁰ B. Mindur,^{81a} M. Mineev,⁷⁷ Y. Minegishi,¹⁵⁸ Y. Mino,⁸³ L. M. Mir,¹² M. Miralles Lopez,¹⁶⁸ M. Mironova,¹²⁹ T. Mitani,¹⁷³ V. A. Mitsou,¹⁶⁸ M. Mittal,^{58c} O. Miu,¹⁶¹ P. S. Miyagawa,⁹⁰ Y. Miyazaki,⁸⁵ A. Mizukami,⁷⁹ J. U. Mjörnmark,⁹⁴ T. Mkrtychyan,^{59a} M. Mlynarikova,¹¹⁶ T. Moa,^{43a,43b} S. Mobius,⁵¹ K. Mochizuki,¹⁰⁶ P. Moder,⁴⁴ P. Mogg,¹¹⁰ A. F. Mohammed,^{13a} S. Mohapatra,³⁷ G. Mokgatitwane,^{31g} B. Mondal,¹⁴⁶ S. Mondal,¹³⁶ K. Mönig,⁴⁴ E. Monnier,⁹⁸ L. Monsonis Romero,¹⁶⁸ A. Montalbano,¹⁴⁷ J. Montejo Berlingen,³⁴ M. Montella,¹²² F. Monticelli,⁸⁶ N. Morange,⁶² A. L. Moreira De Carvalho,^{134a} M. Moreno Llácer,¹⁶⁸ C. Moreno Martinez,¹² P. Morettini,^{53b} S. Morgenstern,¹⁷² D. Mori,¹⁴⁷ M. Morii,⁵⁷ M. Morinaga,¹⁵⁸ V. Morisbak,¹²⁸ A. K. Morley,³⁴ A. P. Morris,⁹² L. Morvaj,³⁴ P. Moschovakos,³⁴ B. Moser,¹¹⁵ M. Mosidze,^{154b} T. Moskalets,⁵⁰ P. Moskvitina,¹¹⁴ J. Moss,^{29,gg} E. J. W. Moyse,⁹⁹ S. Muanza,⁹⁸ J. Mueller,¹³³ R. Mueller,¹⁸ D. Muenstermann,⁸⁷ G. A. Mullier,⁹⁴ J. J. Mullin,¹³¹ D. P. Mungo,^{66a,66b} J. L. Munoz Martinez,¹² F. J. Munoz Sanchez,⁹⁷ M. Murin,⁹⁷ P. Murin,^{26b} W. J. Murray,^{172,138} A. Murrone,^{66a,66b} J. M. Muse,¹²³ M. Muškinja,¹⁶ C. Mwewa,²⁷ A. G. Myagkov,^{118,i} A. J. Myers,⁷ A. A. Myers,¹³³ G. Myers,⁶³ M. Myska,¹³⁶ B. P. Nachman,¹⁶ O. Nackenhorst,⁴⁵ A. Nag Nag,⁴⁶ K. Nagai,¹²⁹ K. Nagano,⁷⁹ J. L. Nagle,²⁷ E. Nagy,⁹⁸ A. M. Nairz,³⁴ Y. Nakahama,¹¹² K. Nakamura,⁷⁹ H. Nanjo,¹²⁷ F. Napolitano,^{59a} R. Narayan,⁴⁰ E. A. Narayanan,¹¹³ I. Naryshkin,¹³² M. Naseri,³² C. Nass,²² T. Naumann,⁴⁴ G. Navarro,^{20a} J. Navarro-Gonzalez,¹⁶⁸ R. Nayak,¹⁵⁶ P. Y. Nechaeva,¹⁰⁷ F. Nechansky,⁴⁴ T. J. Neep,¹⁹ A. Negri,^{68a,68b} M. Negrini,^{21b} C. Nellist,¹¹⁴ C. Nelson,¹⁰⁰ K. Nelson,¹⁰² S. Nemecek,¹³⁵ M. Nessi,^{34,hh} M. S. Neubauer,¹⁶⁷ F. Neuhaus,⁹⁶ J. Neundorf,⁴⁴ R. Newhouse,¹⁶⁹ P. R. Newman,¹⁹ C. W. Ng,¹³³ Y. S. Ng,¹⁷ Y. W. Y. Ng,¹⁶⁵ B. Ngair,^{33e} H. D. N. Nguyen,¹⁰⁶ R. B. Nickerson,¹²⁹ R. Nicolaidou,¹³⁹ D. S. Nielsen,³⁸ J. Nielsen,¹⁴⁰ M. Niemeyer,⁵¹ N. Nikiforou,¹⁰ V. Nikolaenko,^{118,i} I. Nikolic-Audit,¹³⁰ K. Nikolopoulos,¹⁹ P. Nilsson,²⁷ H. R. Nindhito,⁵² A. Nisati,^{70a} N. Nishu,² R. Nisius,¹¹¹ T. Nitta,¹⁷³ T. Nobe,¹⁵⁸ D. L. Noel,³⁰ Y. Noguchi,⁸³ I. Nomidis,¹³⁰ M. A. Nomura,²⁷ M. B. Norfolk,¹⁴⁴ R. R. B. Norisam,⁹² J. Novak,⁸⁹ T. Novak,⁴⁴ O. Novgorodova,⁴⁶ L. Novotny,¹³⁶ R. Novotny,¹¹³ L. Nozka,¹²⁵ K. Ntekas,¹⁶⁵ E. Nurse,⁹² F. G. Oakham,^{32,e} J. Ocariz,¹³⁰ A. Ochi,⁸⁰ I. Ochoa,^{134a} J. P. Ochoa-Ricoux,^{141a} S. Oda,⁸⁵ S. Odaka,⁷⁹ S. Oerdek,¹⁶⁶ A. Ogrodnik,^{81a} A. Oh,⁹⁷ C. C. Ohm,¹⁴⁹ H. Oide,¹⁵⁹ R. Oishi,¹⁵⁸ M. L. Ojeda,⁴⁴ Y. Okazaki,⁸³ M. W. O'Keefe,⁸⁸ Y. Okumura,¹⁵⁸ A. Olariu,^{25b} L. F. Oleiro Seabra,^{134a} S. A. Olivares Pino,^{141e} D. Oliveira Damazio,²⁷ D. Oliveira Goncalves,^{78a} J. L. Oliver,¹⁶⁵ M. J. R. Olsson,¹⁶⁵ A. Olszewski,⁸² J. Olszowska,⁸² Ö. O. Öncel,²² D. C. O'Neil,¹⁴⁷ A. P. O'neill,¹²⁹ A. Onofre,^{134a,134e} P. U. E. Onyisi,¹⁰ R. G. Oreamuno Madriz,¹¹⁶ M. J. Oreglia,³⁵ G. E. Orellana,⁸⁶ D. Orestano,^{72a,72b} N. Orlando,¹² R. S. Orr,¹⁶¹ V. O'Shea,⁵⁵ R. Ospanov,^{58a} G. Otero y Garzon,²⁸ H. Otono,⁸⁵ P. S. Ott,^{59a} G. J. Ottino,¹⁶ M. Ouchrif,^{33d} J. Ouellette,²⁷ F. Ould-Saada,¹²⁸ A. Ouraou,^{139,a} Q. Ouyang,^{13a} M. Owen,⁵⁵ R. E. Owen,¹³⁸ K. Y. Oyulmaz,^{11c} V. E. Ozcan,^{11c} N. Ozturk,⁷ S. Ozturk,^{11c} J. Pacalt,¹²⁵ H. A. Pacey,³⁰ K. Pachal,⁴⁷ A. Pacheco Pages,¹² C. Padilla Aranda,¹² S. Pagan Griso,¹⁶ G. Palacino,⁶³ S. Palazzo,⁴⁸ S. Palestini,³⁴ M. Palka,^{81b} P. Palni,^{81a} D. K. Panchal,¹⁰ C. E. Pandini,⁵² J. G. Panduro Vazquez,⁹¹ P. Pani,⁴⁴ G. Panizzo,^{64a,64c} L. Paolozzi,⁵² C. Papadatos,¹⁰⁶ S. Parajuli,⁴⁰ A. Paramonov,⁵ C. Paraskevopoulos,⁹ D. Paredes Hernandez,^{60b} S. R. Paredes Saenz,¹²⁹ B. Parida,¹⁷⁴ T. H. Park,¹⁶¹ A. J. Parker,²⁹ M. A. Parker,³⁰ F. Parodi,^{53b,53a} E. W. Parrish,¹¹⁶

J. A. Parsons,³⁷ U. Parzefall,⁵⁰ L. Pascual Dominguez,¹⁵⁶ V. R. Pascuzzi,¹⁶ F. Pasquali,¹¹⁵ E. Pasqualucci,^{70a} S. Passaggio,^{53b}
 F. Pastore,⁹¹ P. Pasuwan,^{43a,43b} J. R. Pater,⁹⁷ A. Pathak,¹⁷⁵ J. Patton,⁸⁸ T. Pauly,³⁴ J. Pearkes,¹⁴⁸ M. Pedersen,¹²⁸
 L. Pedraza Diaz,¹¹⁴ R. Pedro,^{134a} T. Peiffer,⁵¹ S. V. Peleganchuk,^{117b,117a} O. Penc,¹³⁵ C. Peng,^{60b} H. Peng,^{58a} M. Penzin,¹⁶⁰
 B. S. Peralva,^{78a} A. P. Pereira Peixoto,^{134a} L. Pereira Sanchez,^{43a,43b} D. V. Perepelitsa,²⁷ E. Perez Codina,^{162a} M. Perganti,⁹
 L. Perini,^{66a,66b} H. Pernegger,³⁴ S. Perrella,³⁴ A. Perrevoort,¹¹⁵ K. Peters,⁴⁴ R. F. Y. Peters,⁹⁷ B. A. Petersen,³⁴
 T. C. Petersen,³⁸ E. Petit,⁹⁸ V. Petousis,¹³⁶ C. Petridou,¹⁵⁷ P. Petroff,⁶² F. Petrucci,^{72a,72b} A. Petrukhin,¹⁴⁶ M. Pettee,¹⁷⁷
 N. E. Pettersson,³⁴ K. Petukhova,¹³⁷ A. Peyaud,¹³⁹ R. Pezoa,^{141f} L. Pezzotti,³⁴ G. Pezzullo,¹⁷⁷ T. Pham,¹⁰¹ P. W. Phillips,¹³⁸
 M. W. Phipps,¹⁶⁷ G. Piacquadio,¹⁵⁰ E. Pianori,¹⁶ F. Piazza,^{66a,66b} A. Picazio,⁹⁹ R. Piegai,²⁸ D. Pietreanu,^{25b} J. E. Pilcher,³⁵
 A. D. Pilkington,⁹⁷ M. Pinamonti,^{64a,64c} J. L. Pinfold,² C. Pitman Donaldson,⁹² D. A. Pizzi,³² L. Pizzimento,^{71a,71b}
 A. Pizzini,¹¹⁵ M.-A. Pleier,²⁷ V. Plesanovs,⁵⁰ V. Pleskot,¹³⁷ E. Plotnikova,⁷⁷ P. Podberezko,^{117b,117a} R. Poettgen,⁹⁴ R. Poggi,⁵²
 L. Poggioli,¹³⁰ I. Pogrebnyak,¹⁰³ D. Pohl,²² I. Pokharel,⁵¹ G. Polesello,^{68a} A. Poley,^{147,162a} A. Policicchio,^{70a,70b} R. Polifka,¹³⁷
 A. Polini,^{21b} C. S. Pollard,¹²⁹ Z. B. Pollock,¹²² V. Polychronakos,²⁷ D. Ponomarenko,¹⁰⁸ L. Pontecorvo,³⁴ S. Popa,^{25a}
 G. A. Popeneciu,^{25d} L. Portales,⁴ D. M. Portillo Quintero,^{162a} S. Pospisil,¹³⁶ P. Postolache,^{25c} K. Potamianos,¹²⁹
 I. N. Potrap,⁷⁷ C. J. Potter,³⁰ H. Potti,¹ T. Poulsen,⁴⁴ J. Poveda,¹⁶⁸ T. D. Powell,¹⁴⁴ G. Pownall,⁴⁴ M. E. Pozo Astigarraga,³⁴
 A. Prades Ibanez,¹⁶⁸ P. Pralavorio,⁹⁸ M. M. Prapa,⁴² S. Prell,⁷⁶ D. Price,⁹⁷ M. Primavera,^{65a} M. A. Principe Martin,⁹⁵
 M. L. Proffitt,¹⁴³ N. Proklova,¹⁰⁸ K. Prokofiev,^{60c} F. Prokoshin,⁷⁷ S. Protopopescu,²⁷ J. Proudfoot,⁵ M. Przybycien,^{81a}
 D. Pudzha,¹³² P. Puzo,⁶² D. Pyatiiizbyantseva,¹⁰⁸ J. Qian,¹⁰² Y. Qin,⁹⁷ T. Qiu,⁹⁰ A. Quadt,⁵¹ M. Queitsch-Maitland,³⁴
 G. Rabanal Bolanos,⁵⁷ F. Ragusa,^{66a,66b} J. A. Raine,⁵² S. Rajagopalan,²⁷ K. Ran,^{13a,13d} D. F. Rassloff,^{59a} D. M. Rauch,⁴⁴
 S. Rave,⁹⁶ B. Ravina,⁵⁵ I. Ravinovich,¹⁷⁴ M. Raymond,³⁴ A. L. Read,¹²⁸ N. P. Readioff,¹⁴⁴ D. M. Rebutzi,^{68a,68b}
 G. Redlinger,²⁷ K. Reeves,⁴¹ D. Reikher,¹⁵⁶ A. Reiss,⁹⁶ A. Rej,¹⁴⁶ C. Rembser,³⁴ A. Renardi,⁴⁴ M. Renda,^{25b}
 M. B. Rendel,¹¹¹ A. G. Rennie,⁵⁵ S. Resconi,^{66a} M. Ressegotti,^{53b,53a} E. D. Resseguie,¹⁶ S. Rettie,⁹² B. Reynolds,¹²²
 E. Reynolds,¹⁹ M. Rezaei Estabragh,¹⁷⁶ O. L. Rezanova,^{117b,117a} P. Reznicek,¹³⁷ E. Ricci,^{73a,73b} R. Richter,¹¹¹ S. Richter,⁴⁴
 E. Richter-Was,^{81b} M. Ridel,¹³⁰ P. Rieck,¹¹¹ P. Riedler,³⁴ O. Rifki,⁴⁴ M. Rijssenbeek,¹⁵⁰ A. Rimoldi,^{68a,68b} M. Rimoldi,⁴⁴
 L. Rinaldi,^{21b,21a} T. T. Rinn,¹⁶⁷ M. P. Rinnagel,¹¹⁰ G. Ripellino,¹⁴⁹ I. Riu,¹² P. Rivadeneira,⁴⁴ J. C. Rivera Vergara,¹⁷⁰
 F. Rizatdinova,¹²⁴ E. Rizvi,⁹⁰ C. Rizzi,⁵² B. A. Roberts,¹⁷² S. H. Robertson,^{100,m} M. Robin,⁴⁴ D. Robinson,³⁰
 C. M. Robles Gajardo,^{141f} M. Robles Manzano,⁹⁶ A. Robson,⁵⁵ A. Rocchi,^{71a,71b} C. Roda,^{69a,69b} S. Rodriguez Bosca,^{59a}
 A. Rodriguez Rodriguez,⁵⁰ A. M. Rodríguez Vera,^{162b} S. Roe,³⁴ A. R. Roepe,¹²³ J. Roggel,¹⁷⁶ O. Røhne,¹²⁸ R. A. Rojas,^{141f}
 B. Roland,⁵⁰ C. P. A. Roland,⁶³ J. Roloff,²⁷ A. Romaniouk,¹⁰⁸ M. Romano,^{21b} A. C. Romero Hernandez,¹⁶⁷ N. Rompotis,⁸⁸
 M. Ronzani,¹²⁰ L. Roos,¹³⁰ S. Rosati,^{70a} B. J. Rosser,¹³¹ E. Rossi,¹⁶¹ E. Rossi,⁴ E. Rossi,^{67a,67b} L. P. Rossi,^{53b} L. Rossini,⁴⁴
 R. Rosten,¹²² M. Rotaru,^{25b} B. Rottler,⁵⁰ D. Rousseau,⁶² D. Rousso,³⁰ G. Rovelli,^{68a,68b} A. Roy,¹⁰ A. Rozanov,⁹⁸ Y. Rozen,¹⁵⁵
 X. Ruan,^{31g} A. J. Ruby,⁸⁸ T. A. Ruggeri,¹ F. Rühr,⁵⁰ A. Ruiz-Martinez,¹⁶⁸ A. Rummeler,³⁴ Z. Rurikova,⁵⁰ N. A. Rusakovich,⁷⁷
 H. L. Russell,³⁴ L. Rustige,³⁶ J. P. Rutherford,⁶ E. M. Rüttinger,¹⁴⁴ M. Rybar,¹³⁷ E. B. Rye,¹²⁸ A. Ryzhov,¹¹⁸
 J. A. Sabater Iglesias,⁴⁴ P. Sabatini,¹⁶⁸ L. Sabetta,^{70a,70b} H. F-W. Sadrozinski,¹⁴⁰ R. Sadykov,⁷⁷ F. Safai Tehrani,^{70a}
 B. Safarzadeh Samani,¹⁵¹ M. Safdari,¹⁴⁸ P. Saha,¹¹⁶ S. Saha,¹⁰⁰ M. Sahinsoy,¹¹¹ A. Sahu,¹⁷⁶ M. Saimpert,¹³⁹ M. Saito,¹⁵⁸
 T. Saito,¹⁵⁸ D. Salamani,³⁴ G. Salamanna,^{72a,72b} A. Salnikov,¹⁴⁸ J. Salt,¹⁶⁸ A. Salvador Salas,¹² D. Salvatore,^{39b,39a}
 F. Salvatore,¹⁵¹ A. Salzburger,³⁴ D. Sammel,⁵⁰ D. Sampsonidis,¹⁵⁷ D. Sampsonidou,^{58d,58c} J. Sánchez,¹⁶⁸
 A. Sanchez Pineda,⁴ V. Sanchez Sebastian,¹⁶⁸ H. Sandaker,¹²⁸ C. O. Sander,⁴⁴ I. G. Sanderswood,⁸⁷ J. A. Sandesara,⁹⁹
 M. Sandhoff,¹⁷⁶ C. Sandoval,^{20b} D. P. C. Sankey,¹³⁸ M. Sannino,^{53b,53a} A. Sansoni,⁴⁹ C. Santoni,³⁶ H. Santos,^{134a,134b}
 S. N. Santpur,¹⁶ A. Santra,¹⁷⁴ K. A. Saoucha,¹⁴⁴ A. Saponov,⁷⁷ J. G. Saraiva,^{134a,134d} J. Sardain,⁹⁸ O. Sasaki,⁷⁹ K. Sato,¹⁶³
 C. Sauer,^{59b} F. Sauerburger,⁵⁰ E. Sauvan,⁴ P. Savard,^{161,e} R. Sawada,¹⁵⁸ C. Sawyer,¹³⁸ L. Sawyer,⁹³ I. Sayago Galvan,¹⁶⁸
 C. Sbarra,^{21b} A. Sbrizzi,^{64a,64c} T. Scanlon,⁹² J. Schaarschmidt,¹⁴³ P. Schacht,¹¹¹ D. Schaefer,³⁵ U. Schäfer,⁹⁶ A. C. Schaffer,⁶²
 D. Schaile,¹¹⁰ R. D. Schamberger,¹⁵⁰ E. Schanet,¹¹⁰ C. Scharf,¹⁷ N. Scharmberg,⁹⁷ V. A. Schegelsky,¹³² D. Scheirich,¹³⁷
 F. Schenck,¹⁷ M. Schernau,¹⁶⁵ C. Schiavi,^{53b,53a} L. K. Schildgen,²² Z. M. Schillaci,²⁴ E. J. Schioppa,^{65a,65b}
 M. Schioppa,^{39b,39a} B. Schlag,⁹⁶ K. E. Schleicher,⁵⁰ S. Schlenker,³⁴ K. Schmieden,⁹⁶ C. Schmitt,⁹⁶ S. Schmitt,⁴⁴
 L. Schoeffel,¹³⁹ A. Schoening,^{59b} P. G. Scholer,⁵⁰ E. Schopf,¹²⁹ M. Schott,⁹⁶ J. Schovancova,³⁴ S. Schramm,⁵²
 F. Schroeder,¹⁷⁶ H-C. Schultz-Coulon,^{59a} M. Schumacher,⁵⁰ B. A. Schumm,¹⁴⁰ Ph. Schune,¹³⁹ A. Schwartzman,¹⁴⁸
 T. A. Schwarz,¹⁰² Ph. Schwemling,¹³⁹ R. Schwenhorst,¹⁰³ A. Sciandra,¹⁴⁰ G. Sciolla,²⁴ F. Scuri,^{69a} F. Scutti,¹⁰¹
 C. D. Sebastiani,⁸⁸ K. Sedlaczek,⁴⁵ P. Seema,¹⁷ S. C. Seidel,¹¹³ A. Seiden,¹⁴⁰ B. D. Seidlitz,²⁷ T. Seiss,³⁵ C. Seitz,⁴⁴
 J. M. Seixas,^{78b} G. Sekhniaidze,^{67a} S. J. Sekula,⁴⁰ L. P. Selem,⁴ N. Semprini-Cesari,^{21b,21a} S. Sen,⁴⁷ C. Serfon,²⁷ L. Serin,⁶²

L. Serkin,^{64a,64b} M. Sessa,^{72a,72b} H. Severini,¹²³ S. Sevova,¹⁴⁸ F. Sforza,^{53b,53a} A. Sfyrla,⁵² E. Shabalina,⁵¹ R. Shaheen,¹⁴⁹ J. D. Shahinian,¹³¹ N. W. Shaikh,^{43a,43b} D. Shaked Renous,¹⁷⁴ L. Y. Shan,^{13a} M. Shapiro,¹⁶ A. Sharma,³⁴ A. S. Sharma,¹ S. Sharma,⁴⁴ P. B. Shatalov,¹¹⁹ K. Shaw,¹⁵¹ S. M. Shaw,⁹⁷ P. Sherwood,⁹² L. Shi,⁹² C. O. Shimmin,¹⁷⁷ Y. Shimogama,¹⁷³ J. D. Shinner,⁹¹ I. P. J. Shipsey,¹²⁹ S. Shirabe,⁵² M. Shiyakova,⁷⁷ J. Shlomi,¹⁷⁴ M. J. Shochet,³⁵ J. Shojaii,¹⁰¹ D. R. Shope,¹⁴⁹ S. Shrestha,¹²² E. M. Shrif,^{31g} M. J. Shroff,¹⁷⁰ E. Shulga,¹⁷⁴ P. Sicho,¹³⁵ A. M. Sickles,¹⁶⁷ E. Sideras Haddad,^{31g} O. Sidiropoulou,³⁴ A. Sidoti,^{21b} F. Siegert,⁴⁶ Dj. Sijacki,¹⁴ J. M. Silva,¹⁹ M. V. Silva Oliveira,³⁴ S. B. Silverstein,^{43a} S. Simion,⁶² R. Simoniello,³⁴ N. D. Simpson,⁹⁴ S. Simsek,^{11b} P. Sinervo,¹⁶¹ V. Sinetckii,¹⁰⁹ S. Singh,¹⁴⁷ S. Singh,¹⁶¹ S. Sinha,⁴⁴ S. Sinha,^{31g} M. Sioli,^{21b,21a} I. Siral,¹²⁶ S. Yu. Sivoklov,¹⁰⁹ J. Sjölin,^{43a,43b} A. Skaf,⁵¹ E. Skorda,⁹⁴ P. Skubic,¹²³ M. Slawinska,⁸² K. Sliwa,¹⁶⁴ V. Smakhtin,¹⁷⁴ B. H. Smart,¹³⁸ J. Smiesko,¹³⁷ S. Yu. Smirnov,¹⁰⁸ Y. Smirnov,¹⁰⁸ L. N. Smirnova,^{109,ii} O. Smirnova,⁹⁴ E. A. Smith,³⁵ H. A. Smith,¹²⁹ M. Smizanska,⁸⁷ K. Smolek,¹³⁶ A. Smykiewicz,⁸² A. A. Snesev,¹⁰⁷ H. L. Snoek,¹¹⁵ S. Snyder,²⁷ R. Sobie,^{170,m} A. Soffer,¹⁵⁶ F. Sohns,⁵¹ C. A. Solans Sanchez,³⁴ E. Yu. Soldatov,¹⁰⁸ U. Soldevila,¹⁶⁸ A. A. Solodkov,¹¹⁸ S. Solomon,⁵⁰ A. Soloshenko,⁷⁷ O. V. Solovyanov,¹¹⁸ V. Solovyeve,¹³² P. Sommer,¹⁴⁴ H. Son,¹⁶⁴ A. Sonay,¹² W. Y. Song,^{162b} A. Sopczak,¹³⁶ A. L. Sopio,⁹² F. Sopkova,^{26b} S. Sottocornola,^{68a,68b} R. Soualah,^{64a,64c} A. M. Soukharev,^{117b,117a} Z. Soumami,^{33c} D. South,⁴⁴ S. Spagnolo,^{65a,65b} M. Spalla,¹¹¹ M. Spangenberg,¹⁷² F. Spanò,⁹¹ D. Sperlich,⁵⁰ T. M. Spieker,^{59a} G. Spigo,³⁴ M. Spina,¹⁵¹ D. P. Spiteri,⁵⁵ M. Spousta,¹³⁷ A. Stabile,^{66a,66b} B. L. Stamas,¹¹⁶ R. Stamen,^{59a} M. Stamenkovic,¹¹⁵ A. Stampekis,¹⁹ M. Standke,²² E. Stanecka,⁸² B. Stanislaus,³⁴ M. M. Stanitzki,⁴⁴ M. Stankaityte,¹²⁹ B. Stapf,⁴⁴ E. A. Starchenko,¹¹⁸ G. H. Stark,¹⁴⁰ J. Stark,⁹⁸ D. M. Starko,^{162b} P. Staroba,¹³⁵ P. Starovoitov,^{59a} S. Stärz,¹⁰⁰ R. Staszewski,⁸² G. Stavropoulos,⁴² P. Steinberg,²⁷ A. L. Steinhebel,¹²⁶ B. Stelzer,^{147,162a} H. J. Stelzer,¹³³ O. Stelzer-Chilton,^{162a} H. Stenzel,⁵⁴ T. J. Stevenson,¹⁵¹ G. A. Stewart,³⁴ M. C. Stockton,³⁴ G. Stoicea,^{25b} M. Stolarski,^{134a} S. Stonjek,¹¹¹ A. Straessner,⁴⁶ J. Strandberg,¹⁴⁹ S. Strandberg,^{43a,43b} M. Strauss,¹²³ T. Streblner,⁹⁸ P. Strizenec,^{26b} R. Ströhmer,¹⁷¹ D. M. Strom,¹²⁶ L. R. Strom,⁴⁴ R. Stroynowski,⁴⁰ A. Strubig,^{43a,43b} S. A. Stucci,²⁷ B. Stugu,¹⁵ J. Stupak,¹²³ N. A. Styles,⁴⁴ D. Su,¹⁴⁸ S. Su,^{58a} W. Su,^{58d,143,58c} X. Su,^{58a} K. Sugizaki,¹⁵⁸ V. V. Sulin,¹⁰⁷ M. J. Sullivan,⁸⁸ D. M. S. Sultan,⁵² L. Sultanaliev,¹⁰⁷ S. Sultansoy,^{3c} T. Sumida,⁸³ S. Sun,¹⁰² S. Sun,¹⁷⁵ X. Sun,⁹⁷ O. Sunneborn Gudnadottir,¹⁶⁶ C. J. E. Suster,¹⁵² M. R. Sutton,¹⁵¹ M. Svatos,¹³⁵ M. Swiatkowski,^{162a} T. Swirski,¹⁷¹ I. Sykora,^{26a} M. Sykora,¹³⁷ T. Sykora,¹³⁷ D. Ta,⁹⁶ K. Tackmann,^{44,ij} A. Taffard,¹⁶⁵ R. Tafirout,^{162a} R. H. M. Taibah,¹³⁰ R. Takashima,⁸⁴ K. Takeda,⁸⁰ T. Takeshita,¹⁴⁵ E. P. Takeva,⁴⁸ Y. Takubo,⁷⁹ M. Talby,⁹⁸ A. A. Talyshev,^{117b,117a} K. C. Tam,^{60b} N. M. Tamir,¹⁵⁶ A. Tanaka,¹⁵⁸ J. Tanaka,¹⁵⁸ R. Tanaka,⁶² J. Tang,^{58c} Z. Tao,¹⁶⁹ S. Tapia Araya,⁷⁶ S. Tapprogge,⁹⁶ A. Tarek Abouelfadl Mohamed,¹⁰³ S. Tarem,¹⁵⁵ K. Tariq,^{58b} G. Tarna,^{25b} G. F. Tartarelli,^{66a} P. Tas,¹³⁷ M. Tasevsky,¹³⁵ E. Tassi,^{39b,39a} G. Tatenò,¹⁵⁸ Y. Tayalati,^{33e} G. N. Taylor,¹⁰¹ W. Taylor,^{162b} H. Teagle,⁸⁸ A. S. Tee,¹⁷⁵ R. Teixeira De Lima,¹⁴⁸ P. Teixeira-Dias,⁹¹ H. Ten Kate,³⁴ J. J. Teoh,¹¹⁵ K. Terashi,¹⁵⁸ J. Terron,⁹⁵ S. Terzo,¹² M. Testa,⁴⁹ R. J. Teuscher,^{161,m} N. Themistokleous,⁴⁸ T. Thevenaux-Pelzer,¹⁷ O. Thielmann,¹⁷⁶ D. W. Thomas,⁹¹ J. P. Thomas,¹⁹ E. A. Thompson,⁴⁴ P. D. Thompson,¹⁹ E. Thomson,¹³¹ E. J. Thorpe,⁹⁰ Y. Tian,⁵¹ V. O. Tikhomirov,^{107,kk} Yu. A. Tikhonov,^{117b,117a} S. Timoshenko,¹⁰⁸ P. Tipton,¹⁷⁷ S. Tisserant,⁹⁸ S. H. Tlou,^{31g} A. Tmourji,³⁶ K. Todome,^{21b,21a} S. Todorova-Nova,¹³⁷ S. Todt,⁴⁶ M. Togawa,⁷⁹ J. Tojo,⁸⁵ S. Tokár,^{26a} K. Tokushuku,⁷⁹ E. Tolley,¹²² R. Tombs,³⁰ M. Tomoto,^{79,112} L. Tompkins,¹⁴⁸ P. Tornambe,⁹⁹ E. Torrence,¹²⁶ H. Torres,⁴⁶ E. Torró Pastor,¹⁶⁸ M. Toscani,²⁸ C. Toscirì,³⁵ J. Toth,^{98,ll} D. R. Tovey,¹⁴⁴ A. Traeet,¹⁵ C. J. Treado,¹²⁰ T. Trefzger,¹⁷¹ A. Tricoli,²⁷ I. M. Trigger,^{162a} S. Trincaz-Duvoid,¹³⁰ D. A. Trischuk,¹⁶⁹ W. Trischuk,¹⁶¹ B. Trocmé,⁵⁶ A. Trofymov,⁶² C. Troncon,^{66a} F. Trovato,¹⁵¹ L. Truong,^{31c} M. Trzebinski,⁸² A. Trzupek,⁸² F. Tsai,¹⁵⁰ A. Tsiamis,¹⁵⁷ P. V. Tsiarehka,^{104,cc} A. Tsirigotis,^{157,dd} V. Tsiskaridze,¹⁵⁰ E. G. Tskhadadze,^{154a} M. Tsopoulou,¹⁵⁷ I. I. Tsukerman,¹¹⁹ V. Tsulaia,¹⁶ S. Tsuno,⁷⁹ O. Tsur,¹⁵⁵ D. Tsybychev,¹⁵⁰ Y. Tu,^{60b} A. Tudorache,^{25b} V. Tudorache,^{25b} A. N. Tuna,³⁴ S. Turchikhin,⁷⁷ I. Turk Cakir,^{3a} R. J. Turner,¹⁹ R. Turra,^{66a} P. M. Tuts,³⁷ S. Tzamarias,¹⁵⁷ P. Tzanis,⁹ E. Tzovara,⁹⁶ K. Uchida,¹⁵⁸ F. Ukegawa,¹⁶³ G. Unal,³⁴ M. Unal,¹⁰ A. Undrus,²⁷ G. Unel,¹⁶⁵ F. C. Ungaro,¹⁰¹ K. Uno,¹⁵⁸ J. Urban,^{26b} P. Urquijo,¹⁰¹ G. Usai,⁷ R. Ushioda,¹⁵⁹ M. Usman,¹⁰⁶ Z. Uysal,^{11d} V. Vacek,¹³⁶ B. Vachon,¹⁰⁰ K. O. H. Vadla,¹²⁸ T. Vafeiadis,³⁴ C. Valderanis,¹¹⁰ E. Valdes Santurio,^{43a,43b} M. Valente,^{162a} S. Valentinetti,^{21b,21a} A. Valero,¹⁶⁸ L. Valéry,⁴⁴ R. A. Vallance,¹⁹ A. Vallier,⁹⁸ J. A. Valls Ferrer,¹⁶⁸ T. R. Van Daalen,¹⁴³ P. Van Gemmeren,⁵ S. Van Stroud,⁹² I. Van Vulpen,¹¹⁵ M. Vanadia,^{71a,71b} W. Vandelli,³⁴ M. Vandenbroucke,¹³⁹ E. R. Vandewall,¹²⁴ D. Vannicola,¹⁵⁶ L. Vannoli,^{53b,53a} R. Vari,^{70a} E. W. Varnes,⁶ C. Varni,¹⁶ T. Varol,¹⁵³ D. Varouchas,⁶² K. E. Varvell,¹⁵² M. E. Vasile,^{25b} L. Vaslin,³⁶ G. A. Vasquez,¹⁷⁰ F. Vazeille,³⁶ D. Vazquez Furelos,¹² T. Vazquez Schroeder,³⁴ J. Veatch,⁵¹ V. Vecchio,⁹⁷ M. J. Veen,¹¹⁵ I. Veliscek,¹²⁹ L. M. Veloce,¹⁶¹ F. Veloso,^{134a,134c} S. Veneziano,^{70a} A. Ventura,^{65a,65b} A. Verbytskyi,¹¹¹ M. Verducci,^{69a,69b} C. Vergis,²² M. Verissimo De Araujo,^{78b} W. Verkerke,¹¹⁵ A. T. Vermeulen,¹¹⁵ J. C. Vermeulen,¹¹⁵

C. Vernieri,¹⁴⁸ P. J. Verschuuren,⁹¹ M. Vessella,⁹⁹ M. L. Vesterbacka,¹²⁰ M. C. Vetterli,^{147,e} A. Vgenopoulos,¹⁵⁷
 N. Viaux Maira,^{141f} T. Vickey,¹⁴⁴ O. E. Vickey Boeriu,¹⁴⁴ G. H. A. Viehhauser,¹²⁹ L. Vigani,^{59b} M. Villa,^{21b,21a}
 M. Villaplana Perez,¹⁶⁸ E. M. Villhauer,⁴⁸ E. Vilucchi,⁴⁹ M. G. Vinciter,³² G. S. Virdee,¹⁹ A. Vishwakarma,⁴⁸ C. Vittori,^{21b,21a}
 I. Vivarelli,¹⁵¹ V. Vladimirov,¹⁷² E. Voevodina,¹¹¹ M. Vogel,¹⁷⁶ P. Vokac,¹³⁶ J. Von Ahnen,⁴⁴ E. Von Toerne,²² V. Vorobel,¹³⁷
 K. Vorobev,¹⁰⁸ M. Vos,¹⁶⁸ J. H. Vosseveld,⁸⁸ M. Vozak,⁹⁷ L. Vozdecky,⁹⁰ N. Vranjes,¹⁴ M. Vranjes Milosavljevic,¹⁴
 V. Vrba,^{136,a} M. Vreeswijk,¹¹⁵ N. K. Vu,⁹⁸ R. Vuillermet,³⁴ O. V. Vujanovic,⁹⁶ I. Vukotic,³⁵ S. Wada,¹⁶³ C. Wagner,⁹⁹
 W. Wagner,¹⁷⁶ S. Wahdan,¹⁷⁶ H. Wahlberg,⁸⁶ R. Wakasa,¹⁶³ M. Wakida,¹¹² V. M. Walbrecht,¹¹¹ J. Walder,¹³⁸ R. Walker,¹¹⁰
 S. D. Walker,⁹¹ W. Walkowiak,¹⁴⁶ A. M. Wang,⁵⁷ A. Z. Wang,¹⁷⁵ C. Wang,^{58a} C. Wang,^{58c} H. Wang,¹⁶ J. Wang,^{60a} P. Wang,⁴⁰
 R.-J. Wang,⁹⁶ R. Wang,⁵⁷ R. Wang,¹¹⁶ S. M. Wang,¹⁵³ S. Wang,^{58b} T. Wang,^{58a} W. T. Wang,⁷⁵ W. X. Wang,^{58a} X. Wang,^{13c}
 X. Wang,¹⁶⁷ X. Wang,^{58c} Y. Wang,^{58a} Z. Wang,¹⁰² C. Wanotayaroj,³⁴ A. Warburton,¹⁰⁰ C. P. Ward,³⁰ R. J. Ward,¹⁹
 N. Warrack,⁵⁵ A. T. Watson,¹⁹ M. F. Watson,¹⁹ G. Watts,¹⁴³ B. M. Waugh,⁹² A. F. Webb,¹⁰ C. Weber,²⁷ M. S. Weber,¹⁸
 S. A. Weber,³² S. M. Weber,^{59a} C. Wei,^{58a} Y. Wei,¹²⁹ A. R. Weidberg,¹²⁹ J. Weingarten,⁴⁵ M. Weirich,⁹⁶ C. Weiser,⁵⁰
 T. Wenaus,²⁷ B. Wendland,⁴⁵ T. Wengler,³⁴ S. Wenig,³⁴ N. Wermes,²² M. Wessels,^{59a} K. Whalen,¹²⁶ A. M. Wharton,⁸⁷
 A. S. White,⁵⁷ A. White,⁷ M. J. White,¹ D. Whiteson,¹⁶⁵ L. Wickremasinghe,¹²⁷ W. Wiedenmann,¹⁷⁵ C. Wiel,⁴⁶
 M. Wielers,¹³⁸ N. Wieseotte,⁹⁶ C. Wiglesworth,³⁸ L. A. M. Wiik-Fuchs,⁵⁰ D. J. Wilbern,¹²³ H. G. Wilkens,³⁴ L. J. Wilkins,⁹¹
 D. M. Williams,³⁷ H. H. Williams,¹³¹ S. Williams,³⁰ S. Willocq,⁹⁹ P. J. Windischhofer,¹²⁹ I. Wingerter-Seez,⁴
 F. Winklmeier,¹²⁶ B. T. Winter,⁵⁰ M. Wittgen,¹⁴⁸ M. Wobisch,⁹³ A. Wolf,⁹⁶ R. Wölker,¹²⁹ J. Wollrath,¹⁶⁵ M. W. Wolter,⁸²
 H. Wolters,^{134a,134c} V. W. S. Wong,¹⁶⁹ A. F. Wongel,⁴⁴ S. D. Worm,⁴⁴ B. K. Wosiek,⁸² K. W. Woźniak,⁸² K. Wraight,⁵⁵
 J. Wu,^{13a,13d} S. L. Wu,¹⁷⁵ X. Wu,⁵² Y. Wu,^{58a} Z. Wu,^{139,58a} J. Wuerzinger,¹²⁹ T. R. Wyatt,⁹⁷ B. M. Wynne,⁴⁸ S. Xella,³⁸
 L. Xia,^{13c} M. Xia,^{13b} J. Xiang,^{60c} X. Xiao,¹⁰² M. Xie,^{58a} X. Xie,^{58a} I. Xiotidis,¹⁵¹ D. Xu,^{13a} H. Xu,^{58a} H. Xu,^{58a} L. Xu,^{58a}
 R. Xu,¹³¹ T. Xu,^{58a} W. Xu,¹⁰² Y. Xu,^{13b} Z. Xu,^{58b} Z. Xu,¹⁴⁸ B. Yabsley,¹⁵² S. Yacoob,^{31a} N. Yamaguchi,⁸⁵ Y. Yamaguchi,¹⁵⁹
 M. Yamatani,¹⁵⁸ H. Yamauchi,¹⁶³ T. Yamazaki,¹⁶ Y. Yamazaki,⁸⁰ J. Yan,^{58c} S. Yan,¹²⁹ Z. Yan,²³ H. J. Yang,^{58c,58d}
 H. T. Yang,¹⁶ S. Yang,^{58a} T. Yang,^{60c} X. Yang,^{58a} X. Yang,^{13a} Y. Yang,¹⁵⁸ Z. Yang,^{102,58a} W.-M. Yao,¹⁶ Y. C. Yap,⁴⁴ H. Ye,^{13c}
 J. Ye,⁴⁰ S. Ye,²⁷ I. Yeletsikh,⁷⁷ M. R. Yexley,⁸⁷ P. Yin,³⁷ K. Yorita,¹⁷³ K. Yoshihara,⁷⁶ C. J. S. Young,⁵⁰ C. Young,¹⁴⁸
 R. Yuan,^{58b,mm} X. Yue,^{59a} M. Zaazoua,^{33e} B. Zabinski,⁸² G. Zacharis,⁹ E. Zaid,⁴⁸ A. M. Zaitsev,^{118,i} T. Zakareishvili,^{154b}
 N. Zakharchuk,³² S. Zambito,³⁴ D. Zanzi,⁵⁰ S. V. Zeiβner,⁴⁵ C. Zeitnitz,¹⁷⁶ J. C. Zeng,¹⁶⁷ D. T. Zenger Jr.,²⁴ O. Zenin,¹¹⁸
 T. Ženiš,^{26a} S. Zenz,⁹⁰ S. Zerradi,^{33a} D. Zerwas,⁶² B. Zhang,^{13c} D. F. Zhang,¹⁴⁴ G. Zhang,^{13b} J. Zhang,⁵ K. Zhang,^{13a}
 L. Zhang,^{13c} M. Zhang,¹⁶⁷ R. Zhang,¹⁷⁵ S. Zhang,¹⁰² X. Zhang,^{58c} X. Zhang,^{58b} Z. Zhang,⁶² P. Zhao,⁴⁷ Y. Zhao,¹⁴⁰ Z. Zhao,^{58a}
 A. Zhemchugov,⁷⁷ Z. Zheng,¹⁴⁸ D. Zhong,¹⁶⁷ B. Zhou,¹⁰² C. Zhou,¹⁷⁵ H. Zhou,⁶ N. Zhou,^{58c} Y. Zhou,⁶ C. G. Zhu,^{58b}
 C. Zhu,^{13a,13d} H. L. Zhu,^{58a} H. Zhu,^{13a} J. Zhu,¹⁰² Y. Zhu,^{58a} X. Zhuang,^{13a} K. Zhukov,¹⁰⁷ V. Zhulanov,^{117b,117a} D. Zieminska,⁶³
 N. I. Zimine,⁷⁷ S. Zimmermann,^{50,a} J. Zinsser,^{59b} M. Ziolkowski,¹⁴⁶ L. Živković,¹⁴ A. Zoccoli,^{21b,21a} K. Zoch,⁵²
 T. G. Zorbas,¹⁴⁴ O. Zormpa,⁴² W. Zou,³⁷ and L. Zwalinski³⁴

(ATLAS Collaboration)

¹*Department of Physics, University of Adelaide, Adelaide, Australia*²*Department of Physics, University of Alberta, Edmonton, Alberta, Canada*^{3a}*Department of Physics, Ankara University, Ankara, Turkey*^{3b}*Istanbul Aydin University, Application and Research Center for Advanced Studies, Istanbul, Turkey*^{3c}*Division of Physics, TOBB University of Economics and Technology, Ankara, Turkey*⁴*LAPP, Univ. Savoie Mont Blanc, CNRS/IN2P3, Annecy, France*⁵*High Energy Physics Division, Argonne National Laboratory, Argonne, Illinois, USA*⁶*Department of Physics, University of Arizona, Tucson, Arizona, USA*⁷*Department of Physics, University of Texas at Arlington, Arlington, Texas, USA*⁸*Physics Department, National and Kapodistrian University of Athens, Athens, Greece*⁹*Physics Department, National Technical University of Athens, Zografou, Greece*¹⁰*Department of Physics, University of Texas at Austin, Austin, Texas, USA*^{11a}*Bahcesehir University, Faculty of Engineering and Natural Sciences, Istanbul, Turkey*^{11b}*Istanbul Bilgi University, Faculty of Engineering and Natural Sciences, Istanbul, Turkey*^{11c}*Department of Physics, Bogazici University, Istanbul, Turkey*^{11d}*Department of Physics Engineering, Gaziantep University, Gaziantep, Turkey*^{11e}*Department of Physics, Istanbul University, Istanbul, Turkey*

- ^{11f}*Istinye University, Sariyer, Istanbul, Turkey*
- ¹²*Institut de Física d'Altes Energies (IFAE), Barcelona Institute of Science and Technology, Barcelona, Spain*
- ^{13a}*Institute of High Energy Physics, Chinese Academy of Sciences, Beijing, China*
- ^{13b}*Physics Department, Tsinghua University, Beijing, China*
- ^{13c}*Department of Physics, Nanjing University, Nanjing, China*
- ^{13d}*University of Chinese Academy of Science (UCAS), Beijing, China*
- ¹⁴*Institute of Physics, University of Belgrade, Belgrade, Serbia*
- ¹⁵*Department for Physics and Technology, University of Bergen, Bergen, Norway*
- ¹⁶*Physics Division, Lawrence Berkeley National Laboratory and University of California, Berkeley, California, USA*
- ¹⁷*Institut für Physik, Humboldt Universität zu Berlin, Berlin, Germany*
- ¹⁸*Albert Einstein Center for Fundamental Physics and Laboratory for High Energy Physics, University of Bern, Bern, Switzerland*
- ¹⁹*School of Physics and Astronomy, University of Birmingham, Birmingham, United Kingdom*
- ^{20a}*Facultad de Ciencias y Centro de Investigaciones, Universidad Antonio Nariño, Bogotá, Colombia*
- ^{20b}*Departamento de Física, Universidad Nacional de Colombia, Bogotá, Colombia*
- ^{21a}*Dipartimento di Fisica e Astronomia A. Righi, Università di Bologna, Bologna, Italy*
- ^{21b}*INFN Sezione di Bologna, Bologna, Italy*
- ²²*Physikalisches Institut, Universität Bonn, Bonn, Germany*
- ²³*Department of Physics, Boston University, Boston, Massachusetts, USA*
- ²⁴*Department of Physics, Brandeis University, Waltham, Massachusetts, USA*
- ^{25a}*Transilvania University of Brasov, Brasov, Romania*
- ^{25b}*Horia Hulubei National Institute of Physics and Nuclear Engineering, Bucharest, Romania*
- ^{25c}*Department of Physics, Alexandru Ioan Cuza University of Iasi, Iasi, Romania*
- ^{25d}*National Institute for Research and Development of Isotopic and Molecular Technologies, Physics Department, Cluj-Napoca, Romania*
- ^{25e}*University Politehnica Bucharest, Bucharest, Romania*
- ^{25f}*West University in Timisoara, Timisoara, Romania*
- ^{26a}*Faculty of Mathematics, Physics and Informatics, Comenius University, Bratislava, Slovak Republic*
- ^{26b}*Department of Subnuclear Physics, Institute of Experimental Physics of the Slovak Academy of Sciences, Kosice, Slovak Republic*
- ²⁷*Physics Department, Brookhaven National Laboratory, Upton, New York, USA*
- ²⁸*Departamento de Física (FCEN) and IFIBA, Universidad de Buenos Aires and CONICET, Buenos Aires, Argentina*
- ²⁹*California State University, California, USA*
- ³⁰*Cavendish Laboratory, University of Cambridge, Cambridge, United Kingdom*
- ^{31a}*Department of Physics, University of Cape Town, Cape Town, South Africa*
- ^{31b}*iThemba Labs, Western Cape, South Africa*
- ^{31c}*Department of Mechanical Engineering Science, University of Johannesburg, Johannesburg, South Africa*
- ^{31d}*National Institute of Physics, University of the Philippines Diliman (Philippines), Quezon City, Philippines*
- ^{31e}*University of South Africa, Department of Physics, Pretoria, South Africa*
- ^{31f}*University of Zululand, KwaDlangezwa, South Africa*
- ^{31g}*School of Physics, University of the Witwatersrand, Johannesburg, South Africa*
- ³²*Department of Physics, Carleton University, Ottawa, Ontario, Canada*
- ^{33a}*Faculté des Sciences Ain Chock, Réseau Universitaire de Physique des Hautes Energies—Université Hassan II, Casablanca, Morocco*
- ^{33b}*Faculté des Sciences, Université Ibn-Tofail, Kénitra, Morocco*
- ^{33c}*Faculté des Sciences Semlalia, Université Cadi Ayyad, LPHEA-Marrakech, Morocco*
- ^{33d}*LPMR, Faculté des Sciences, Université Mohamed Premier, Oujda, Morocco*
- ^{33e}*Faculté des sciences, Université Mohammed V, Rabat, Morocco*
- ^{33f}*Mohammed VI Polytechnic University, Ben Guerir, Morocco*
- ³⁴*CERN, Geneva, Switzerland*
- ³⁵*Enrico Fermi Institute, University of Chicago, Chicago, Illinois, USA*
- ³⁶*LPC, Université Clermont Auvergne, CNRS/IN2P3, Clermont-Ferrand, France*
- ³⁷*Nevis Laboratory, Columbia University, Irvington, New York, USA*
- ³⁸*Niels Bohr Institute, University of Copenhagen, Copenhagen, Denmark*
- ^{39a}*Dipartimento di Fisica, Università della Calabria, Rende, Italy*

- ^{39b}INFN Gruppo Collegato di Cosenza, Laboratori Nazionali di Frascati, Frascati, Italy
- ⁴⁰Physics Department, Southern Methodist University, Dallas, Texas, USA
- ⁴¹Physics Department, University of Texas at Dallas, Richardson, Texas, USA
- ⁴²National Centre for Scientific Research “Demokritos”, Agia Paraskevi, Greece
- ^{43a}Department of Physics, Stockholm University, Stockholm, Sweden
- ^{43b}Oskar Klein Centre, Stockholm, Sweden
- ⁴⁴Deutsches Elektronen-Synchrotron DESY, Hamburg and Zeuthen, Germany
- ⁴⁵Lehrstuhl für Experimentelle Physik IV, Technische Universität Dortmund, Dortmund, Germany
- ⁴⁶Institut für Kern- und Teilchenphysik, Technische Universität Dresden, Dresden, Germany
- ⁴⁷Department of Physics, Duke University, Durham, North Carolina, USA
- ⁴⁸SUPA—School of Physics and Astronomy, University of Edinburgh, Edinburgh, United Kingdom
- ⁴⁹INFN e Laboratori Nazionali di Frascati, Frascati, Italy
- ⁵⁰Physikalisches Institut, Albert-Ludwigs-Universität Freiburg, Freiburg, Germany
- ⁵¹II. Physikalisches Institut, Georg-August-Universität Göttingen, Göttingen, Germany
- ⁵²Département de Physique Nucléaire et Corpusculaire, Université de Genève, Genève, Switzerland
- ^{53a}Dipartimento di Fisica, Università di Genova, Genova, Italy
- ^{53b}INFN Sezione di Genova, Genova, Italy
- ⁵⁴II. Physikalisches Institut, Justus-Liebig-Universität Giessen, Giessen, Germany
- ⁵⁵SUPA—School of Physics and Astronomy, University of Glasgow, Glasgow, United Kingdom
- ⁵⁶LPSC, Université Grenoble Alpes, CNRS/IN2P3, Grenoble INP, Grenoble, France
- ⁵⁷Laboratory for Particle Physics and Cosmology, Harvard University, Cambridge, Massachusetts, USA
- ^{58a}Department of Modern Physics and State Key Laboratory of Particle Detection and Electronics, University of Science and Technology of China, Hefei, China
- ^{58b}Institute of Frontier and Interdisciplinary Science and Key Laboratory of Particle Physics and Particle Irradiation (MOE), Shandong University, Qingdao, China
- ^{58c}School of Physics and Astronomy, Shanghai Jiao Tong University, Key Laboratory for Particle Astrophysics and Cosmology (MOE), SKLPPC, Shanghai, China
- ^{58d}Tsung-Dao Lee Institute, Shanghai, China
- ^{59a}Kirchhoff-Institut für Physik, Ruprecht-Karls-Universität Heidelberg, Heidelberg, Germany
- ^{59b}Physikalisches Institut, Ruprecht-Karls-Universität Heidelberg, Heidelberg, Germany
- ^{60a}Department of Physics, Chinese University of Hong Kong, Shatin, N.T., Hong Kong, China
- ^{60b}Department of Physics, University of Hong Kong, Hong Kong, China
- ^{60c}Department of Physics and Institute for Advanced Study, Hong Kong University of Science and Technology, Clear Water Bay, Kowloon, Hong Kong, China
- ⁶¹Department of Physics, National Tsing Hua University, Hsinchu, Taiwan
- ⁶²IJCLab, Université Paris-Saclay, CNRS/IN2P3, 91405, Orsay, France
- ⁶³Department of Physics, Indiana University, Bloomington, Indiana, USA
- ^{64a}INFN Gruppo Collegato di Udine, Sezione di Trieste, Udine, Italy
- ^{64b}ICTP, Trieste, Italy
- ^{64c}Dipartimento Politecnico di Ingegneria e Architettura, Università di Udine, Udine, Italy
- ^{65a}INFN Sezione di Lecce, Lecce, Italy
- ^{65b}Dipartimento di Matematica e Fisica, Università del Salento, Lecce, Italy
- ^{66a}INFN Sezione di Milano, Milano, Italy
- ^{66b}Dipartimento di Fisica, Università di Milano, Milano, Italy
- ^{67a}INFN Sezione di Napoli, Napoli, Italy
- ^{67b}Dipartimento di Fisica, Università di Napoli, Napoli, Italy
- ^{68a}INFN Sezione di Pavia, Pavia, Italy
- ^{68b}Dipartimento di Fisica, Università di Pavia, Pavia, Italy
- ^{69a}INFN Sezione di Pisa, Pisa, Italy
- ^{69b}Dipartimento di Fisica E. Fermi, Università di Pisa, Pisa, Italy
- ^{70a}INFN Sezione di Roma, Roma, Italy
- ^{70b}Dipartimento di Fisica, Sapienza Università di Roma, Roma, Italy
- ^{71a}INFN Sezione di Roma Tor Vergata, Roma, Italy
- ^{71b}Dipartimento di Fisica, Università di Roma Tor Vergata, Roma, Italy
- ^{72a}INFN Sezione di Roma Tre, Roma, Italy
- ^{72b}Dipartimento di Matematica e Fisica, Università Roma Tre, Roma, Italy
- ^{73a}INFN-TIFPA, Trento, Italy
- ^{73b}Università degli Studi di Trento, Trento, Italy
- ⁷⁴Institut für Astro- und Teilchenphysik, Leopold-Franzens-Universität, Innsbruck, Austria
- ⁷⁵University of Iowa, Iowa City, Iowa, USA

- ⁷⁶*Department of Physics and Astronomy, Iowa State University, Ames, Iowa, USA*
- ⁷⁷*Joint Institute for Nuclear Research, Dubna, Russia*
- ^{78a}*Departamento de Engenharia Elétrica, Universidade Federal de Juiz de Fora (UFJF), Juiz de Fora, Brazil*
- ^{78b}*Universidade Federal do Rio De Janeiro COPPE/EE/IF, Rio de Janeiro, Brazil*
- ^{78c}*Instituto de Física, Universidade de São Paulo, São Paulo, Brazil*
- ^{78d}*Rio de Janeiro State University, Rio de Janeiro, Brazil*
- ⁷⁹*KEK, High Energy Accelerator Research Organization, Tsukuba, Japan*
- ⁸⁰*Graduate School of Science, Kobe University, Kobe, Japan*
- ^{81a}*AGH University of Science and Technology, Faculty of Physics and Applied Computer Science, Krakow, Poland*
- ^{81b}*Marian Smoluchowski Institute of Physics, Jagiellonian University, Krakow, Poland*
- ⁸²*Institute of Nuclear Physics Polish Academy of Sciences, Krakow, Poland*
- ⁸³*Faculty of Science, Kyoto University, Kyoto, Japan*
- ⁸⁴*Kyoto University of Education, Kyoto, Japan*
- ⁸⁵*Research Center for Advanced Particle Physics and Department of Physics, Kyushu University, Fukuoka, Japan*
- ⁸⁶*Instituto de Física La Plata, Universidad Nacional de La Plata and CONICET, La Plata, Argentina*
- ⁸⁷*Physics Department, Lancaster University, Lancaster, United Kingdom*
- ⁸⁸*Oliver Lodge Laboratory, University of Liverpool, Liverpool, United Kingdom*
- ⁸⁹*Department of Experimental Particle Physics, Jožef Stefan Institute and Department of Physics, University of Ljubljana, Ljubljana, Slovenia*
- ⁹⁰*School of Physics and Astronomy, Queen Mary University of London, London, United Kingdom*
- ⁹¹*Department of Physics, Royal Holloway University of London, Egham, United Kingdom*
- ⁹²*Department of Physics and Astronomy, University College London, London, United Kingdom*
- ⁹³*Louisiana Tech University, Ruston, Louisiana, USA*
- ⁹⁴*Fysiska institutionen, Lunds universitet, Lund, Sweden*
- ⁹⁵*Departamento de Física Teórica C-15 and CIAFF, Universidad Autónoma de Madrid, Madrid, Spain*
- ⁹⁶*Institut für Physik, Universität Mainz, Mainz, Germany*
- ⁹⁷*School of Physics and Astronomy, University of Manchester, Manchester, United Kingdom*
- ⁹⁸*CPPM, Aix-Marseille Université, CNRS/IN2P3, Marseille, France*
- ⁹⁹*Department of Physics, University of Massachusetts, Amherst, Massachusetts, USA*
- ¹⁰⁰*Department of Physics, McGill University, Montreal, Québec, Canada*
- ¹⁰¹*School of Physics, University of Melbourne, Victoria, Australia*
- ¹⁰²*Department of Physics, University of Michigan, Ann Arbor, Michigan, USA*
- ¹⁰³*Department of Physics and Astronomy, Michigan State University, East Lansing, Michigan, USA*
- ¹⁰⁴*B.I. Stepanov Institute of Physics, National Academy of Sciences of Belarus, Minsk, Belarus*
- ¹⁰⁵*Research Institute for Nuclear Problems of Byelorussian State University, Minsk, Belarus*
- ¹⁰⁶*Group of Particle Physics, University of Montreal, Montreal, Québec, Canada*
- ¹⁰⁷*P.N. Lebedev Physical Institute of the Russian Academy of Sciences, Moscow, Russia*
- ¹⁰⁸*National Research Nuclear University MEPhI, Moscow, Russia*
- ¹⁰⁹*D.V. Skobeltsyn Institute of Nuclear Physics, M.V. Lomonosov Moscow State University, Moscow, Russia*
- ¹¹⁰*Fakultät für Physik, Ludwig-Maximilians-Universität München, München, Germany*
- ¹¹¹*Max-Planck-Institut für Physik (Werner-Heisenberg-Institut), München, Germany*
- ¹¹²*Graduate School of Science and Kobayashi-Maskawa Institute, Nagoya University, Nagoya, Japan*
- ¹¹³*Department of Physics and Astronomy, University of New Mexico, Albuquerque, New Mexico, USA*
- ¹¹⁴*Institute for Mathematics, Astrophysics and Particle Physics, Radboud University/Nikhef, Nijmegen, Netherlands*
- ¹¹⁵*Nikhef National Institute for Subatomic Physics and University of Amsterdam, Amsterdam, Netherlands*
- ¹¹⁶*Department of Physics, Northern Illinois University, DeKalb, Illinois, USA*
- ^{117a}*Budker Institute of Nuclear Physics and NSU, SB RAS, Novosibirsk, Russia*
- ^{117b}*Novosibirsk State University, Novosibirsk, Russia*
- ¹¹⁸*Institute for High Energy Physics of the National Research Centre Kurchatov Institute, Protvino, Russia*
- ¹¹⁹*Institute for Theoretical and Experimental Physics named by A.I. Alikhanov of National Research Centre “Kurchatov Institute”, Moscow, Russia*
- ¹²⁰*Department of Physics, New York University, New York, New York, USA*
- ¹²¹*Ochanomizu University, Otsuka, Bunkyo-ku, Tokyo, Japan*
- ¹²²*Ohio State University, Columbus, Ohio, USA*

- ¹²³Homer L. Dodge Department of Physics and Astronomy, University of Oklahoma, Norman, Oklahoma, USA
- ¹²⁴Department of Physics, Oklahoma State University, Stillwater, Oklahoma, USA
- ¹²⁵Palacký University, Joint Laboratory of Optics, Olomouc, Czech Republic
- ¹²⁶Institute for Fundamental Science, University of Oregon, Eugene, Oregon, USA
- ¹²⁷Graduate School of Science, Osaka University, Osaka, Japan
- ¹²⁸Department of Physics, University of Oslo, Oslo, Norway
- ¹²⁹Department of Physics, Oxford University, Oxford, United Kingdom
- ¹³⁰LPNHE, Sorbonne Université, Université de Paris, CNRS/IN2P3, Paris, France
- ¹³¹Department of Physics, University of Pennsylvania, Philadelphia, Pennsylvania, USA
- ¹³²Konstantinov Nuclear Physics Institute of National Research Centre “Kurchatov Institute”, PNPI, St. Petersburg, Russia
- ¹³³Department of Physics and Astronomy, University of Pittsburgh, Pittsburgh, Pennsylvania, USA
- ^{134a}Laboratório de Instrumentação e Física Experimental de Partículas—LIP, Lisboa, Portugal
- ^{134b}Departamento de Física, Faculdade de Ciências, Universidade de Lisboa, Lisboa, Portugal
- ^{134c}Departamento de Física, Universidade de Coimbra, Coimbra, Portugal
- ^{134d}Centro de Física Nuclear da Universidade de Lisboa, Lisboa, Portugal
- ^{134e}Departamento de Física, Universidade do Minho, Braga, Portugal
- ^{134f}Departamento de Física Teórica y del Cosmos, Universidad de Granada, Granada (Spain), Spain
- ^{134g}Dep Física and CEFITEC of Faculdade de Ciências e Tecnologia, Universidade Nova de Lisboa, Caparica, Portugal
- ^{134h}Instituto Superior Técnico, Universidade de Lisboa, Lisboa, Portugal
- ¹³⁵Institute of Physics of the Czech Academy of Sciences, Prague, Czech Republic
- ¹³⁶Czech Technical University in Prague, Prague, Czech Republic
- ¹³⁷Charles University, Faculty of Mathematics and Physics, Prague, Czech Republic
- ¹³⁸Particle Physics Department, Rutherford Appleton Laboratory, Didcot, United Kingdom
- ¹³⁹IRFU, CEA, Université Paris-Saclay, Gif-sur-Yvette, France
- ¹⁴⁰Santa Cruz Institute for Particle Physics, University of California Santa Cruz, Santa Cruz, California, USA
- ^{141a}Departamento de Física, Pontificia Universidad Católica de Chile, Santiago, Chile
- ^{141b}Millennium Institute for Subatomic physics at high energy frontier (SAPHIR), Santiago, Chile
- ^{141c}Universidad de la Serena, La Serena, Chile
- ^{141d}Universidad Andres Bello, Department of Physics, Santiago, Chile
- ^{141e}Instituto de Alta Investigación, Universidad de Tarapacá, Arica, Chile
- ^{141f}Departamento de Física, Universidad Técnica Federico Santa María, Valparaíso, Chile
- ¹⁴²Universidade Federal de São João del Rei (UFSJ), São João del Rei, Brazil
- ¹⁴³Department of Physics, University of Washington, Seattle, Washington, USA
- ¹⁴⁴Department of Physics and Astronomy, University of Sheffield, Sheffield, United Kingdom
- ¹⁴⁵Department of Physics, Shinshu University, Nagano, Japan
- ¹⁴⁶Department Physik, Universität Siegen, Siegen, Germany
- ¹⁴⁷Department of Physics, Simon Fraser University, Burnaby, British Columbia, Canada
- ¹⁴⁸SLAC National Accelerator Laboratory, Stanford, California, USA
- ¹⁴⁹Department of Physics, Royal Institute of Technology, Stockholm, Sweden
- ¹⁵⁰Departments of Physics and Astronomy, Stony Brook University, Stony Brook, New York, USA
- ¹⁵¹Department of Physics and Astronomy, University of Sussex, Brighton, United Kingdom
- ¹⁵²School of Physics, University of Sydney, Sydney, Australia
- ¹⁵³Institute of Physics, Academia Sinica, Taipei, Taiwan
- ^{154a}E. Andronikashvili Institute of Physics, Iv. Javakhishvili Tbilisi State University, Tbilisi, Georgia
- ^{154b}High Energy Physics Institute, Tbilisi State University, Tbilisi, Georgia
- ¹⁵⁵Department of Physics, Technion, Israel Institute of Technology, Haifa, Israel
- ¹⁵⁶Raymond and Beverly Sackler School of Physics and Astronomy, Tel Aviv University, Tel Aviv, Israel
- ¹⁵⁷Department of Physics, Aristotle University of Thessaloniki, Thessaloniki, Greece
- ¹⁵⁸International Center for Elementary Particle Physics and Department of Physics, University of Tokyo, Tokyo, Japan
- ¹⁵⁹Department of Physics, Tokyo Institute of Technology, Tokyo, Japan
- ¹⁶⁰Tomsk State University, Tomsk, Russia
- ¹⁶¹Department of Physics, University of Toronto, Toronto, Ontario, Canada
- ^{162a}TRIUMF, Vancouver, British Columbia, Canada
- ^{162b}Department of Physics and Astronomy, York University, Toronto, Ontario, Canada

- ¹⁶³*Division of Physics and Tomonaga Center for the History of the Universe, Faculty of Pure and Applied Sciences, University of Tsukuba, Tsukuba, Japan*
- ¹⁶⁴*Department of Physics and Astronomy, Tufts University, Medford, Massachusetts, USA*
- ¹⁶⁵*Department of Physics and Astronomy, University of California Irvine, Irvine, California, USA*
- ¹⁶⁶*Department of Physics and Astronomy, University of Uppsala, Uppsala, Sweden*
- ¹⁶⁷*Department of Physics, University of Illinois, Urbana, Illinois, USA*
- ¹⁶⁸*Instituto de Física Corpuscular (IFIC), Centro Mixto Universidad de Valencia—CSIC, Valencia, Spain*
- ¹⁶⁹*Department of Physics, University of British Columbia, Vancouver, British Columbia, Canada*
- ¹⁷⁰*Department of Physics and Astronomy, University of Victoria, Victoria, British Columbia, Canada*
- ¹⁷¹*Fakultät für Physik und Astronomie, Julius-Maximilians-Universität Würzburg, Würzburg, Germany*
- ¹⁷²*Department of Physics, University of Warwick, Coventry, United Kingdom*
- ¹⁷³*Waseda University, Tokyo, Japan*
- ¹⁷⁴*Department of Particle Physics and Astrophysics, Weizmann Institute of Science, Rehovot, Israel*
- ¹⁷⁵*Department of Physics, University of Wisconsin, Madison, Wisconsin, USA*
- ¹⁷⁶*Fakultät für Mathematik und Naturwissenschaften, Fachgruppe Physik, Bergische Universität Wuppertal, Wuppertal, Germany*
- ¹⁷⁷*Department of Physics, Yale University, New Haven, Connecticut, USA*

^aDeceased.

^bAlso at Department of Physics, King's College London, London, United Kingdom.

^cAlso at Istanbul University, Department of Physics, Istanbul, Turkey.

^dAlso at Instituto de Física Teórica, IFT-UAM/CSIC, Madrid, Spain.

^eAlso at TRIUMF, Vancouver, British Columbia, Canada.

^fAlso at Department of Physics, University of Fribourg, Fribourg, Switzerland.

^gAlso at Department of Physics and Astronomy, University of Louisville, Louisville, Kentucky, USA.

^hAlso at Departament de Física de la Universitat Autònoma de Barcelona, Barcelona, Spain.

ⁱAlso at Moscow Institute of Physics and Technology State University, Dolgoprudny, Russia.

^jAlso at Faculty of Physics, Sofia University, 'St. Kliment Ohridski', Sofia, Bulgaria.

^kAlso at Department of Physics, Ben Gurion University of the Negev, Beer Sheva, Israel.

^lAlso at Università di Napoli Parthenope, Napoli, Italy.

^mAlso at Institute of Particle Physics (IPP), Canada.

ⁿAlso at Bruno Kessler Foundation, Trento, Italy.

^oAlso at Department of Physics, St. Petersburg State Polytechnical University, St. Petersburg, Russia.

^pAlso at Borough of Manhattan Community College, City University of New York, New York, New York, USA.

^qAlso at Department of Physics, California State University, Fresno, California, USA.

^rAlso at Department of Financial and Management Engineering, University of the Aegean, Chios, Greece.

^sAlso at Centro Studi e Ricerche Enrico Fermi, Italy.

^tAlso at Department of Physics, California State University, East Bay, California, USA.

^uAlso at Institutio Catalana de Recerca i Estudis Avancats, ICREA, Barcelona, Spain.

^vAlso at Graduate School of Science, Osaka University, Osaka, Japan.

^wAlso at Physikalisches Institut, Albert-Ludwigs-Universität Freiburg, Freiburg, Germany.

^xAlso at University of Chinese Academy of Sciences (UCAS), Beijing, China.

^yAlso at Institute of Physics, Azerbaijan Academy of Sciences, Baku, Azerbaijan.

^zAlso at Yeditepe University, Physics Department, Istanbul, Turkey.

^{aa}Also at Institute of Theoretical Physics, Ilia State University, Tbilisi, Georgia.

^{bb}Also at CERN, Geneva, Switzerland.

^{cc}Also at Joint Institute for Nuclear Research, Dubna, Russia.

^{dd}Also at Hellenic Open University, Patras, Greece.

^{ee}Also at Center for High Energy Physics, Peking University, China.

^{ff}Also at The City College of New York, New York, New York, USA.

^{gg}Also at Department of Physics, California State University, Sacramento, California, USA.

^{hh}Also at Département de Physique Nucléaire et Corpusculaire, Université de Genève, Genève, Switzerland.

ⁱⁱAlso at Faculty of Physics, M.V. Lomonosov Moscow State University, Moscow, Russia.

^{jj}Also at Institut für Experimentalphysik, Universität Hamburg, Hamburg, Germany.

^{kk}Also at National Research Nuclear University MEPhI, Moscow, Russia.

^{ll}Also at Institute for Particle and Nuclear Physics, Wigner Research Centre for Physics, Budapest, Hungary.

^{mm}Also at Department of Physics and Astronomy, Michigan State University, East Lansing, Michigan, USA.